Modelling and Applications of Autonomous Flow Control Devices

Eltazy Mohammed Khalid Eltaher

Submitted for the degree of Doctor of Philosophy

Heriot-Watt University
School of Energy Geoscience Infrastructure and Society
Institute of Petroleum Engineering

May, 2017

Volume II

This Thesis is submitted in two volumes

Abstract

Inflow Control technology has been employed in long, horizontal wells completions since the early 1990s. Their introduction prompted the extension of reservoir and well simulators to support their modelling and optimisation. More recently, Autonomous Flow Control Devices (AFCDs) have further improved well performance. However, the impact of AFCDs on reservoir management cannot yet be confidently predicted since their (autonomous) discrimination and control of the different fluid phases presents new modelling challenges that require extension of today's wellbore/reservoir models and workflows. Novel methods to visualise and optimise AFCD completions are also required.

This thesis shows how to use widely available, commercial codes to reliably simulate wells completed with AFCDs. Workflows for the optimal design and quantification of the economic value of such completions have been developed.

The resulting predictions are compared with published data (AFCD calibration curves). They are used to evaluate the AFCD-completions "added-value" for a range of reservoir types, device specifications and fluids. This work particularly addresses:

i. *Performance of the device* - little published data on AFCD multi-phase flow performance is available. Also, commercial reservoir simulators provide just one equation to capture the underlying physics of all AFCD types.

ii. *Wellbore model* - a representative reservoir/wellbore model and the previously ignored physics (stratified flow in the annulus and well trajectory alteration) are now essential since an AFCD's performance is strongly fluid-sensitive.

The above AFCD modelling and optimisation challenges are addressed by:

1) Developing an AFCD performance model that honours published data. Equations and modelling recommendations for several commercial AFCDs along with a range of modelling options, some novel and bespoke, are presented. The impact of uncertain multiphase flow performance on the AFCD well's "Added-Value" is quantified.

2) Increasing the accuracy of commercial well/reservoir simulators when modelling AFCD completions by recommending how to model the well trajectory, the reservoir/well segmentation and the multiphase flow performance.

3) Comparing the performance of optimised AFCD- and ICD-completions in multiple reservoir models to illustrate how various reservoir management challenges can be met.

Acknowledgement

All praise is to Allah.

I would like to express my sincere appreciation to all those who supported and helped me during my study.

I owe a special gratitude to my supervisors Prof. David Davies and Dr. Khafiz Muradov who provided a great support and invaluable help during the period of my PhD study.

A big thank you to Prof. Eric Mackay and Prof. Bernt Aadnoy for agreeing to be my examiners and spending their valuable time in reading this thesis.

I would like to thank all sponsors of VAWE project for the financial support and data provided for my study, as well as valuable discussions and suggestions during the JIP meetings (special thanks to Juan Videla, Atle Gyllensten, Kristine Arland and Craig Durham). I am also thankful to Schlumberger, CMG, Landmark, WEATHERFORD and Petex for allowing access to their software.

My colleagues in the office: Ivan Grebenkin, Misfer Almari, Bona Prakasa, Akindola Dada, Morteza Highighat, Ehsan Nikjoo and Mojtaba Moradi (Thank you all).

Thanks to Heriot-Watt University: the computer support group, the career advisers, the International Student Support Office and all the wonderful staff. A special thanks to the IPE staff.

Thank you all, my friends at Heriot-Watt University and Edinburgh. Thanks to Edinburgh for being such a great city, the people and everything about it.

Special thanks to Dr. Osman Elfeel, Dr. Mohamed Ahmed and Omer Ahmed (you have been a great help, I don’t have enough words).

My final and deepest gratitude to my parents (Mohamed Khalid & Mahasin Eltazy), my wife and my Sun Mohammed who have played a major role in my success.

Sondos Ahmed, Thank you so much.

DECLARATION STATEMENT

ACADEMIC REGISTRY
Research Thesis Submission

Name:	Eltazy Mohammed Khalid Eltaher		
School/PGI:	Energy Geoscience Infrastructure and Society		
Version: *(i.e. First, Resubmission, Final)*	Final	Degree Sought (Award and Subject area)	PhD in Petroleum Engineering

Declaration

In accordance with the appropriate regulations I hereby submit my thesis and I declare that:

1) The thesis embodies the results of my own work and has been composed by myself
2) Where appropriate, I have made acknowledgement of the work of others and have made reference to work carried out in collaboration with other persons
3) The thesis is the correct version of the thesis for submission and is the same version as any electronic versions submitted*.
4) My thesis for the award referred to, deposited in the Heriot-Watt University Library, should be made available for loan or photocopying and be available via the Institutional Repository, subject to such conditions as the Librarian may require
5) I understand that as a student of the University I am required to abide by the Regulations of the University and to conform to its discipline.

* *Please note that it is the responsibility of the candidate to ensure that the correct version of the thesis is submitted.*

Signature of Candidate:		Date:	

Submission

Submitted By *(name in capitals):*	ELTAZY MOHAMMED KHALID ELTAHER
Signature of Individual Submitting:	
Date Submitted:	

For Completion in the Student Service Centre (SSC)

Received in the SSC by *(name in capitals):*			
1.1 Method of Submission (Handed in to SSC; posted through internal/external mail):			
1.2 E-thesis Submitted (mandatory for final theses)			
Signature:		Date:	

TABLE OF CONTENTS

Chapter 4 Annular Flow and its influence on the Performance of AFCD completions

4.1 Introduction

The functions of the various wellbore completion components and their impact on the given well performance need to be fully understood to achieve the full potential of AWCs. As detailed in chapter 3, the multi-segment well model introduced by (Holmes, J.A., 1998) has provided a tool to model the pressure drop along the wellbore in a coupled well-reservoir simulator with the simplification of , oil and water treated as a homogeneous emulsion [73]. Most of the commercially-available reservoir simulators divide the wellbore into a number of segments that represent sections of the tubing, annulus and the flow control devices. The connection between the segments is designed such that the flow from one or more segments always converges in a single downstream segment (further details can be found in chapter 3) [18]. This modelling technique was suitable to model the performance of wells completed with inflow control valves ICVs and/or ICDs (where the ICD flow coefficient is assumed to be independent of Reynolds number). But for AFCD completions it is inaccurate and over simplified - unless annular flow isolation is installed in the annular space between the formation and the production tubing at every AFCD joint; this is a challenging completion to install (both technically and economically). It can only be assumed if the annulus is fully packed with gravel and the model is designed with enough resolution to capture the flow from the reservoir into each AFCD joint (12 m). Even then, there is the uncertainty within the same joint that the valves will be exposed to different fluids due to natural stratification {Figure 4-1}.

The modelling accuracy and added value quantification of AFCDs, unlike the passive FCDs, requires further research due to their (designed) multiphase flow sensitivity.

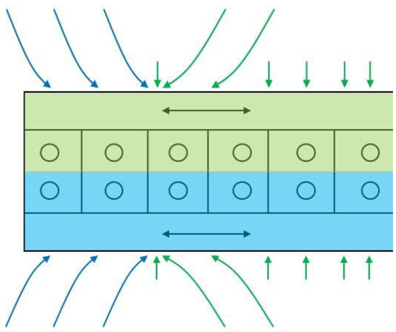

Figure 4-1 A conceptual picture illustrating several devices installed in a stratified flow environment in a zone that produces both oil and water

The reason for this complexity is the simulators' inability to accurately model the multi-phase annular flow that occurs (i.e. splitting each phase inflows within the annulus and then between the annulus and the AFCDs depending on their locations, number and flow resistance to achieve equilibrium). Reservoir simulators offer an option to introduce the volumetric fraction weighted fluid density ρ_{mix} and viscosity μ_{mix} shown in Equation 4-1 and Equation 4-2 (arbitrary values are used here, e.g. 1). However, this cannot capture the reservoir and wellbore conditions dependant, complex MPF performance in the annulus (upstream of the valves) that is responsible for inflow phase re-distribution and dynamic changes at various locations in the annulus.

$$\rho_{mix} = (\alpha_{oil})^a * \rho_{oil} + (\alpha_{water})^b * \rho_{water} + \left(\alpha_{gas}\right)^c * \rho_{gas} \qquad \text{Equation 4-1}$$

$$\mu_{mix} = (\alpha_{oil})^d * \mu_{oil} + (\alpha_{water})^e * \mu_{water} + \left(\alpha_{gas}\right)^f * \mu_{gas} \qquad \text{Equation 4-2}$$

Furthermore, the recent MPF data published for the performance of a single RCP valve, despite being limited, show a stricter performance than can be derived from these formula (Equation 4-1 and Equation 4-2) and could be difficult to incorporate in simulation whereby (a, b, c, d, e, f) are commonly assumed to equal 1.

The MPF regime in horizontal wellbores is normally stratified over a large part of the completion (around toe) since the flow velocity increases gradually from zero at the toe to maximum at the heel. In segmented wells the maximum annular flow in each zone is limited to this zone’s inflow, which promotes the stratified flow in the annulus even further with varying water hold-up with the position within the zone. That makes it unrealistic to apply the homogenous models or assumptions, e.g. as (Equation 4-1 and Equation 4-2 with the exponents equal 1), to such wells where the flow is stratified and the AFCDs strongly respond to this.

In this chapter we explain and examine various aspects of AFCD-completion modelling. Observations of stratified flow in advanced wells, its reasons and implications are discussed.

4.1.1 Introduction to Multiphase Flow in Pipes

The multiphase flow is greatly simplified, in the coupled well/reservoir modelling tools available today (further discussion can be found in chapter 3). This is due to the assumption that the fluids behave as a homogeneous mixture whose properties were averaged (volume weighted) from the individual phases’ properties. Experiments have shown that this is not the case [86]. The impact of such simplification is pronounced with AFCD-completions. Being fluid sensitive and accordingly autonomously active, their published MPF shows a significant difference to the routine modelling practice (assumptions and simplifications) as described above [10, 85].

The fundamental MPF phenomenon occurring in horizontal and vertical pipes for oil-gas, water-oil, etc. include the concepts of SLIP and HOLD UP [87]:

I. SLIP refers to "the ability of the less dense (e.g. "lighter" for upward flow) phase to flow at a greater velocity than the denser (e.g. "heavier" for upward flow) phase".
II. HOLD UP (HL) is "the volume fraction of the pipe occupied by one phase. As a consequence of slip - the HL of the denser phase is greater than would be expected from the (relative) in – and outflow of the two phases - since its flow velocity is slower than that for the light phase".
III. The accumulation of the denser phase in the pipe (or the annulus) is "an equilibrium phenomenon i.e. the in- and out-let flow rates of a particular phase flowing in the pipe are the same".

The importance of these phenomena is further pronounced in the case of gas/liquid flow, due to the density differences being greatest. These concepts are further explained in Appendix (6).

Depending on the flow regime in the tubing/annulus, "the oil and water are flowing as separated phases with one phase will form the continuous phase, with the second phase being dispersed as small droplets within this continuous phase" [87].

The flow patterns in the tubing/annulus is a function of:

a) gas and liquid flow rates
b) pipe angle of inclination
c) pipe diameter
d) fluid properties

The MPF in tubing and annuli is briefly described below. The main focus of this chapter is to study the applications of AFCD-completion in horizontal wells and the associated MPF concerns (inherited assumptions and routine simplifications).

4.1.1.1 Flow in Inclined and Horizontal Tubing

In vertical pipes, the low density (e.g. gas) tends to rise in the same direction as the main flow. Therefore, the gas/liquid multiphase flow is somewhat simplified. For inclined or horizontal flow on the other hand, it is much easier for the gas to separate from the liquid under these conditions. The difference between the actual and superficial phase velocities becomes greater than for the corresponding vertical flow conditions. Therefore, the flow regime is significantly altered with the increasing (θ) (angle of inclination) from the vertical "large variations observed in the fluid distribution and the flow pattern along the pipes when the angle of inclination is changed from +1° to -1° under stratified or (relatively) low velocity flow conditions" [86]. A second effect is that the tubing length (L) becomes greater than H (the vertical depth) as θ increases [87]:

$$L = {}^{H}\!/_{\cos\theta} \qquad \text{Equation 4-3}$$

As the angle θ increases to 90º "a horizontal well", the hydrostatic head component becomes of minor importance and the phase separation tendency "due to density difference" is at its greatest. Experiments have been carried out in transparent pipes and have identified the flow regimes in Figure 4-2 [87].

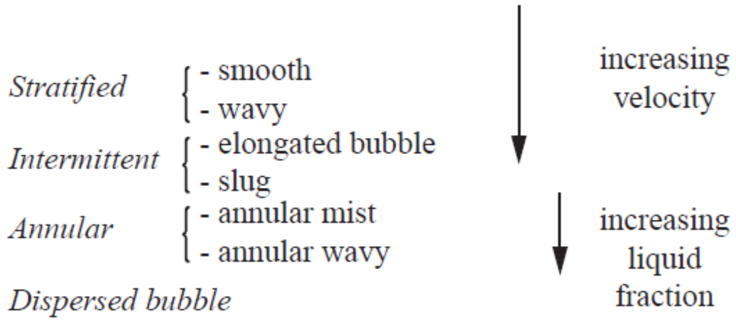

Figure 4-2: flow regimes and fluid velocity [87]

Such effect are considered to be of paramount importance for "horizontal" wells, especially when such wells are completed with AFCDs. Note: "horizontal" wells are never "exactly" horizontal and their liner/casing diameter is larger than that of a normal production tubing (which further signify the problem).

Flow maps which delineated the boundaries between the different flow regimes have been produced experimentally {Figure 4-3}. Accordingly, correlations between pressure drop and liquid and gas phase properties and velocities have been developed, as a function of tubing diameter, within each flow regime {Table 4-1}.

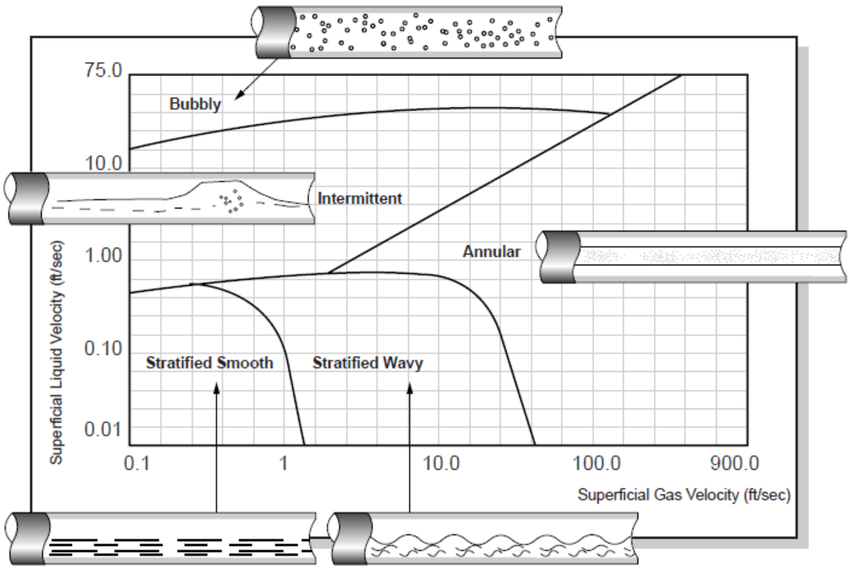

Figure 4-3: Taitel-Dukler horizontal flow map

In order to model and thereby optimize the performance of wells coupled to reservoirs, accurate multiphase pipe flow models must be incorporated into reservoir simulators [75]. More details available in chapter 3 [87].

Table 4-1: flow correlations [87]

Reference	Data Source	Fluids	Comments
Gilbert	Field data	G, O, W	Introduced vertical, multiphase gradient curves
Duns and Ros	Field and Lab. Data (air, oil & water flow in 11/4 - 31/8 in. pipes)	G, O, W	Vertical flow over wide flow rate range
Griffith and Wallis	Laboratory data (air & water flow in narrow pipes)	G, W	Good slug flow correlation used by later investigators
Hagedoorn and Brown	Field experiment (gas, oil & water flow in 1 - 4in. pipes)	G, O, W	Forms basis for widely used correlation
Aziz and Govier	Field & Lab. Data (air, oil & water flow in a wide range of pipes)	G, W	Correlations developed by mechanistic fluid mechanical study tested against field data

Beggs and Brill	Laboratory data (air & water flow in 1-11/2 in. pipes)	G, W	Correlations at all inclination angles

The coupled well/reservoir simulator rely on either the homogeneous model or the drift flux model to apply the above described physics (as discussed in chapter 3). This is mainly because they are considered to provide fast and efficient calculations governed by [74]:

(a) Simplicity:

The calculation has to be done many times in each segment at every time-step.

(b) Continuity:

The model must cover the complete range of flowing conditions without any first order discontinuities. Any such discontinuities would prevent the iterations of the well solution from converging (appendix 3). This requirement rules out methods involving flow regime maps, because the calculated pressure gradient changes discontinuously from one flow regime to another, unless some form of smoothing is applied.

(c) Differentiability:

The fully implicit solution of the multi-segment well model requires the calculation of derivatives of the phase flow rates and the pressure drop.

The drift flux model in particular can simulate countercurrent flow regime, allowing the heavy and light phases to flow in opposite directions when the overall flow velocity is small. This enables the software to model the separation of phases within the wellbore that occurs when, e.g., a well is shut-in at the surface, and also the accumulation of water in undulating sections of a "horizontal" well [74].

4.1.2 Field Experience and Engineering Data Related to Directional Wells

Engineering data provided by Production Logging Tools (PLT) in a real well or by experiments in the laboratory, have indicated stratified multiphase flow to be the most frequently encountered flow environment in horizontal and highly deviated wellbores. Observations by Espinoza, I. B., et al., 2015, Oddie, G., et al., 2003 and Bamforth, S., et al., 1996 and others include [31, 86, 88-90]:

1) Most horizontal wells exhibit stratified flow.

2) Almost all horizontal wells have a snake-like trajectory that results in complex flow regimes and holdup variation {Figure 4-4}.
3) Almost all wells had water present at the heel during PLT analysis.
4) Stagnating or circulating water asymmetrically re-invades the formation on the low-side of the horizontal wellbore with the consequence of increased unwanted fluid saturations in the near wellbore zone.
5) The static productivity index calculated from the rock properties often differ significantly from the dynamic productivity index calculated from PLT data.

Stratified flow in the annulus and the screen has also been verified both experimentally and computationally by Aakre, H., et al., 2014 [85].

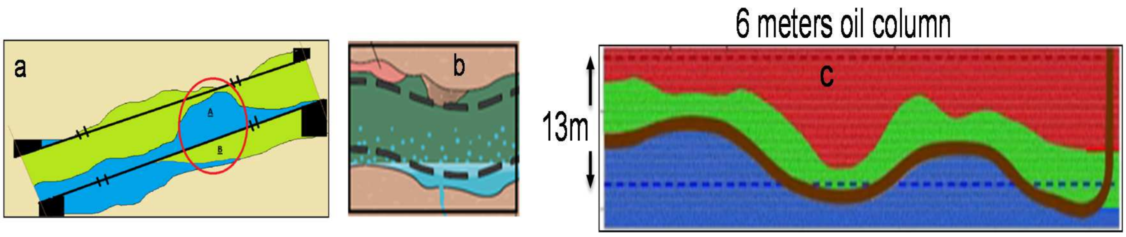

Figure 4-4: (a) Phase separation in inclined wells and (b) Denser fluid accumulation at low point of well trajectory [86]. (c) Example of well placement challenges driven by lithology and fluid contacts (Courtesy of Statoil)

A so-called horizontal well is almost never actually horizontal. Laboratory experiments {Figure 4-5} have demonstrated a considerable difference in phase velocities and holdup values resulting from small ($\pm 1^0$) changes in wellbore inclination from the horizontal. In fact, hold up is one of the most important factors characterizing multiphase flow in wellbores [75]. The localised fluid holdup of an advanced well completion defines the fluid phase that the active element of the FCD exposed to, and the subsequent control action of the AFCDs [69, 85]. This physics needs to be included in the modelling workflow since it will certainly impact the predicted performance of the AFCDs behaviour. The problem is further exacerbated by accumulation of the denser fluid at low points {Figure 4-4 (b)} and the gas at the high points of the well trajectory.

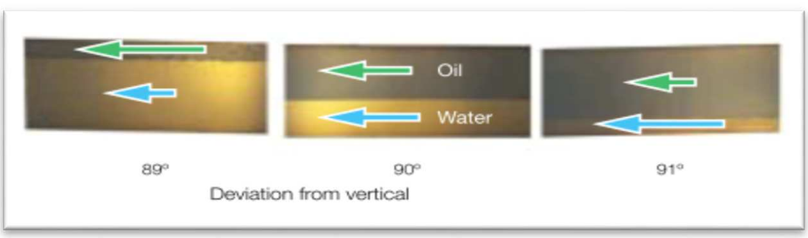

Figure 4-5: Laboratory experiments demonstrate a large change in phase velocities and holdup values from small (1^0) changes in wellbore inclination [86]

Table 4-2: Challenges for wellbore modelling of (near) horizontal completions incorporating AFCDs

Concern	Implications
1) Well inclination	Controls the multiphase hold-up of each fluid phase Can stratified flow in annulus be assumed?
2) Hold-up calculation	Defines which fluid controls the AFCD response.
3) Well undulation	Phase accumulation affects flow velocities and may result in triggering the Active module of the adjacent AFCD.
4) Annular Multi-phase flow calculation	Fluids within a segment assumed to be a homogeneous mixture with properties calculated based on the volumetric average: $\mu_{mix} = \propto_o . \mu_o + \propto_w . \mu_w + \propto_g . \mu_g$ $\rho_{mix} = \propto_o . \rho_o + \propto_w . \rho_w + \propto_g . \rho_g$ This is incorrect for stratified flow and will affect the AFCD's modelled response.
5) FCD locations	Not considered in current Modelling Workflow. However, it will control the fluid flowing through the AFCD and the response of the AFCD's active element.

The inevitable consequences of the above explained scenario {Table 4-2} is an inaccurate AFCD modelling! The currently used AFCD performance modelling approach, that was suitable enough for a passive FCD, is physically controversial for modelling phase selective FCDs therefore is recognised as needing update.

4.2 Impact of Annular Multiphase Flow on AFCD-completion Performance

4.2.1 The Modelled Wellbore Trajectory, Discretisation and AFCD Design

As detailed in section (4.1.2) above, the directional wells are never actually horizontal. Moreover, several challenges can hinder the originally planned trajectory resulting in a shorter well, varying inclinations and perhaps different target (sand unit) in some cases. This fact is resulting from several factors that take place during well placement operations some of which are listed in Table 4-3.

Table 4-3: example directional drilling challenges affecting the planned trajectory

Well placement challenges	Impact on well design/trajectory
Sand continuity and uncertainty	Shorter well or changing the targeted sand unit (zone).
Structural description uncertainty	Varying inclinations while maintaining the well within a specific zone.
Distorted contacts in mature fields	Varying inclinations to avoid drilling the well in zones interpreted to contain high unwanted fluid saturation (Figure 4-4 "c").
Drilling challenges (geo-steering)	Changing trajectory due to: loss of an equipment, problems with washout, and rocks with similar resistivity response to the reservoir.

Furthermore, AFCD(s) can be installed at every tubing joint (12.5 m), as is normally the case for ICDs (hundreds of ICDs are installed in a horizontal well completion). However, the number of packers installed in order to segment the wellbore into zones is limited (up to a few tens), hence, normally several devices are installed in the same zone, i.e. sharing the same annulus. Figure 4-6 is a conceptual picture of two completion zones separated by a packer:

- Assuming stratified flow in the annulus, the right zone produces oil while the left zone produces both oil and water with stratified flow in the annulus. Stratified flow exposes the lower valves to water and the upper valves to oil.
- One alternative scenario is that homogeneous flow exists in the left annulus, a situation that will result in a significantly different zonal production performance (the impact of this is evaluated in the following sections).

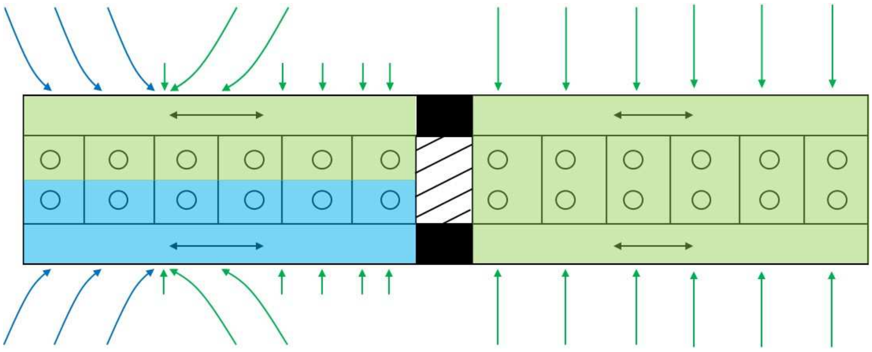

Figure 4-6: A conceptual illustration of several AFCDs installed in two zones separated by a packer. The right zone produces oil while the left zone produces both oil and water with stratified flow in the annulus.

In the case of AFCDs this raises a serious concern of how to model the Multi-Phase Flow (MPF) accurately to capture the effect of AFCDs exposed to the different fluid composition in the same annulus. This problem was previously ignored for ICDs and ICVs because they were lacking such strong phase selectivity.

It's important to realise that the models discussed in chapter (3) refer to the stand-alone AFCD performance. The AFCD-completion performance is expected to be intrinsically reliant on wellbore multiphase flow description (e.g. flow regime, velocities, conduit geometry, etc.).

4.2.2 Traditional Wellbore Model Segmentation Evaluated for AICVs

The frequently observed stratified flow in horizontal wells means that some devices will be receiving one fluid and others may receive a mixture. Such flow conditions has been reported for AICV-completion as depicted in Figure 4-7.

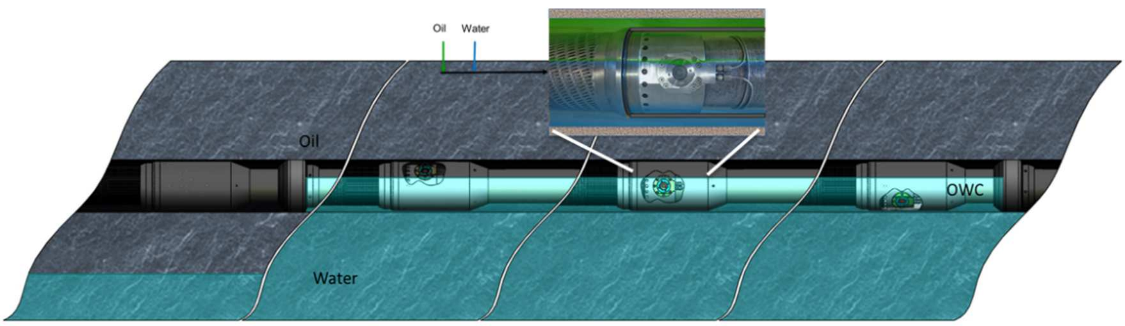

Figure 4-7: Illustration of the stratified flow in a well section completed with several AICVs sharing the same annulus (courtesy of Inflowcontrol)

To illustrate the implications of the homogeneous flow assumption on the horizontal AFCDs performance modelling results, we will take AICVs, first, as a case study. This is because they are simpler in terms of their multiphase performance definition compared with the remaining AICDs (for illustration). The AICV as explained in chapter 2, has only two positions: (1) "ON" for oil and multiphase flow up to a specific threshold for unwanted fluid flow above which it takes (2) the "OFF" position. The threshold is determined from laboratory experiments to be 98% for oil water system and 98% for gas oil system [85]. Similar observation were made from the first field application of AICV-completion in an Enhanced Oil Recovery (EOR) project to stop CO2 and water production [34]. In this field test, one completion-section was producing with WC of (91%) with AICV-completion open. The main contributing section of the well was producing with WC of (99%) and this is where the AICV reaction was triggered and the production from this section is stopped. Note: in separate discussion with the provider, a new AICV design that has a selective adjustable MPF performance is being developed and possible based on simple alteration of the current design geometries.

The AICV situation shown in Figure 4-7 above, describe the system as: (a) one valve immersed in oil, (b) one valve immersed in water and (c) the third valve is in multiphase flow condition. If homogeneous MPF is assumed in the annulus for modelling this section's performance, neither of the three valves will actually reach the 98% threshold. Hence none of them will close (during the simulation period illustrated in Figure 4-8. The AICV in this case behaves exactly as an ICD with equivalent nozzle size and no autonomous reaction will be triggered. In reality, as observed from published tests; one AICV is closed, and the others are open. Hence **the flow rate** from that section of the well will have **dropped less than half** for the same reservoir pressure (P_r) and tubing pressure (P_{tube}) (calculated from Equation 3-13 with the nozzle area reduced by one third).

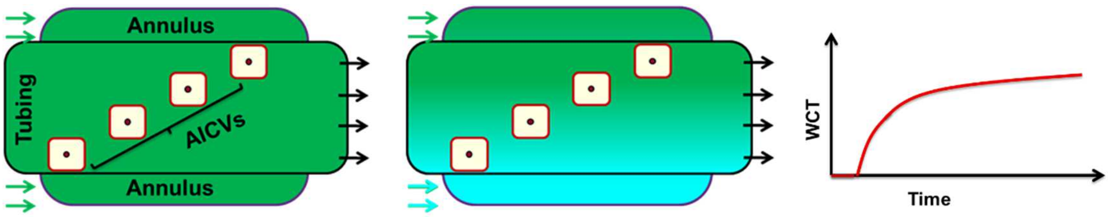

Figure 4-8: AICV modelling under homogeneous flow assumption behave as an ICD

The impact of modelling accuracy is exacerbated with AICDs since the MPF performance is expected to play a greater role in flow rate and pressure drop calculations since AICDs continue to react for the full range of MPF conditions, unlike the AICVs which are only active at a specific MPF threshold.

4.2.3 Modulation of the MPF Performance on the Generalised AICD Formula

Section 3.4.1 illustrates the impact of the stand-alone AFCD MPF assumptions on the AICD completion modelling. In this section a generalised equation {Equation 4-4} is provided, assuming:

1) More than one valve installed in the annulus defined by two packers (see e.g. Figure 4-7).
2) The valves are placed at different locations and exposed to different fluids, influenced by the fluid segregation in the annulus.
3) Equilibrium conditions in the system require:
    a) Inflow rate = outflow rate such that: $\mathrm{Q}_{total} = \mathrm{Q}_{AICD1} + \mathrm{Q}_{AICD2} + \mathrm{Q}_{AICD3}$ and
    b) The pressure drop between the annulus upstream of the valves and the tubing downstream is constant such that:
    $\Delta \mathrm{p}_{total} = \Delta \mathrm{p}_{AICD1} = \Delta \mathrm{p}_{AICD2} = \Delta \mathrm{p}_{AICD3}$

Equation 4-4 incorporates both, the improved single phase performance formula {Equation 3-18} and the annulus fluid segregation impact. Equation 4-4 is also dimensionally consistent and assumes pseudo-volumetric averaging of single-phase AFCD response. It employs several variable parameters to match the AFCD MPF performance. The mathematical form was chosen to model [79]:

i. A "slow", or tolerant, AFCD response to an increase in the water or gas fraction.
ii. A "fast", or highly restrictive, AFCD response to the unwanted fluid phase.
iii. A "linear" response to MPF performance.

This wide range of MPF performance curves has been observed during extensive AFCD flow loop laboratory tests (personal communication).

$$\Delta p = \frac{b_{\mathrm{AICD}}}{\left\{\left[\left(\frac{\mu_{mix,AICD1}^{x-2}}{\rho_{mix,AICD1}^{x-1}}\right)\right]^{1/x} + \left[\left(\frac{\mu_{mix,AICD2}^{x-2}}{\rho_{mix,AICD2}^{x-1}}\right)\right]^{1/x} + \left[\left(\frac{\mu_{mix,AICD3}^{x-2}}{\rho_{mix,AICD3}^{x-1}}\right)\right]^{1/x} + \cdots\right\}^{x}} q^{x}$$

Equation 4-4

The mixture property for each valve is affected by the fluid segregation in the annulus and the valve location. For instance, one of the valves might be completely immersed in one of the phases (e.g. pure oil or pure water).

The MPF can take various forms depending on the expected AFCD's multiphase flow performance (e.g. when it is not only oil or only water), e.g.:

$$
\begin{cases}
\rho_{mix} = (\alpha_{oil})^{a} * \rho_{oil} + (\alpha_{water})^{b} * \rho_{water} + \left(\alpha_{gas}\right)^{c} * \rho_{gas} \\
\mu_{mix} = (\alpha_{oil})^{e} * \mu_{oil} + (\alpha_{water})^{f} * \mu_{water} + \left(\alpha_{gas}\right)^{g} * \mu_{gas}
\end{cases}
$$

Equation 4-5

In the example given in Equation 4-5, the parameters (a, b, c, d, e, f, and g) can be used to match the MPF obtained from the flow loop test while accurately honouring the single phase performance (pressure drop vs. liquid rate) as depicted in Figure 4-9 for a device sensitive-to-wc (i.e. 'fast' response), or a less sensitive one ('slow').

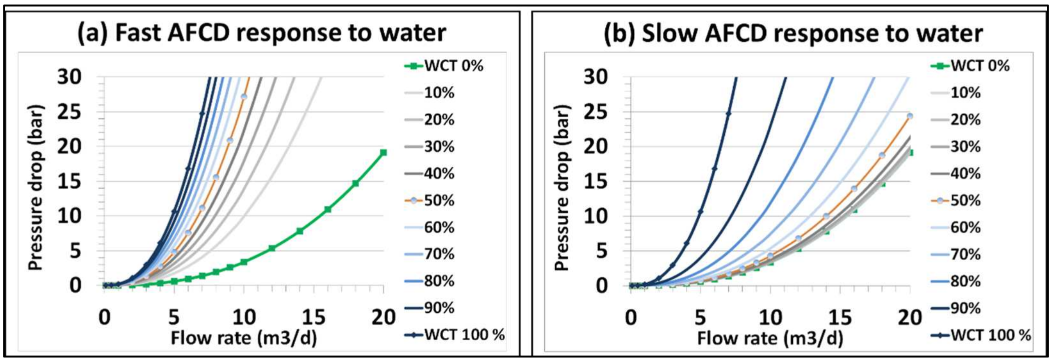

Figure 4-9: Example AFCD multi-phase performance generated using Equation 4-4, Equation 4-5 and Equation 3-19

Figure 4-9 "a", is an example MPF performance curve of an AFCD that has been designed to react in a fast (highly restrictive) manner to the arrival of an unwanted fluid.

Figure 4-9 "b", shows the opposite performance as experienced by a slow AFCD that "tolerates" a WC increase by not changing its MPF.

The parameters a, b, c, d, e, f, g (or maybe other set of parameters) can also be used to perform a robust and informative sensitivity study of the stand-alone performance of any AFCD (provided in chapter 5). The range of several possible MPF performance for all commercial AFCD types can be generated by varying the parameters as appropriate.

4.2.4 Traditional Wellbore Model Segmentation Evaluated for AICDs

Figure 4-10 illustrates the importance of the annulus flow regime on AICD completion modelling by considering a wellbore zone with 2 AICDs, installed one above the other. Let us, for example, take the production constraints listed in Table 4-4 (the inclined well PLT data in Figure 4-4 "a" is also relevant here).

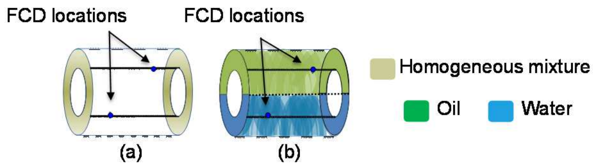

Figure 4-10: Well segment with (a) Homogeneous & (b) Stratified Annular Flow

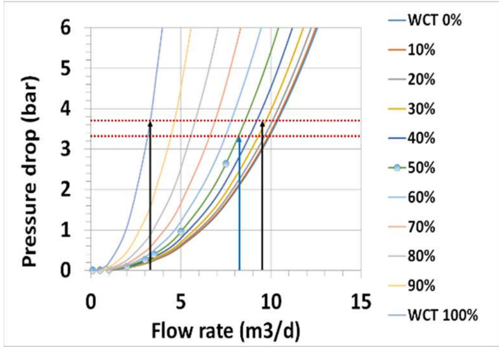

Figure 4-11: Flow performance of a “slow” standalone AICD

Table 4-4: Example production constraints

Parameter	Value	Units
Liquid productivity index (PI)	10	m^3/d/bar
Reservoir pressure (Pr)	150	bar
Pressure downstream of the device (Pt)	145	bar
Water cut (WC)	0.50	Fraction

Figure 4-11, the performance of a “slow” AICD (i.e. the AICD reacts slowly to the increasing water cut), illustrates the impact of the annular flow regime on AFCD’s completion performance. Note that the pressure drop along the annulus and tubing is negligible compared to the pressure drop across the AFCD.

1. Homogeneous (ideally mixed, Figure 4-10 “a”) illustrates the MPF flow regime traditionally assumed in reservoir simulation. The system production was 16.5 m^3/d with each AFCD passing 8.25 m^3/d of fluid at 50% WC and a pressure drop of 3.35 bar across the AICD (Table 4-5 and the vertical, blue line in Figure 4-11).
2. Stratified annular flow (separate, Figure 4-10 “b”), exposes the lower AFCD to water flow while the upper device produces a mixture of oil and water. The system production is reduced to 12.9 m^3/d at 50% WC and a pressure drop of 3.7 bar across the AICD (vertical, black line in Figure 4-11). The flow rates was 3.3 m^3/d for the lower AFCD and 9.6 m^3/d for the upper one. The above performance was calculated with Equation 4-6:

$$Q_{AICD1} = Q_{total} / \left[1 + \left(\left[\left(\frac{\rho^{x-1}_{mix,AICD2}}{\mu^{x-2}_{mix,AICD2}}\right)\right] \Big/ \left[\left(\frac{\rho^{x-1}_{mix,AICD1}}{\mu^{x-2}_{mix,AICD1}}\right)\right]\right)^{1/x}\right]$$

Equation 4-6

Where: $\mathrm{Q}_{total} = \mathrm{Q}_{AICD1} + \mathrm{Q}_{AICD2}$ and $\Delta\mathrm{p}_{total} = \Delta\mathrm{p}_{AICD1} = \Delta\mathrm{p}_{AICD2}$ under the assumption that one valve will be producing single-phase and the other will produce the remaining mixture (i.e. the term mix in the equation will be either oil or water for one of the valves - AICD1 & AICD2 - depending on the percentage of each within the annulus and the location of the valves).

Note: for x ≤ 2, the following expression can be used:

$$Q_{AICD1} = Q_{total} / \left[1 + \left(\left[\left(\frac{\rho^{2}_{mix,AICD2}}{\mu^{y}{}_{mix,AICD2}}\right)\right] \Big/ \left[\left(\frac{\rho^{2}_{mix,AICD1}}{\mu^{y}{}_{mix,AICD1}}\right)\right]\right)^{1/x}\right]$$

Equation 4-7

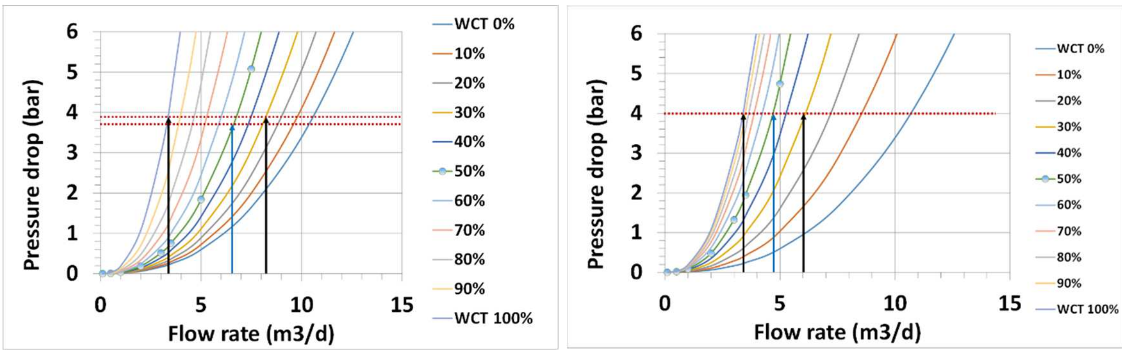

Figure 4-12: Flow performance of a "fast" and a "linear" AICD

In addition to the annulus flow, the AFCD MPF performance model also has a strong impact on the result. Figure 4-12 presents the corresponding results to Figure 4-11 for a "linear" and a "fast" AICD designs with the same performance to 100% oil and 100% water, but reacting differently at intermediate water cut values. The "fast" AICD responds the most aggressively to the increasing water cut. The corresponding pressure drops and flow rate splits between the upper and lower AFCDs (for 50% WC) are summarised in Table 4-5. Note that:

a) The pressure drop across the AICD increases and the rate decreases as the device's response to water becomes more restrictive.
b) The total flow rate for segregated annular flow is somewhat (up to 20%) lower than when modelled with homogeneous annular flow (except for fast MPF

performance where MPF parameters can be calculated (iteratively) that allow for a similar performance for both cases, i.e. one specific MPF performance matching the whole "WC" range for both homogeneous and stratified flow {Figure 4-13}).

c) Up to 44% difference in the system performance (flow rate) observed at 50% WC for the MPF designs applied (slow, linear and fast).

Table 4-5: Performance of "slow", "linear" and "fast" AICD designs for Homogeneous and Stratified annular flow at 5 bar Δp

AICD reaction to water	Total Flow Rate (50% WC, 5 bar drawdown)	Lower AICD		Upper AICD		Zonal Parameters	
		Flow Rate	WC	Flow Rate	WC	ΔP across AICD	Annular Flow Regime
	m^3/d	m^3/d	fraction	m^3/d	fraction	bar	
"Slow"	16.5	8.25	0.5	8.25	0.50	3.35	homogeneous
	12.9	3.3	1.0	9.6	0.33	3.71	segregated
"Linear"	13.2	6.6	0.5	6.6	0.50	3.68	homogeneous
	11.6	3.3	1.0	8.3	0.30	3.84	segregated
"Fast"	9.4	4.7	0.5	4.7	0.50	4.06	homogeneous
	9.4	3.4	1.0	6.0	0.32	4.06	segregated

Table 4-6 is a repeat of the Table 4-5 calculations for a downstream of the AICD pressure (Pt) of 140 bar and a drawdown of 10 bar.

Table 4-6: Performance of "slow", "linear" and "fast" AICD designs for Homogeneous and Stratified annular flow at 10 bar Δp

AICD reaction to water	Total Flow Rate (50% WC, 10 bar drawdown)	Lower AICD		Upper AICD		Zonal Parameters	
		Flow Rate	WC	Flow Rate	WC	ΔP across AICD	Annular Flow Regime
	m^3/d	m^3/d	fraction	m^3/d	fraction	bar	
"Slow"	23	11.5	0.5	11.5	0.50	7.7	homogeneous
	17.7	4.5	1.0	13.2	0.33	8.23	segregated
"Linear"	18.2	9.1	0.5	9.1	0.50	8.18	homogeneous
	15.8	4.5	1.0	11.3	0.30	8.42	segregated
"Fast"	12.7	6.35	0.5	6.35	0.50	8.72	homogeneous
	12.7	4.6	1.0	8.1	0.32	8.72	segregated

Table 4-6 results follow the same pattern as was observed for Table 4-5. The flow rate has increased less rapidly than the drawdown, as expected from Equation 3-13, et seq. which reflect the function of an ICD to reduce high flow velocities by increasing the drawdown. Such changes in the sandface pressure and the inflow rate due to the combination of the devices autonomous reaction to water with this "ICD" response will significantly affect the reservoir's dynamic response during depletion.

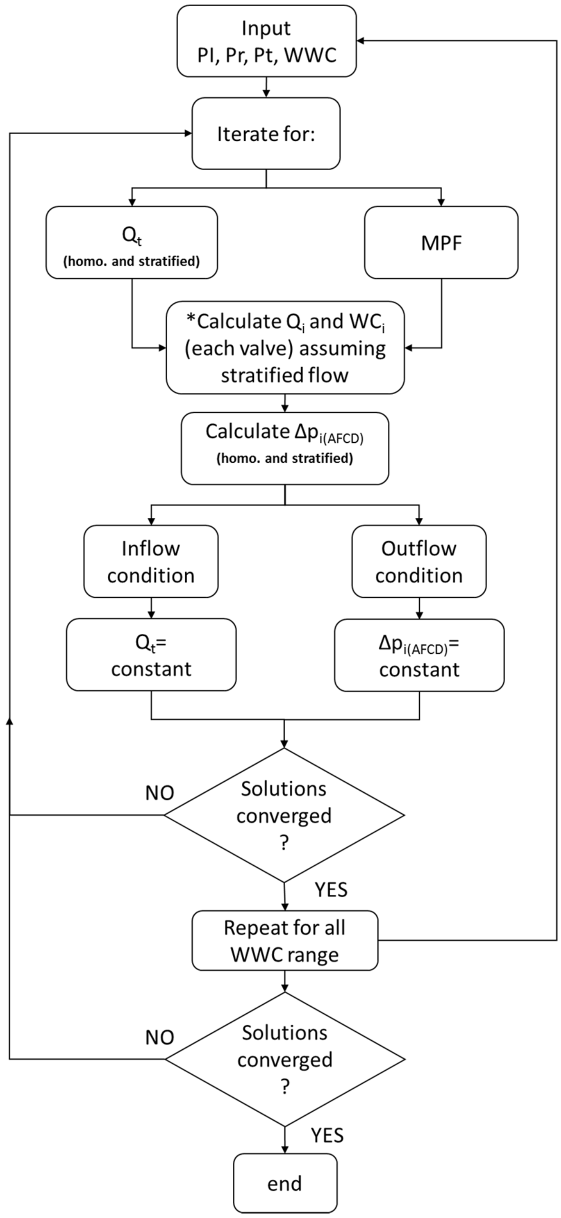

Figure 4-13: workflow (2) joining the well's inflow/outflow, and the AFCD performance to obtain (b, v) values allowing the homogeneous AFCD MPF to incorporate the fluid stratification effects

4.2.4.1 AICD Completion Flow Efficiency

Table 4-7 and Table 4-8 summarise the data from Table 4-5 and Table 4-6 with the addition of the single-phase flow performance (i.e. 0% and 100% WC), also re calculated at 5 bar and 10 bar reservoir drawdown respectively.

Table 4-7: AICD flow rate (sm^3/d/bar) at 5 bar drawdown

AICD reaction to water	Annular Flow Regime	Total Flow Rate at 0% WC (m^3/d)	Total flow Rate at 50% WC (m^3/d)	Total Flow Rate at 100% WC (m^3/d)
"Slow"	homogeneous	19.3	16.5	7.0
	segregated		12.9	
"Linear"	homogeneous		13.2	
	segregated		11.6	
"Fast"	homogeneous		9.4	
	segregated		9.4	

Table 4-8: AICD flow rates ($sm^3/d/$) at 10 bar drawdown

AICD reaction to water	Annular Flow Regime	Total Flow Rate at 0% WC (m^3/d)	Total flow Rate at 50% WC (m^3/d)	Total Flow Rate at 100% WC (m^3/d)
"Slow"	homogeneous	27.2	23	9.4
	Segregated		17.7	
"Linear"	homogeneous		18.2	
	Segregated		15.8	
"Fast"	Homogeneous		12.7	
	Segregated		12.7	

The above tables illustrate the AICD's ability to reduce the liquid flow rate by 65% as the inflow changes from 100% oil to 100% water. The flexibility generated by the range of possible AICD designs illustrated in Figure 4-11 and Figure 4-12 has been quantified for 50% WC in the above tables (please note, 44% difference in the system performance observed at 50% WC for the MPF designs applied). Table 4-9 and Table 4-10 use the above data in the form of a Completion Flow Efficiency (CFE), defined by Equation 4-8. This parameter combines the interaction between the flow rate, the pressure drop, the annular MPF regime and the aggressiveness of the AICDs reaction to water.

$$CFE = Q_{AICD} / \Delta p_{AICD} \qquad \text{Equation 4-8}$$

Table 4-9: Completion Flow Efficiency ($sm^3/d/bar$) at 5 bar drawdown

AICD reaction to water	Annular Flow Regime	Completion Flow Efficiency ($sm^3/d/bar$)		
		WC = 0%	WC = 50%	WC = 100%
"Slow"	homogeneous	6.26	4.93	1.62
	segregated		3.47	
"Linear"	homogeneous		3.58	
	segregated		3.00	
"Fast"	homogeneous		2.32	
	segregated		2.32	

Table 4-10: Completion Flow Efficiency ($sm^3/d/bar$) at 10 bar drawdown

AICD reaction to water	Annular Flow Regime	Completion Flow Efficiency ($sm^3/d/bar$)		
		WC = 0%	WC = 50%	WC = 100%
"Slow"	homogeneous	3.73	2.99	1.03
	segregated		2.15	
"Linear"	homogeneous		2.22	
	segregated		1.88	
"Fast"	homogeneous		1.45	
	segregated		1.45	

Inspection of Table 4-9 and Table 4-10, and Table 4-7 and Table 4-8, indicate that the ratio between the equivalent figures for the higher and the lower drawdown is approximately constant (see Equation 4-9).

$$\frac{CFE_1}{CFE_2} = \left\{\frac{Q_{1AICD}}{Q_{2AICD}}\right\} \Big/ \left\{\frac{\Delta p_{1AICD}}{\Delta p_{2AICD}}\right\} \qquad \text{Equation 4-9}$$

This analysis proves that a fast MPF performance for AFCDs is more likely to occur downhole (compared with slow and linear) when more than one valve are sharing the same annulus, mostly influenced by fluid stratification/segregation in the annulus. The current industry practice of assuming simple values, e.g. (1), for the homogeneous mixture parameters is very simplistic and can lead to misleading simulation results and, therefore, completion designs. The methodology presented here facilitates incorporating the MPF performance within the current simulators capabilities while capturing the fluid stratification effects.

4.3 Requirements for an Improved AFCD Modelling

Depending on the completion method used in a horizontal, inclined or undulating wells, fluids may enter or leave the wellbore radially through the production tubing at various locations. Various parameters can play a significant role on the AFCD-completion: e.g. multiphase flow regime, the flow rates of various fluids, inflow/outflow format, well inclination, fluid properties, and well geometry.

These challenges along with the challenges listed in Table 4-2 and their impact on the AFCD-completion performance in an advanced well have not yet been captured in the well/reservoir modelling workflow. These parameters {Figure 4-14} are categorised and discussed in this chapter.

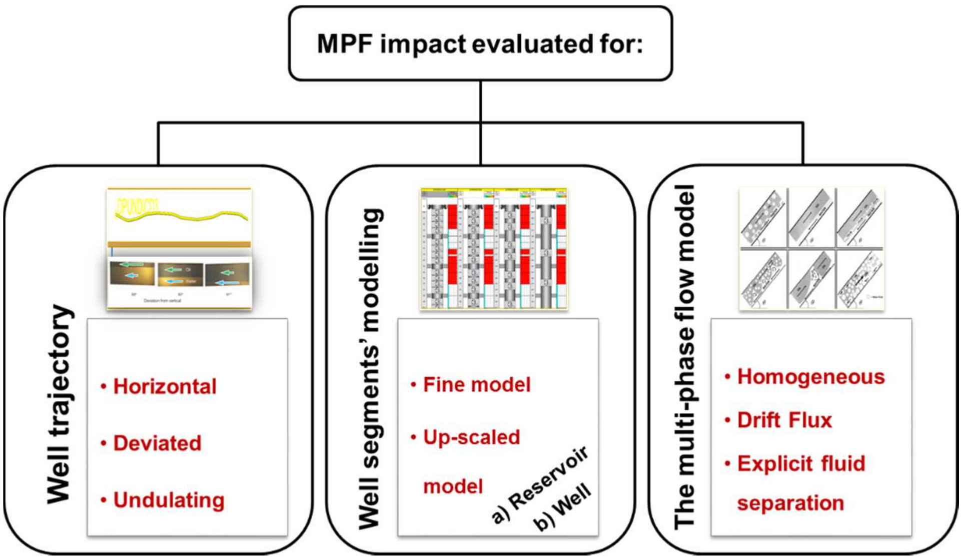

Figure 4-14: MPF impact evaluated for the definition of well trajectory, well/reservoir segmentation and the MPF model adopted for the wellbore solution.

4.3.1 *Sensitivity to Real Well Trajectory Analysis Should be investigated*

It is a common practice in the industry to model the so-called "horizontal" wells as a perfectly horizontal trajectory (an uncommon condition challenged by several geological, design, mechanical and operational constraints). This assumption was not of significance (within the wellbore mode) when passive FCDs where modelled. Its impact on wellbore/AFCD modelling and optimisation has not yet been analysed. Note: it is important to highlight that, the modelling of the correct well trajectory is important for well/reservoir connection deliverability calculation in all situations (see for example connection factor calculation in Reveal, ECLIPSE and Petrel) [74, 91].

4.3.2 *Well Model Segmentation/Discretization Should be Reviewed/Modified*

4.3.2.1 *The Device Model*

It is also a common practice to simulate the performance of several adjacent FCDs as a single representative FCD segment with appropriately modified properties – an upscaled wellbore model of the combined performance of all the FCDs connected to a reservoir grid block is required {Figure 4-15}. Annular isolation is an important factor to be considered in all cases. The number & location of these packers, etc. should also be considered in the completion design process. The options for defining the scaling factor is described in Equation 3-26 and Equation 3-27 (see also section 3.2.2).

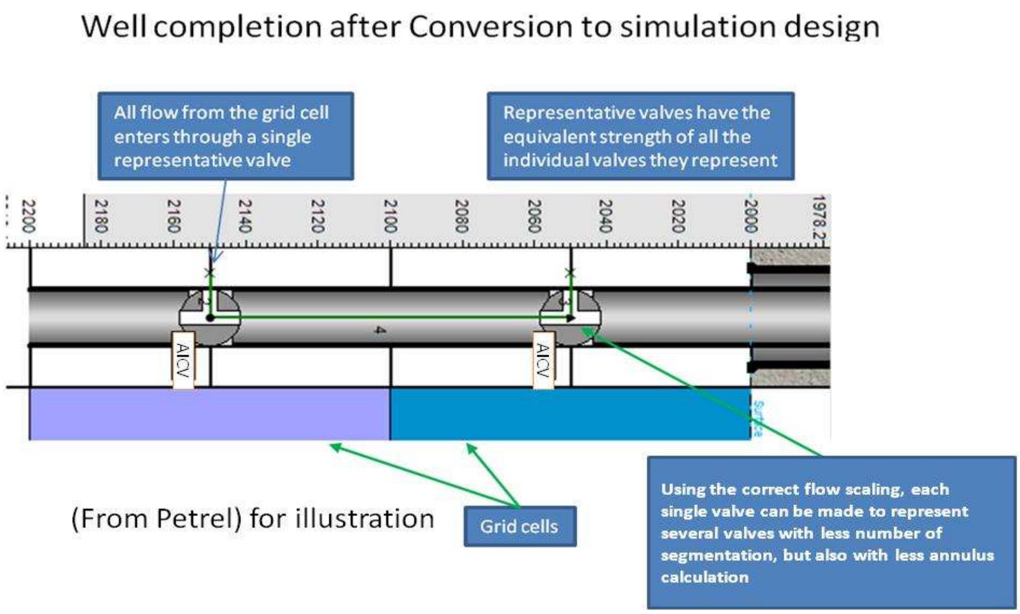

Figure 4-15: A Single, but representative valve, per wellbore and reservoir grid block. Adjusted from [92]

The completion depicted in Figure 4-15 can be designed to provide the same total fluid rate as inflows from the reservoir cell to the wellbore. Pressure drop calculations are based on a single, representative (A)FCD that mimics the performance of the real number of (A)FCDs in this well segment. A reasonable pressure drop value is calculated and the annulus flow calculation within this section can be omitted. It is only calculated between adjacent segments. This approach upscales the “annulus” & “tubing sections” of the wellbore (see also section 3.6).

Another approach (computationally demanding) is to model the number of valves explicitly – i.e. to allocate a segment to every joint. The annulus flow should now be accounted for {Figure 4-16}. The impact of such LGR on the results is addressed in chapter 5.

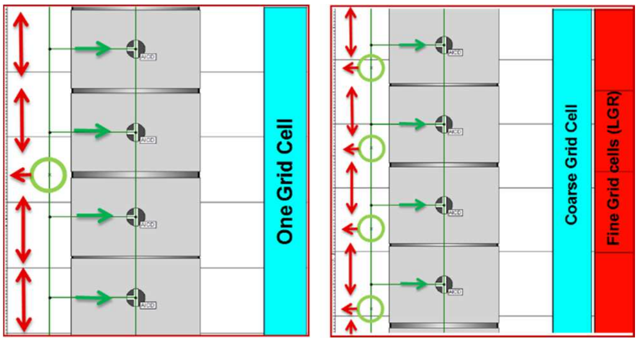

Figure 4-16: LGR and annulus flow with multiple FCDs between backers

4.3.2.2 The Annulus Flow Model

As discussed above, the annulus is divided into segments (axially) {Figure 4-16} and for simplicity the flow within each section of the pipe is considered to be an ideal homogeneous mixture whose properties are the averaged value of the individual phase properties. The annulus sections are separated by packers (axially). Several AFCDs can be allocated to each section where they are routinely modelled, as described above, as sharing the same fluid properties, flow rates and (consequently) the same pressure drop to the production tubing. However, due to fluid segregation (stratified flow, fluid accumulation at undulating sections etc.) such AFCDs do not actually flow the same fluid {Figure 4-4, Figure 4-5, Figure 4-6 and Figure 4-10}.

4.3.2.2.1 The MPF Model

The three models available within a commercial software that capture the physics as discussed in chapter 3. The: (1) Homogeneous model, (2) Drift flux model and (3) Multi-dimensional tables. The impact of these models has been studied and improvements develop where necessary.

4.3.3 *Summary of the Analysis*

Accurate multiphase pipe/annulus flow models must be incorporated into reservoir simulators in order to model and thereby optimize the performance of wells (completed with AFCDs) coupled to reservoir and surface facilities.

To summarize:

1) The routine modelling approach assumes each (axial) section of the wellbore has one MPF mixture properties. It ignores separation occurring within this section and, as a result, the devices will be in different locations and receive different fluids. Hence, not all the flow is converging at a single point as modelled. Therefore, the widely applied MSW model require modifications.
2) The drift flux model allow fluid slippage but does not rectify the problem above, e.g., for horizontal sections.
3) Assumptions such as “perfectly horizontal” trajectory should be evaluated for impact on AFCD-completion performance.
4) A new annulus model is required which allows for both slip velocity and fluid separation at different locations to be recognised by the individual AFCD.
5) The impact of uncertain standalone-AFCD performance should be evaluated with the expected MPF environment in the annulus coupled with a reservoir simulator.
6) The upscaling of (A)FCD performance in non-horizontal trajectories require investigation, especially for AICDs due to their continuous MPF reaction.
7) The accurate AFCD-completion model is envisaged to incorporate both solutions: (1) accurate stand-alone AFCD multi-phase flow (following the solutions provided in this paper along with published laboratory data) and (2) accurate annulus flow model (following the renowned fluid segregation physics).

In chapter 3 we discussed the modelling and optimization of a standalone AFCD design based on the published single phase, and the perceived performance from the limited multiphase flow performance for AFCDs. In the following sections we focus on the accuracy of the wellbore model defining which fluid the device will receive (considering the important coupling of well and reservoir models). Yet their limitations and how we can solve these issues. What is their impact in modelling results? We looked at the general engineering practice and the routine assumptions made for modelling AWCs to illustrate their validity/significance when applied to model AFCD-completion.

Chapter 5 adresses their impact on reservoir performance and completion optimisation.

4.4 Discretised Wellbore Model with Fluid Segregation for Horizontal Wells

4.4.1 Introduction to the Extended Multi-Segment Well (MSW) Application

Advanced well completion design optimization, and hence the proper deployment of (A)FCDs, requires that a sophisticated well model be implemented within the reservoir simulator. The model must be able to determine the local flowing conditions (the flow rate of each fluid phase and its pressure) throughout the well. Furthermore, it should allow for pressure losses calculation along the wellbore and across all specific completion items [73].

A new modelling approach for liquid-liquid and gas-liquid stratified flow in horizontal annuli through an FCD has been developed, coupled to the reservoir model. The two phase flow is captured by a “multi-branch” multi-segment well application. The content of the mixture flowing into the wellbore is modified relative to the immiscible fluids’ densities (assuming no emulsion is formed). This is done by transforming the free fluids holdup fractions in the relevant sections of the wellbore. The unwanted fluid is separated downhole and allocated to the lower branches (water) or the upper branches (gas) and the oil will be flowing at the top (for oil/water systems) or at the bottom for the (oil/gas) systems.

The model is able to determine the local flowing conditions (the flow rate of each fluid phase and its pressure) throughout the well. Furthermore, it allows for pressure losses calculation along the wellbore and across all specific completion items (e.g. AFCDs).

4.4.2 Description of the Proposed Network Topology

The extended MSW workflow is based on further discretisation of the wellbore both axially (separation of the annulus by packers) and laterally (i.e. separation of the annulus into several connected branches one on top of the other, e.g. Upper Segments (US) and Lower Segments (LS)). The length of the axial segment can be adjusted by upscaling to a convenient value since the well is perfectly horizontal. The MSW option within ECLIPSE is used to define several segments laterally depending on the number of FCDs. Different areas and pressure drop calculations can be assigned to different axial and radial segments when simulating either homogeneous or stratified flow. For example, an annulus section which has two AFCD joints with an open annulus is modelled by creating, two branches with a connection between the two annuli. Communication is allowed between adjacent segments {Figure 4-17}.

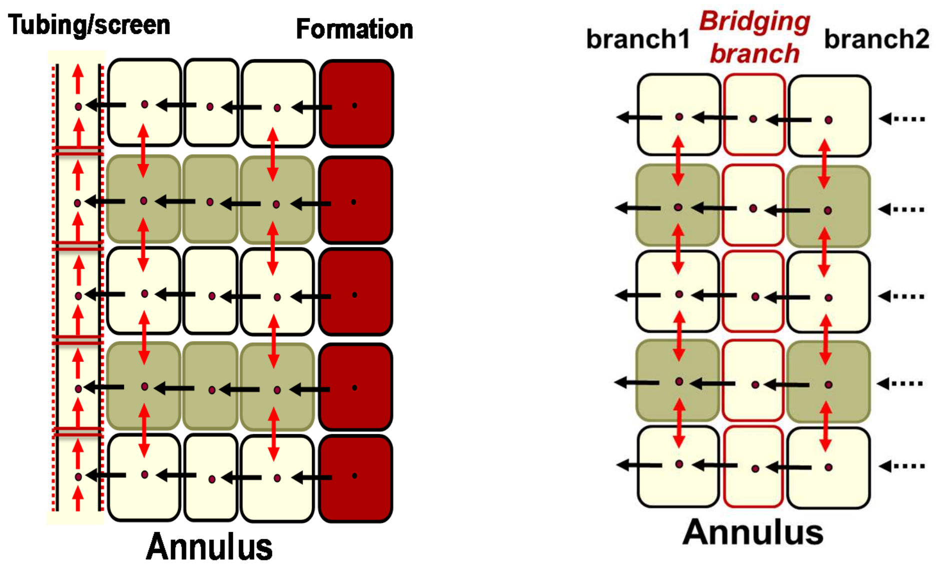

Figure 4-17: The extended MSW model for simulation of an open annulus

The wellbore modelling flexibility allowed by simulators, such as ECLIPSE, gives an opportunity to model various topologies. It therefore potentially provides a solution to several wellbore modelling challenges. The above topology can be used for modelling:

1. Inefficient gravel pack.
2. A leaking packer.
3. Flow through different completion items (behind casing, screen, etc.).

However, to apply such solution for the AFCD-completion modelling required further modification. Even with lateral discretisation and with individual AFCDs connected to different sections of the "discretised annulus", still the same homogeneous fluid flows through these valves. Figure 4-18 is an illustration that provides an example of a wellbore section containing several AFCDs with each two devices separated by a packer.

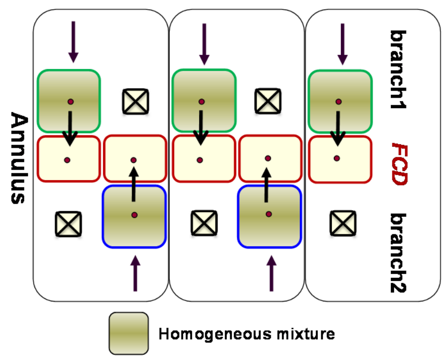

Figure 4-18: The extended MSW topology for simulation of a closed annulus with homogeneous flow

Capturing the phase separation in the annulus is required to be able to apply the method above as a solution for the AFCD-completion modelling challenges discussed earlier.

This is achieved by numerically separating the fluids without altering the system's pressure, as illustrated in Figure 4-19. For example, consider an oil/water system with two AFCD joints separated by a packer. The separation is introduced by:

- ✓ Modifying the phase content of the fluid flowing in the lower segment (water) by increasing the fraction of the denser phase using the downhole separator option in ECLIPSE.
- ✓ The free oil and water holdup fractions are then appropriately adjusted in the upper (mostly oil) and the lower (mostly water) segments. The separator option in ECLIPSE is used to separate the water downhole and re-allocate it to the LS and the oil to the US. The action of the separator is to modify the content of the mixture flowing into the lower branch thought the separator increasing the fraction of the output preferential phase allocated to the specified section of the well, **while ensuring equilibrium condition** (pressure and rate).
- ✓ FCDs are connected to each branch independently and the resulting **flow-and-pressure solution is found iteratively** (appendix 3).

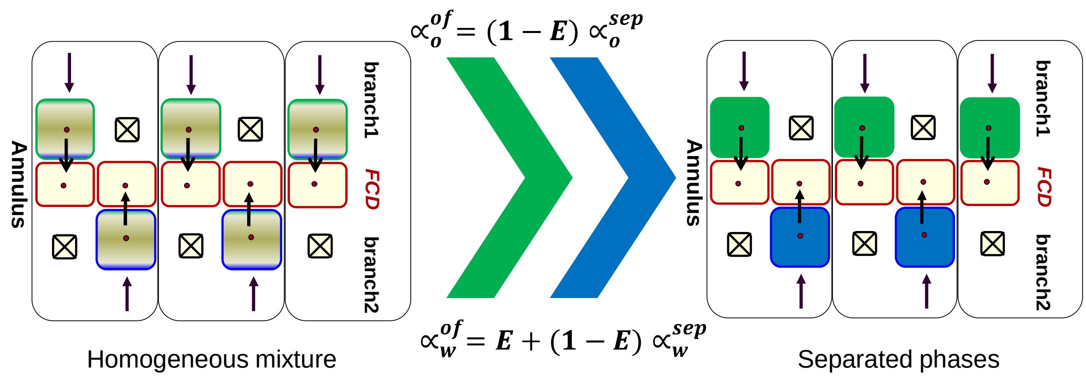

Figure 4-19: Theory of phase separation in a horizontal well section

The addition of this extra step allows the methodology to model the physics of segregated flow. This modification solves some of the modelling challenges discussed in section 4.1:

1) The fluid hold up, being one of the most important factors characterizing multiphase flow in wellbores [75], determines the fluid that the FCD responds to.
2) Improved multi-phase flow calculation model for stratified flow.
3) FCD locations are now included in Modelling Workflow {Figure 4-4 and Figure 4-10}.

4.4.3 Defining the Function of the Downhole MPF Separator

Any segment can be designated as a downhole separator. The downhole separator can separate water or free gas from the flowing mixture within the well, and send it along to another branch/segment. The separator segment should have [74]:

- An inlet segment, from which the well stream enters the separator, e.g. from a cell/connection.
- A water or gas offtake segment, for which the separated fluid (water or gas) is allocated based on the separation efficiency.
- An outlet segment, through which the remaining fluid is ought to continue its flow towards the wellhead.

The only action of the separator, as mentioned earlier, is to modify the content of the mixture flowing into the offtake branch through the separator offtake, increasing the fraction of the offtake's preferential phase. The fluid flow rate along the water/gas branch for the resulting well configuration depends on the:

1) Pressure in the segments.
2) Pressure in the tubing.
3) Pressure losses along the segments.
4) Performance of the segment's flow control device(s).
5) The inflow and outflow rates.

The holdup fractions $\propto^{of}$ of the mixture entering the offtake are calculated as a function of the holdup fractions $\propto^{sep}$ of the remaining fluid within the separator segment and a separation efficiency (E). For a water separator offtake the transformation is [74]:

$$\propto_{\mathrm{w}}^{\mathrm{of}} = \mathrm{E} + (1 - \mathrm{E}) \propto_{\mathrm{w}}^{\mathrm{sep}} \qquad \text{Equation 4-10}$$

$$\propto_{\mathrm{g}}^{\mathrm{of}} = (1 - \mathrm{E}) \propto_{\mathrm{g}}^{\mathrm{sep}} \qquad \text{Equation 4-11}$$

$$\propto_{\mathrm{o}}^{\mathrm{of}} = (1 - \mathrm{E}) \propto_{\mathrm{o}}^{\mathrm{sep}} \qquad \text{Equation 4-12}$$

Obviously, water cannot be taken off unless it is present within the separator. Hence "E" approaches zero as $\propto_{\mathrm{w}}^{\mathrm{sep}}$ approaches zero. This functionality is provided by keeping E as a constant (defined independently) when $\propto_{\mathrm{w}}^{\mathrm{sep}}$ is above a certain value $\propto_{lim}$ and letting E linearly approach zero when $\propto_{\mathrm{w}}^{\mathrm{sep}}$ falls below the value $\propto_{lim}$ as follows:

$$E = E_{max} \qquad when \quad \propto_{w}^{sep} > \propto_{lim}$$

$$E = \frac{\propto_{w}^{sep}}{\propto_{lim}} E_{max} \quad when \quad \propto_{w}^{sep} < \propto_{lim}$$ Equation 4-13

Where E_{max} is the maximum separation efficiency and $\propto_{lim}$ is the limiting holdup fraction below which the separation efficiency begins to decrease. E_{max} and $\propto_{lim}$ are constants defined for the offtake. The local volumetric flow rate of each free phase through the offtake is proportional to its holdup fraction $\propto^{of}$. The separator segment uses the homogeneous flow model, so all phases flow with the same velocity within the separator segment (not necessary for the other segments).

The flow of the remaining fluid flowing towards the wellhead is similar function of the holdup fractions of the fluid remaining within the separator ($\propto^{sep}$).

Gas separators act in a similar manner to remove free gas (**at the separator segment's pressure**) and send it preferentially into the offtake segment. They have an equivalent transformation of holdup fractions between the separator and the offtake [74]:

$$\propto_{w}^{of} = \mathrm{E} + (1 - \mathrm{E}) \propto_{w}^{sep}$$ Equation 4-14

$$\propto_{g}^{of} = (1 - \mathrm{E}) \propto_{g}^{sep}$$ Equation 4-15

$$\propto_{o}^{of} = (1 - \mathrm{E}) \propto_{o}^{sep}$$ Equation 4-16

where,

$$\mathrm{E} = \mathrm{E_{max}} \qquad \mathrm{when} \quad \propto_{w}^{sep} > \propto_{\mathrm{lim}}$$ Equation 4-17

$$\mathrm{E} = \frac{\propto_{w}^{sep}}{\propto_{\mathrm{lim}}} \mathrm{E_{max}} \quad \mathrm{when} \quad \propto_{w}^{sep} < \propto_{\mathrm{lim}}$$

The overall separation efficiency of the system is governed by the 'flow split', the fraction of the inflow that exits through the oil outlet. To explain the process, let us consider the behaviour of the model for a water separator (with E_{max} = 1.0) as the flow split is reduced by steadily increasing the flow rate through the water offtake. At low offtake rates, when the flow through the offtake is less than the inflow rate of water to the separator, the **offtake flow is 100% water**. The remainder of the water exits with the oil through the oil outlet. As the offtake flow increases towards the value of the water inflow rate, the water fraction flowing through the oil outlet decreases to a residual value that depends on

α_{lim}. As the offtake flow increases further to exceed the water inflow rate, the water fraction in the oil outlet remains at a residual value but there is an increasing carryover rate of oil through the water outlet. In general the smaller the α_{lim} value is, the more difficult it is for the well solution to converge [74].

As discussed earlier, the flow rate in the offtake branch depends on the pressure upstream and downstream of the segment and the pressure losses along the flow path. All these calculations are solved simultaneously in the wellbore (containing AFCDs) together with the reservoir model (appendix 3).

4.4.4 Case study (1): Impact of Segregated Flow on (A)ICD-completion Performance

The methodology detailed above has been implemented in the reservoir/well model developed in chapter 3 (model-OW). Comparison of the results from the following three completion modelling scenarios illustrate the impact of segregated flow on (A)FCD performance:

1) An upscaled wellbore model (1 FCD/segment that represents 2 physical valves)
2) A fine wellbore model (2 FCDs/segment)
3) A fine wellbore model with stratified flow (2 FCD/segment)

4.4.4.1 Passive FCD Performance in Segregated Flow Environment

Comparison of cases (1), (2) and (3) indicated that the inclusion of stratified flow in the coupled well/reservoir simulation model **did not** impact the results when a passive inflow control device was present in the well {Figure 4-20}. The figure shows the results for all three cases (ICD upscaled, ICD fine, and ICD fine with segregated flow) match one another. This is mainly attributed to the performance of the passive ICD, the nature of the modelled fluids (heavy oil and water only, no gas) and the performance model of the ICD restriction that was used in this simulation work.

Note that the flow through the ICDs is modelled using Equation 3-13 with a fixed flow coefficient (i.e. independent of Re). The modelled ICD performance is controlled by the density of the flowing fluid. Lauritzen and Martiniussen's, 2011 multiphase flow laboratory work indicated that the ICD flow coefficient is strongly correlated to both the Reynolds number and to the viscosity of the flowing fluid [93]. Passive-ICD modelling should be modelled with the relevant dependence on fluid viscosities as indicated from laboratory experiments. Furthermore, a similar comparison should be performed for gas, oil and/or water system with the observed physics being included in the extended MSW application.

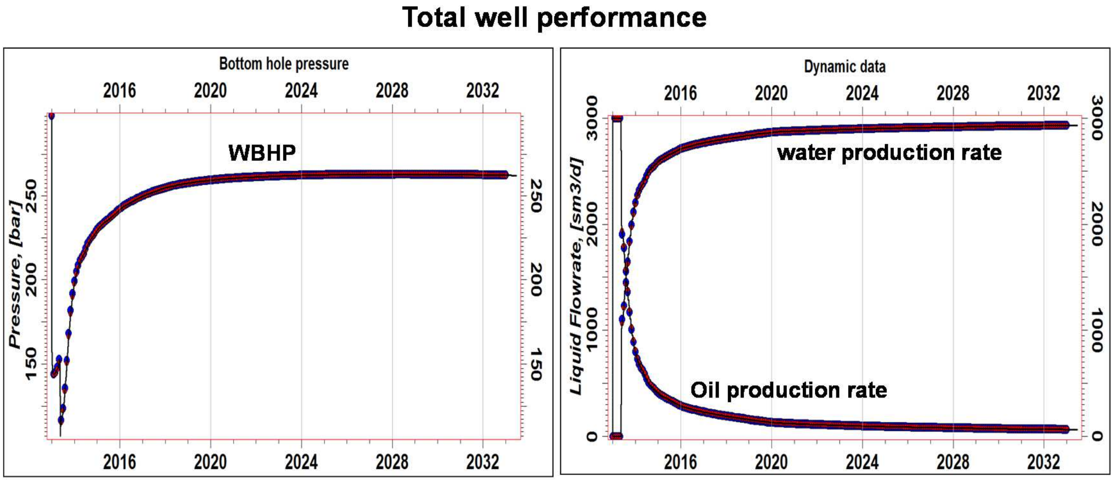

Figure 4-20: Passive FCD performance in segregated flow environment

Further investigation is required before a final conclusion can be drawn on the performance of Passive FCD in a stratified flow environment. However, the objective of the comparison above is (1) to model, a **phase insensitive** device and (2) to validate the modelled topology before a phase selective device is tested.

4.4.4.2 Active FCDs (e.g. AICD) Performance in Segregated Flow Environment

We will now investigate the performance of an active FCD. The Figure 4-21 results are found to be significantly different from the conventional, single axial segment modelling approach when AFCDs are modelled with the extended MSW approach. The results from the upscaled model and fine model match, while differences appear when stratified annulus flow is modified and the AFCDs located in the upper and lower wellbore segments react to different fluids {Figure 4-22}. This can be attributed to the active response of the AFCD to the fluid's viscosity. The viscosities difference were large in this case, resulting in a considerable deviation from the case when a simple homogeneous fluid was modelled.

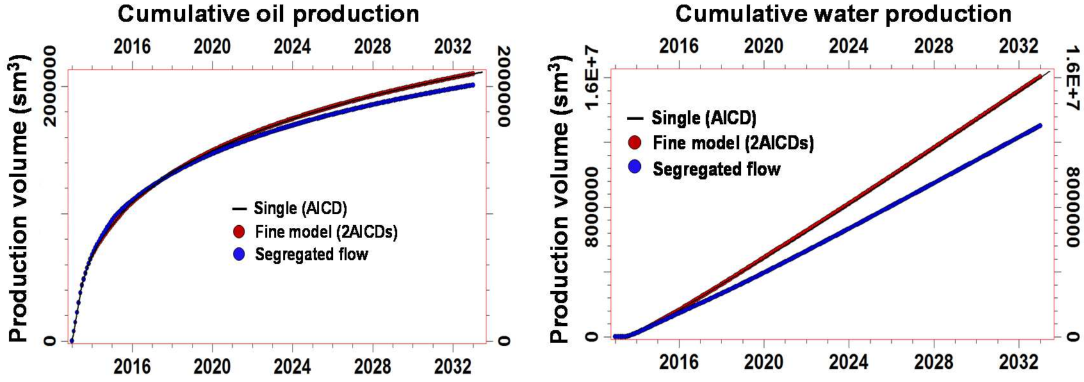

Figure 4-21: Active FCD (AICD) performance in a segregated flow environment

Allowing phase separation in the annulus of a perfectly horizontal well, as described above, is regarded as being a reasonable representation of stratified annulus flows. This allows the properties of the fluid flowing through an (A)FCD to be examined in greater detail since modelling of the performance of each individual AFCD can now be envisaged. Figure 4-22 represents the production from a "high rate" segment in which water breakthrough occurs after 6 months. Figure 4-22's examination of an individual segment's performance shows fluid separation (oil in the upper segment (US) and water in the lower segment (LS)). The single branch (homogeneous model) approach, on the other hand, approximates the solution of the Figure 4-10 scenario by simple averaging. This approximation is currently judged to be acceptable for passive FCDs; but as expected, the extended MSW modelling results will be considerably different when AFCDs are modelled.

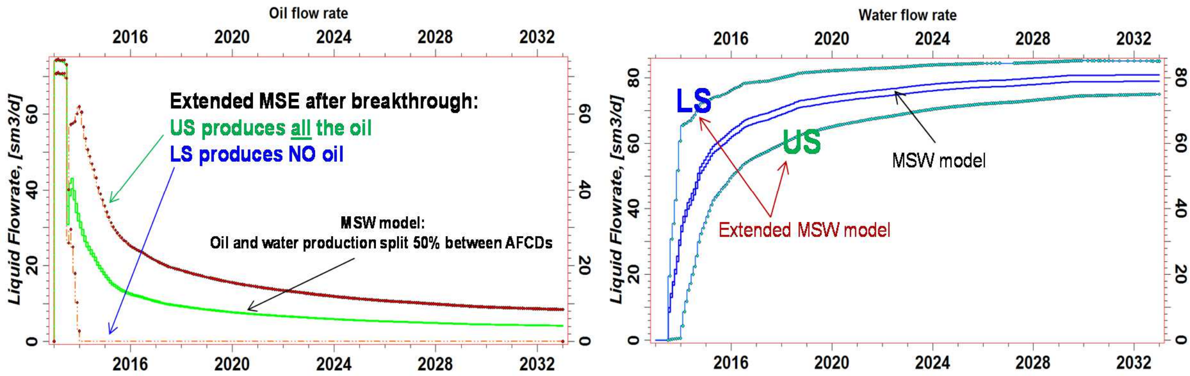

Figure 4-22: Analysis of the performance of a "high rate" two AFCDs segments completion

Figure 4-23 below shows the dynamic connection between the upper and lower segments. By looking at the water hold up we can see that both AFCDs may produce water at high water cuts with water only being produced through the low AFCD until the LS reaches its maximum capacity (hold-up=1). A further increase in the water production allows water to appear in the US which is then produced through the upper AFCD.

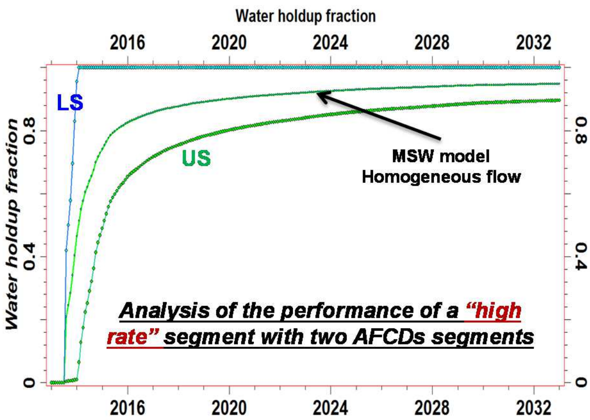

Figure 4-23: Water hold-up fraction of a "high rate" segment with two AFCDs segments

Figure 4-24 examines the performance of a low flow rate segment. The water breakthrough is delayed for 4 years. Initially the AFCDs located in the US and LS produce the same volume of oil (i.e. they are behaving as a passive FCD). The oil production decreases dramatically on water breakthrough due to the extra pressure loss across the LS AFCD caused by the presence of water. After breakthrough there is insufficient produced water to fill the LS (mostly water) segment, i.e. pressure calculations indicated that the maximum flow rate through the AFCD flow control device is greater than the current water production at the initial time steps. Therefore, some of well's total oil production is produced through the AFCD located in the LS; though the majority of the oil enters the tubing through the US which produces only oil. Later, the water cut increases and oil reduces due to an increasing water hold-up fraction. The US starts to produce some water once the LS is "full" (i.e. LS water hold-up fraction = 1). This situation occurs toward the end of simulation period, (the red circles in Figure 4-24).

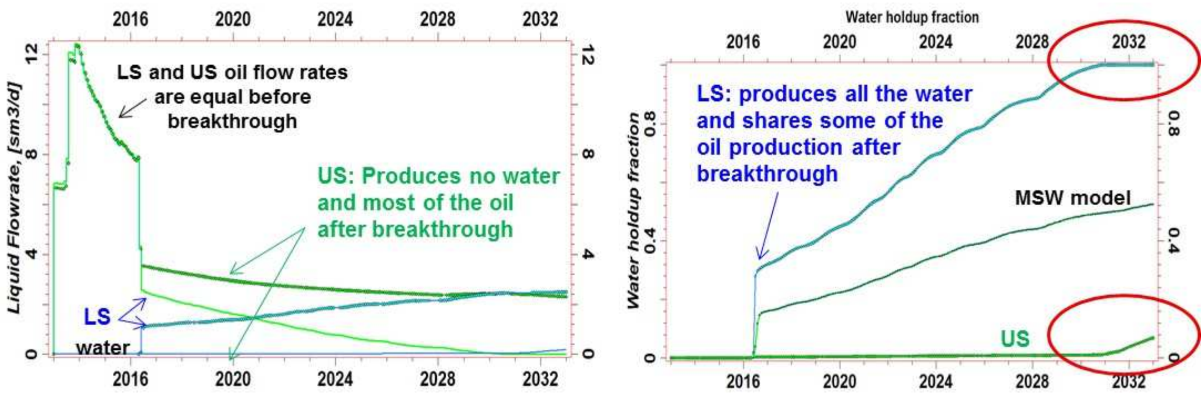

Figure 4-24: Analysis of the performance of a "low rate" segment with two FCD joints

4.4.4.3 Discussion

Initial studies of the extended MSW approach have shown it to be practical to implement within the Petrel-ECLIPSE suite of programs without adding an excessive computational overhead. One way to check the validity of the extended workflow was by obtaining very similar results to the conventional MSW when a single passive FCD was modelled within an isolated annular segment. It has also been shown that the performance of two passive FCDs located in the upper and lower portions of the wellbore produce 50% of the oil and 50% of the water that is flowing. These passive FCD results are due to the nature of the problem being modelled and the published performance equation ($\Delta p \propto (\rho, Q^2)$). Further investigation is required to reveal the impact of Re dependency on passive FCD-completion performance.

Modelling multiphase flow through AFCDs with the extended MSW approach shows their response to a dynamic water coning scenario is understandable. Hence the novel, extended MSW methodology is expected to give a greater insight into their performance.

The importance of this approach is that it allows us to study various scenarios that we were not able to study before given the conventional modelling techniques available. Example applications:

(a) Explicit modelling of the AICVs with 98% threshold was not possible. Tables specifying the conditions at which the AICV should react (shut) were used without direct implementation of the 98% threshold within the software solution. Being able to explicitly apply an AFCD threshold (e.g. 98% for AICVs) is quite important since it would allow exploring the next uncertainty;

(b) What if the valve threshold is not 98%? How does that affect the results?
The impact of relative permeability/outflow performance associated with the action threshold.

(c) Studies for ICV reactive optimisation shows that, the optimum threshold at which the ICVs react to unwanted fluid (e.g. water) depends on (1) the ability of other zones to "at least" replenish the lost oil production by closing a specific zone while trying to control the water, (2) the outflow performance – the well will continue to flow and (3) the changes in flow conditions with time.
Therefore, for a well completed with AICV each zone should have its own threshold and this threshold will change over time.
Hence the question to investigate: Is a fixed threshold along the entire well optimum enough?

(d) Does the wellbore WC thresholds of 25%, 33%, 50%, 98% - still hold? How does it change with changing valve threshold? And what if an AICD with a continuous MPF performance is tested and not an AICV with a specific reaction to one MPF condition.

Next we validate the extended MSW model against the published AICV data.

4.4.5 Case study (2): Extended MSW Model Matches AICV-completion Performance

Aakre, H., et al., 2014 have proposed a specific closing sequence for AICVs sharing the same annulus between two packers [85]. The published performance was based on the flow loop tests commenced for AICV performance. Table 4-11 provides the published closing sequence for 4 valves sharing one annulus.

Table 4-11: published closing sequence for 4 valves sharing one annulus in O/W system [85]

Number of valves open with oil	Number of valves Starting to close (more than 98% water and less than 2% oil)	Number of valves closed	Water Holdup/critical water cut (CWC)
4	1	0	0.2
3	1	1	0.25
2	1	2	0.33
1	1	3	0.50
0	1	4	0.98

This is also depicted in Figure 4-25. At time zero (initially) only oil is flowing and the four valves are open for flow. Once water arrives at the completion, fluid separation takes place in the annulus and the bottom valves will start receiving water and the other three valves will be flowing only oil (depending on the amount of water received and the flow conditions). Based on the AICV tested reaction, the four valves will maintain the open position until time (1) is reach at which the 98% threshold is reached at the bottom valve and it starts closing whereby the resistance to flow will increase and the water will start rising to the next top valve (valve 2). The same sequence of closure is repeated until all of the 4 valves are fully immersed in water and therefore remain in the "OFF" position unless they started to see oil again (Note: the valves are reversible). Importantly, from Table 4-11 the inflow from the reservoir at which the threshold is met for each valve to start shutting is observed to be 25%, 33%, 50% and 98 % for oil water system.

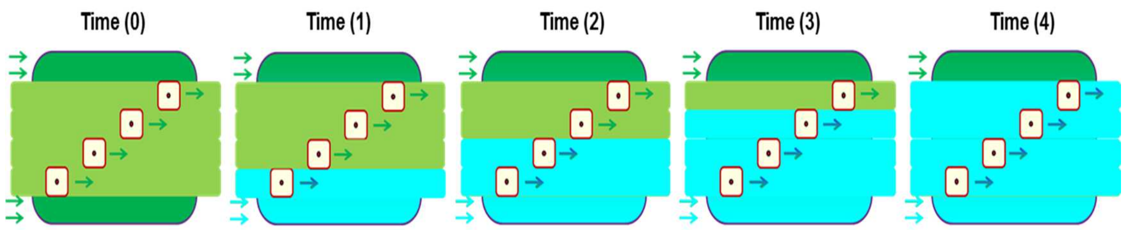

Figure 4-25: Illustration of fluid separation in the annulus and the closing sequence for 4 AICVs sharing one annulus

The expected impact of the flow performance described above {Figure 4-25} on the water cut performance through each valve is depicted in Figure 4-26. Valve-1 takes the full strength of water encroaching in the completion, hence depending on the amount of water a steep increase in the WC flowing through this valve is expected. Note that the water breakthrough here is not controlled. Once AICV-1 starts to react, the total inflow of this section will drop since less flow area is available. Hence the flow of water to the second valve, AICV-2, is expected to be with lower slope compared to the first valve. This sequence is then repeated in the remaining valves as depicted in Figure 4-26.

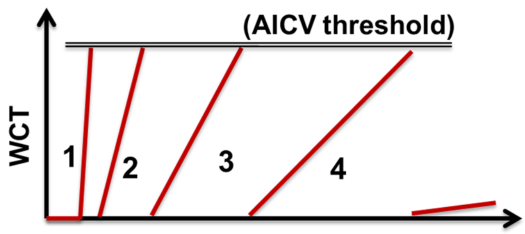

Figure 4-26: The expected impact of the multiple AICV flow performance on the water cut performance through each valve.

For gas system, the same observations were made and the results are tabulated in Figure 4-5 with differences in the inflow values from the reservoir at which the threshold is met for each valve to start shutting.

Table 4-12: Table 4-13: published closing sequence for 4 valves sharing one annulus in O/G system [85]

Number of valves to close (more than 98% Gas based on laboratory experiments)*	Number of valves closed	Critical Gas Volume Fraction (GVF)
5 Open	0	< 0.4
4 Open	1	0.43
3 Open	2	0.50
2 Open	3	0.60
1 Open	4	0.75
All Closed	5	> 0.98

4.4.5.1 4 AICVs Sharing the Same Annulus Flow Conditions

The discretised segregated annulus flow model is validated (next) against the published AICV-completion performance (described above) in different scenarios.

4.4.5.1.1 Oil/Water Systems

4.4.5.1.2 Model Description:

The situation described above is included/tested within Model-X2 (details in chapter 3) wellbore model.

4.4.5.1.3 *Wellbore Description:*

- 4 AICVs/50 m, 96 AICVs installed in total, with 98% unwanted fluid valve shut-in threshold.
- Packer every 50 m. 4 AICVs share each annular section along the wellbore.
- Discretised segregated annulus flow model is applied (details above).

4.4.5.1.4 *Results for an Oil/Water System*

First we highlight that the expected performance described in Figure 4-26 was observed. In Figure 4-27 the WC performance of 4 valves is depicted showing diminishing water development.

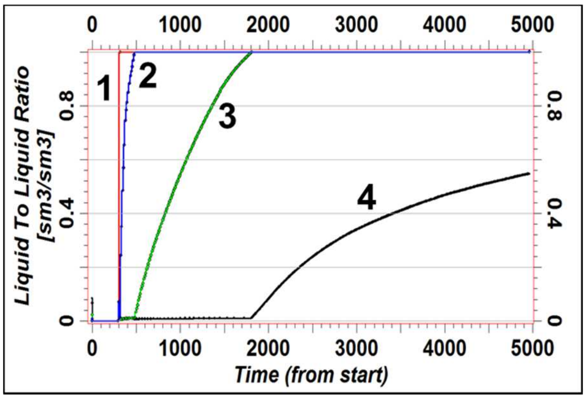

Figure 4-27: The water cut performance through the AICVs in model-X2 with stratified flow in the wellbore

We studied the inflows from the reservoir at which the individual valve threshold (98%) is met for each valve based on its location (for all the sections in the well). The exact same AICV data published observed for all the valves as shown in Figure 4-28 [85]. In this figure, the first valve in each wellbore section separated by packers is observed to reach the 98% threshold at a water influx from the reservoir of 25%. Likewise, 33%, 50% and 98% were observed for the second, the third and the forth valves respectively.

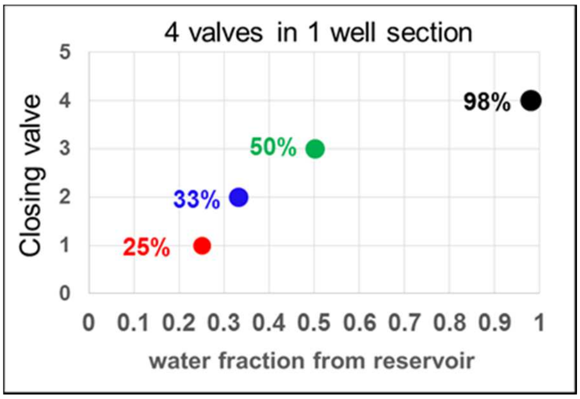

Figure 4-28: Reservoir water influx at which the 4 AICVs in each section of the well is closed individually

4.4.5.1.5 *Oil/Gas Systems*

4.4.5.1.5.1 *Model Description:*

Similarly, using Model case 3 (described in chapter 3), the same study as above is conducted for oil/gas system and the gas volume fraction in the annulus was observed.

4.4.5.1.5.2 *Wellbore Description:*

- 4 AICVs/50 m, 230 AICVs in total installed, with 98% unwanted fluid shut-in threshold for the valve.
- Packer every 50 m. Every 4 AICVs share one annulus section along the wellbore.
- Discretised segregated annulus flow model is applied (details above).

4.4.5.1.5.3 *Results for an Oil/Gas System*

The GVF performance for one completion section (between two packers) is depicted in Figure 4-29. The gas influx (volume fraction) from the reservoir at which each AICV is activated, is obvious from the GVF response.

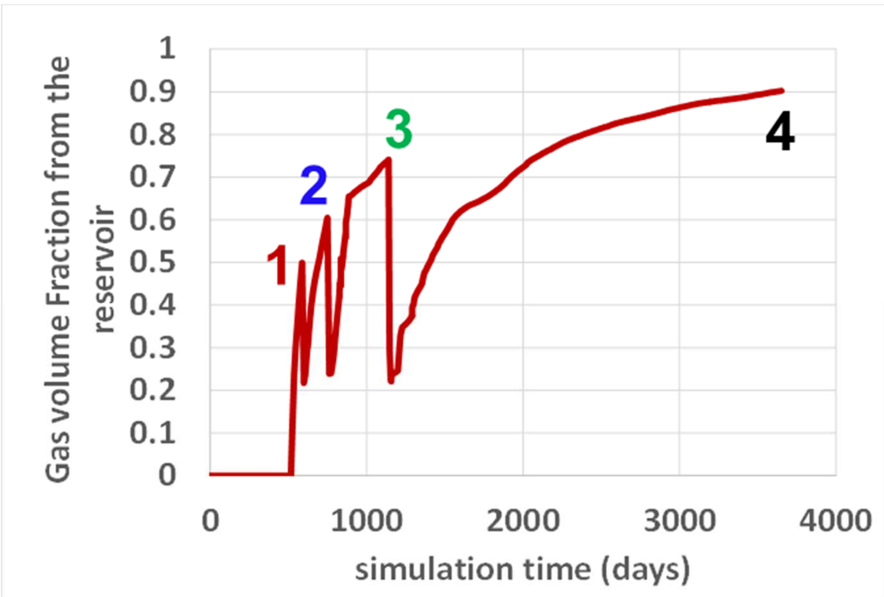

Figure 4-29: The GVF performance through the AICVs in model-GO with stratified flow in the wellbore

The annulus threshold values for AICVs' reaction to gas were also found to be matching with the published AICV performance for all segments {Figure 4-30}.

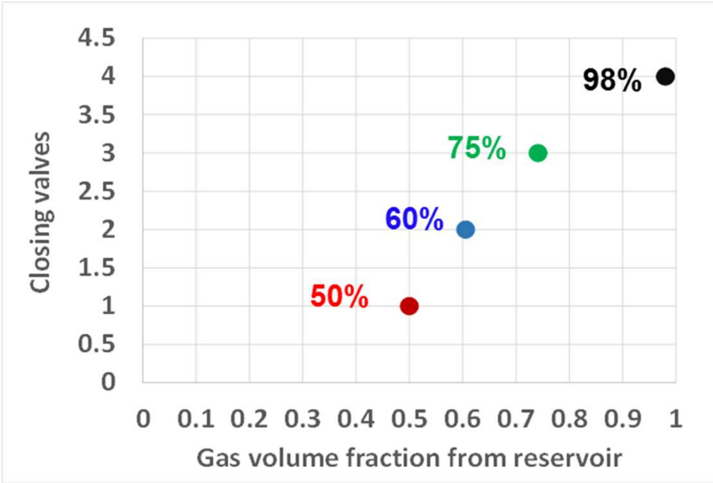

Figure 4-30: Reservoir GVF at which the 4 AICVs in each section of the well is closed individually

Considering that:

(a) The AICV resulting thresholds were defined experimentally, as a consequence of the AICV design, i.e. not consistently designed for.

(b) The AFCDs' designs, in general, can be manipulated in terms of the numbers to be deployed in any completion as well as the AFCDs' dimensions (initial size and the required resistance to unwanted fluids).

Then, the validation above shows that, the proposed model can be used for further investigations to answer several questions as discussed in section (4.4.4.3), to unveil the ambiguity surrounding what can be an optimum AFCD design. Below, several examples of such analysis are provided (see also chapter 5 optimisation study).

4.4.5.2 Is a 98% Threshold Device Optimum?

We will now check the impact on the flow performance with different thresholds, e.g. 95%, 90 % and 80% with respect to improved oil production as the objective function.

4.4.5.2.1 Example (1)

4.4.5.2.1.1 Model Description:

Model X2 (described in detail in chapter 3).

4.4.5.2.1.2 Wellbore Description:

- 4 AICVs/50 m, 96 AICVs in total installed, with 98% unwanted fluid valve shut-in threshold.
- Packer every 50 m. 4 AICVs share each annular section along the wellbore.
- Discretised segregated annulus flow model is applied (details above).

4.4.5.2.1.3 *Example (1) Results*

Figure 4-31 compares the three cases to the 98% case. The well BHP is different, as pictured. The sharper the threshold the higher the pressure loss across the completion at the sections where unwanted fluids are observed (the red lines in the figure). The vertical lines in Figure 4-31, define the times at which a device is active (shut), i.e. where the specified threshold is met for each individual valve.

Now comparing the oil production from the three cases (98%, 95% and 90%), Figure 4-32 shows that the 95% threshold case produced the highest amount of oil. This is expected since it imposes additional pressure drop as compared to the 98% threshold and at the same time continued to produce with a fixed liquid rate. Hence more control on the water production. The 90% threshold case, unlike the 95% case, did impose an additional pressure such that the well's outflow capability is jeopardised and the minimum lifting pressure limit is reached followed by the control changing to BHP control, resulting in a total loss in production (both oil and water).

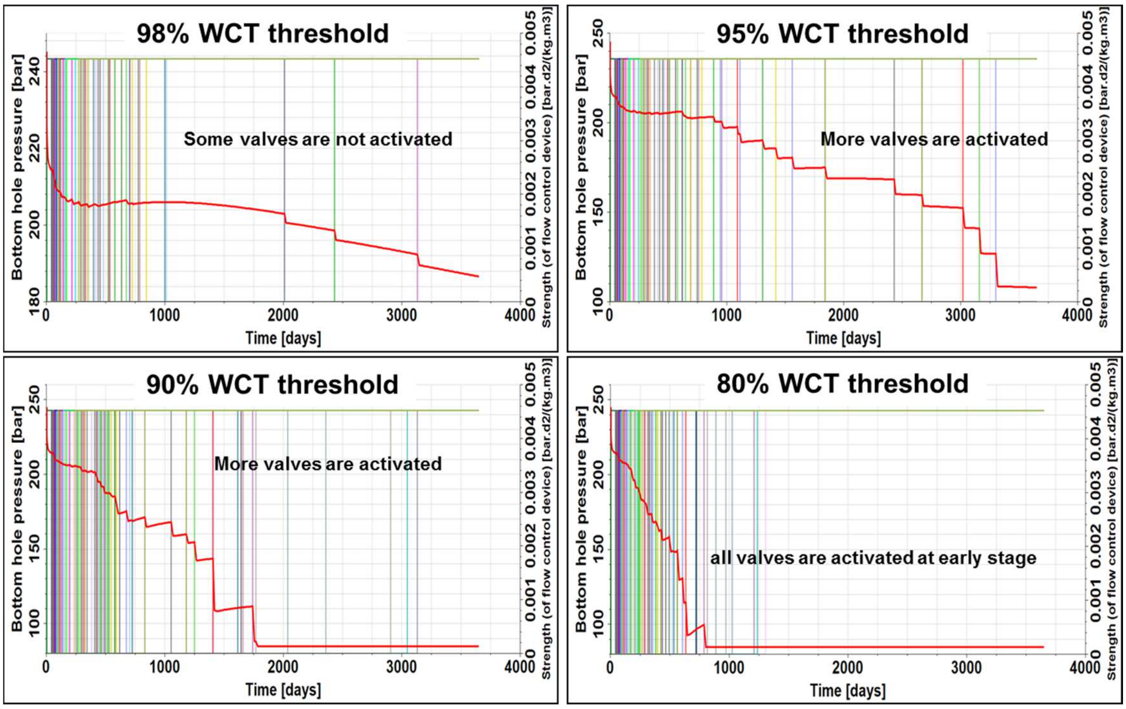

Figure 4-31: Model-X2 BHP and the valves performance tested with different thresholds, 98%, 95%, 90 % and 80%

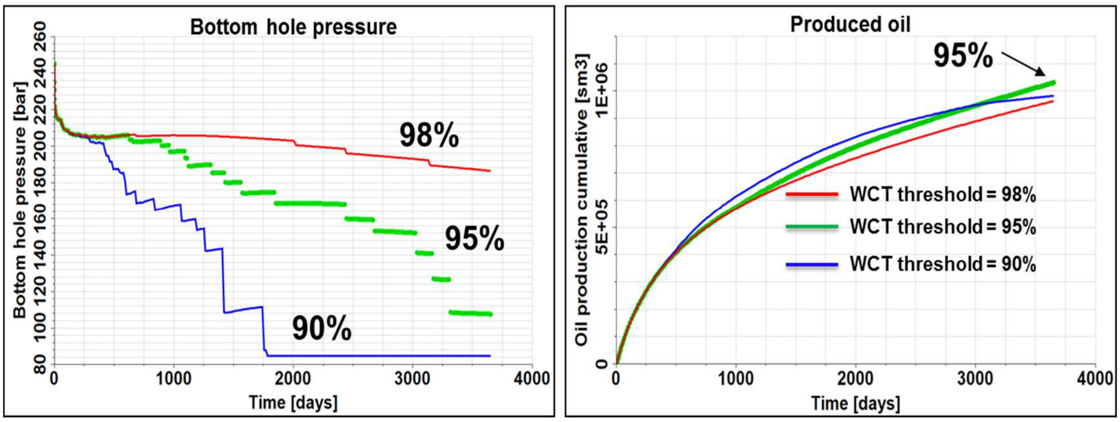

Figure 4-32: Model-X2 BHP and total oil produced considering 98%, 95%, 90 % thresholds for the AICV completion

From here we can see that the 98% unwanted fluid threshold is not always the optimum – it is case specific and it depends on field properties/conditions, zone and time parameters. The critical (optimum) water cut actually depends on variables defining Equation 4-18 [35]:

a) How much oil is lost in the zone of concern?
b) The productivity and water cut for all other zones (i.e. can they "at least" repay the oil lost in point "a" above).
c) The impact of shutting this zone on the outflow performance.
d) The reservoir performance with time (it changes with flow condition which in turn is varying with time). An example formula for critical WC defined by outflow well performance is shown below [35]:

$$WC_n \geq 1 - \frac{\Delta P_{BHP} \sum_{i \neq n}^{N} J_i (1 - WC_i)}{J_n . dP_n} \qquad \text{Equation 4-18}$$

Where, ΔP_{BHP} is the change in the bottom hole pressure and J_i is the productivity index of zone i, $i \in (1..N)$ number of production zones - each of which is separately controlled, n is the zone to be controlled.

The optimum shut-in threshold is case specific/zone specific. However, is it always the case that applying high resistance to unwanted fluid can improve the oil production as long as the outflow performance is not jeopardised? Grebenkin, I.M., 2013 [35] showed that this may not be the case if GOR or fluid density of various production intervals are significantly different (e.g. over 400 scf/b difference for GOR). The next section shows another example designed to illustrate a scenario where this may not be the case.

4.4.5.2.2 Example (2)

In example (1) above, we have shown that with increasing flow resistance to water, above the outflow constraint, the oil is improved. In here we illustrate that this is not the case always. Even above the BHP constraints, un-optimised higher resistance may lead to restricting oil more than water especially in heavy oil environment. According to relative permeability: to produce oil, the completion needs to tolerate some amount of water production (usually referred to as good water).

4.4.5.2.2.1 Model Description:

The aquifer support, in model-OW, has been improved high enough to overcome the limitation of the AICV control applied at breakthrough on the outflow performance. Different AICV thresholds were then applied (98%, 90% and 80%).

4.4.5.2.2.2 Wellbore Description:

- 4 AICVs/50 m, 184 AICVs installed in total, with 98% unwanted fluid valve shut-in threshold.
- Packer every 50 m. 4 AICVs share each annular section along the wellbore.
- Discretised segregated annulus flow model is applied (details above).

4.4.5.2.2.3 Example (2) Results

In Figure 4-33 three thresholds are presented. The 98% AICV threshold is found to be the optimum for this case as applied for all the valves and not selectively different. Whereas, increasing the flow resistance by the applying 90% and 80% thresholds results in a lower oil production for the same liquid flow. This is because the sections which are producing higher amount of liquid (consequently higher water) are strictly controlled at early stage allowing the other sections (with lower productivity) to produce oil and water as long as the threshold is not met. This is a clear example showing that one threshold **applied to all sections** may not be the global optimum and also increasing the resistance to water without optimisation may hinder the maximum oil recovery objective considerably.

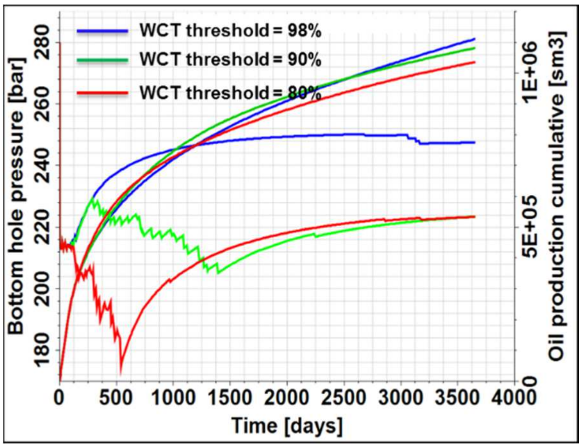

Figure 4-33: Model-OW, with increased aquifer support, BHP and total oil produced considering 98%, 95%, 90 % thresholds for the AICV completion

4.4.5.3 Simplified AICV wellbore model

A simplified (upscaled) wellbore model can be used in full field simulation studies incorporating the exact performance understood from the detailed model for any shut-in threshold. Figure 4-34 gives the exact performance of the detailed wellbore model produces with the upscaled model for 98% AICV threshold. Similarly, Figure 4-35 for 95% AICV threshold. In some cases the detailed model is found to be easier to solve. It depends on the number of valves and reservoir model complexity.

The “upscaled” wellbore description (model X2):

- 1 AICV/50 m, 24 AICVs installed in total, with any shut-in threshold for unwanted fluid flow.
- Packer every 50 m.
- Discretised segregated annulus flow model is applied “implicitly” using multi-dimensional tables (described in chapter 3).

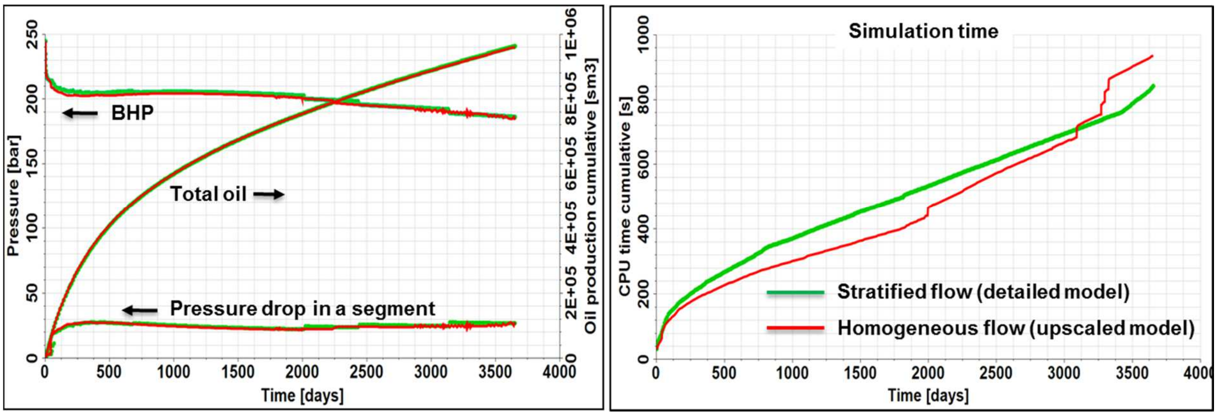

Figure 4-34: Model X2, upscaled wellbore model example with 4 valves compared with 1 valve (98%) threshold device simplified model

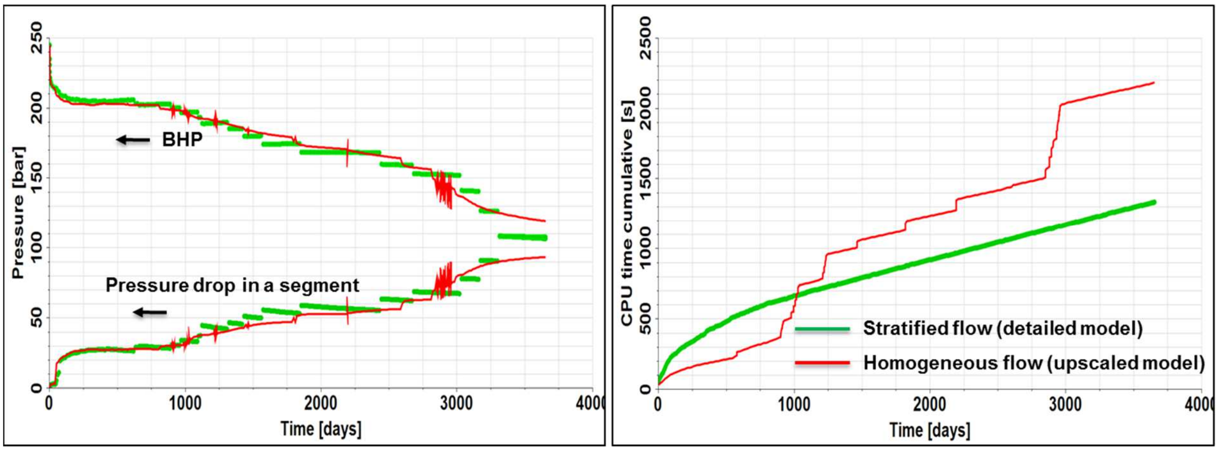

Figure 4-35: Model X2, upscaled wellbore model example with 4 valves compared with 1 valve (95%) threshold device simplified model

4.4.6 Case study (3): Impact of Segregated Flow on AICD-completion Performance

4.4.6.1 Model Description:

The same methodology of discretised wellbore with segregated flow is applied to model X2 with a horizontal well completed with AICDs.

4.4.6.2 Wellbore Description:

- 4 AICDs/50 m, 96 AICDs in total installed.
- Packer every 50 m. 4 AICVs share each annular section along the wellbore.
- Discretised segregated annulus flow model is applied (details above).

4.4.6.2.1.1 AICD-completion Results

Different annulus WC thresholds were observed, depending on the level of AICD restrictive performance applied. Table 4-14 and Figure 4-36 show the modelling parameters and the resulting performances for AICD1 and AICD2 employing Equation 3-12. Completions employing AICD1 and AICD2 were tested.

Figure 4-37 shows: 16%, 30%, 54% and 1% reservoir water influx thresholds for AICD1 design (one section across the well is depicted). AICD2's greater restriction results in a sharper growth of water in the annulus, e.g. 10%, 13%, 20% and 1% annulus thresholds for reaching the water mode for valve 1, 2, 3, and 4 respectively {Figure 4-38}.

Table 4-14: Arbitrary AICD designed tested in a stratified flow environment

Parameter	AICD1	AICD2
a_{AICD}	0.0000235	0.0044
X	2	2
Y	0.3862	1.3728

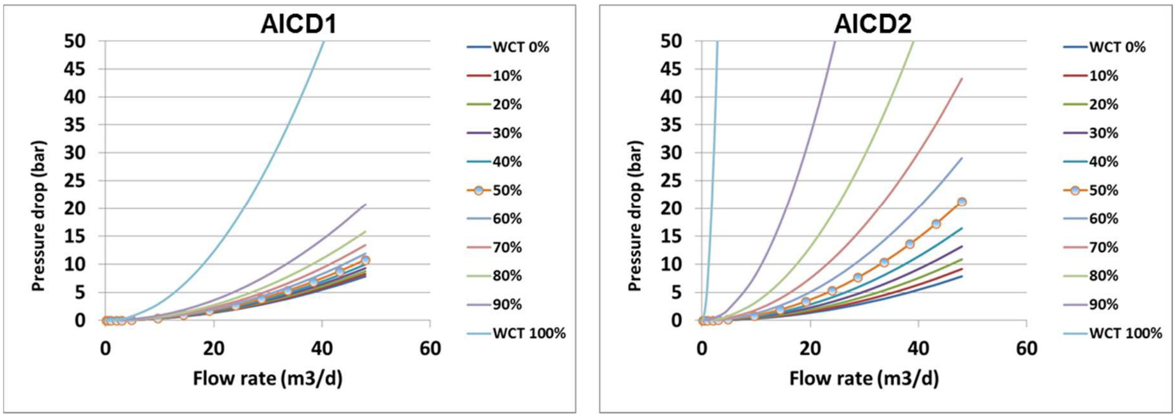

Figure 4-36: pressure drop vs. flow rate performance for AICD1 "restrictive to water" and AICD2 "less restrictive to water"

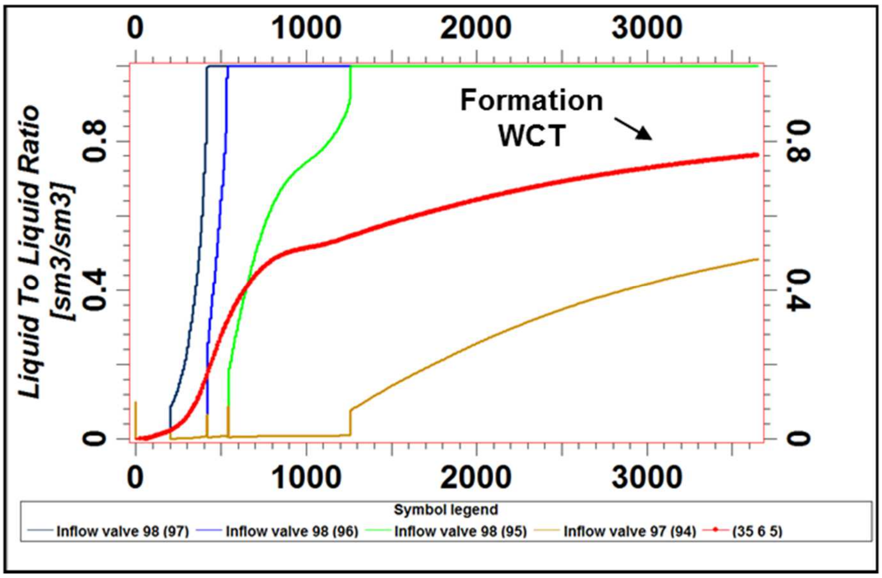

Figure 4-37: model X2 with a horizontal well completed with AICD1

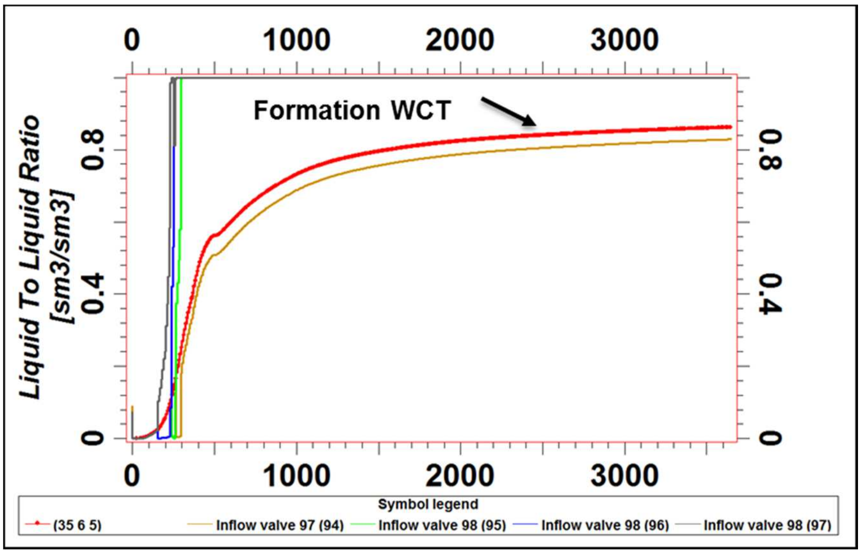

Figure 4-38: Model X2 with a horizontal well completed with AICD2

Figure 4-39 describes the performance of AICD1-completion when one of the main contributing sections of the wellbore had three of the valves changed to water mode (the performance of the section is shown in Figure 4-37). A shift in the BHP (outflow) performance was observed following the AICDs reaction to water. This has also impacted fluid movement within the reservoir as observed by the streamlines illustrated in Figure 4-40.

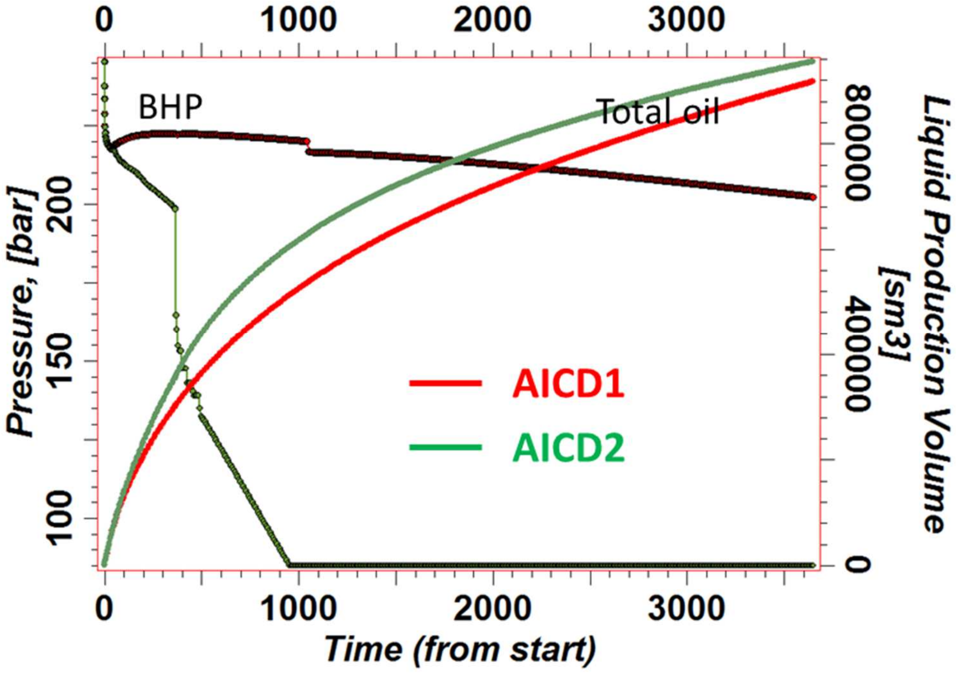

Figure 4-39: AICD1 vs. AICD2 completion performance under segregated flow environment

A considerable difference in the outflow performance is observed between the two AICD designs examined {Figure 4-39}. The oil produced for AICD2 is initially higher, but diminishing after the start of the autonomous reaction to water, due to the outflow constraints being jeopardised. This is not the case for AICD1 completion.

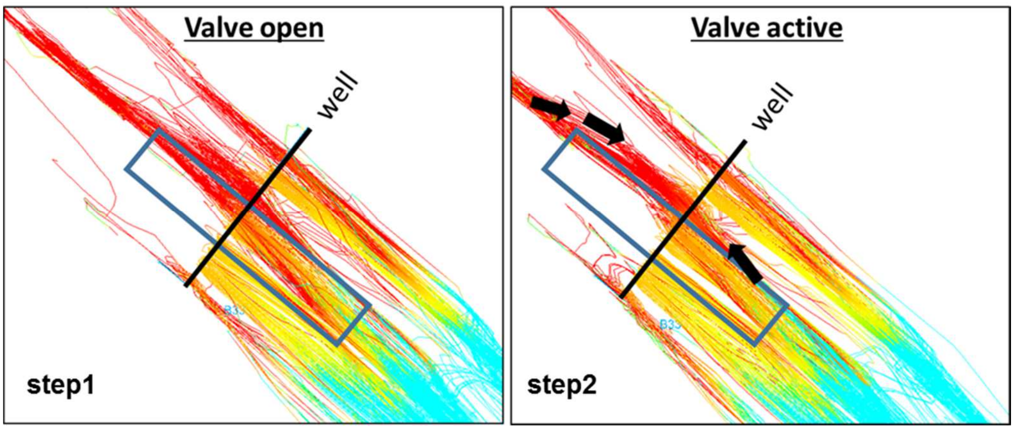

Figure 4-40: Model X2 well reservoir interaction in with AICD1-completion

4.4.6.2.1.2 Comparing AICD-completion Results with and without Stratified Flow

To illustrate the impact of the modelling methodology, we now compare the above results for AICD1 and AICD2 completions with stratified flow against a case where homogeneous fluid flowing through the valves is applied.

For AICD1-completion: the total wellbore performance (BHP and oil produced) shows a small differences between the conventional wellbore model and the stratified flow model {Figure 4-41}. However, a considerable difference is observed at the valve level after the water breakthrough {Figure 4-42}. Please note both modelling methods exhibit same performance before breakthrough.

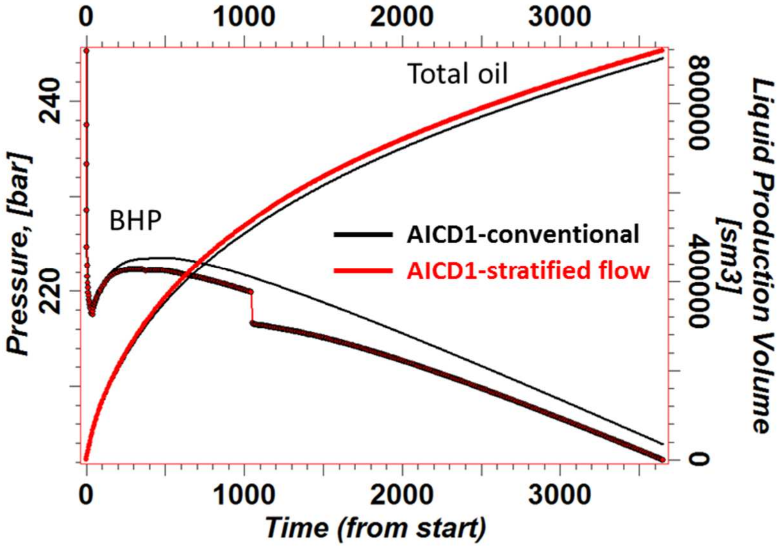

Figure 4-41: AICD1-completion total wellbore performance (BHP and oil produced) for the case of conventional wellbore model vs. the stratified flow model

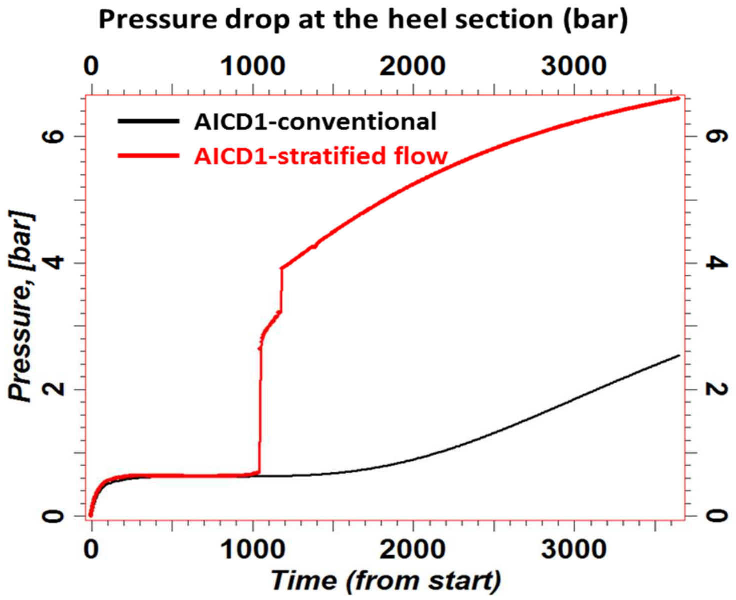

Figure 4-42: AICD1 individual valves performance exhibit large differences for the case of conventional wellbore model vs. the stratified flow model

For AICD2-completion: Both the total wellbore performance (BHP and oil produced) and the individual valve performance exhibit large differences {Figure 4-43 and Figure 4-44}.

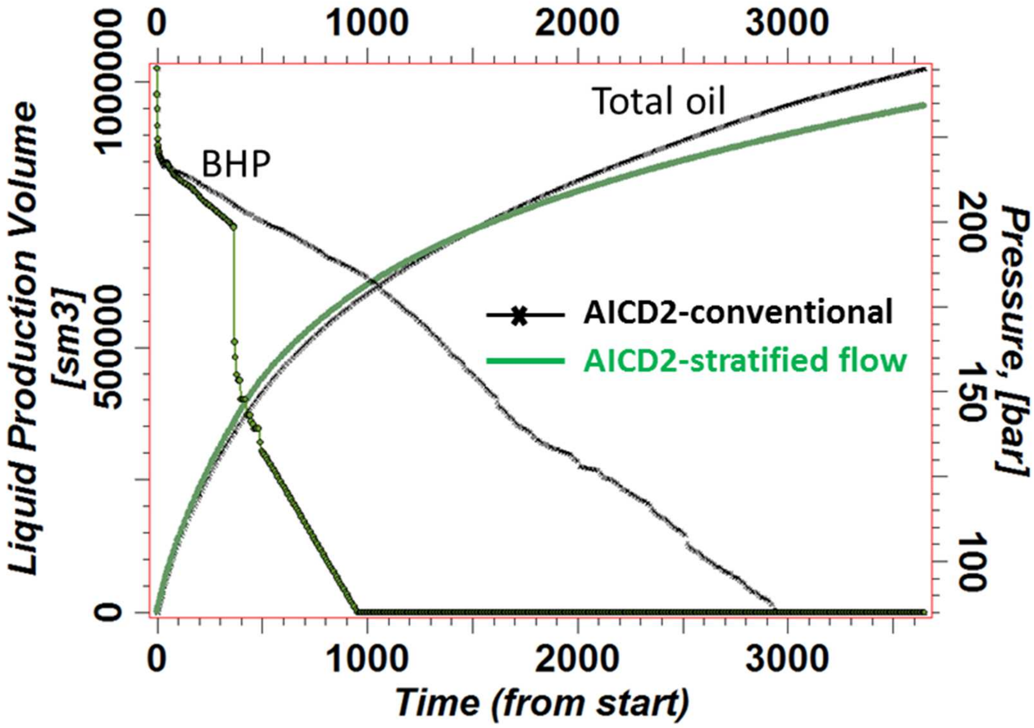

Figure 4-43: AICD2-completion total wellbore performance (BHP and oil produced) for the case of conventional wellbore model vs. the stratified flow model

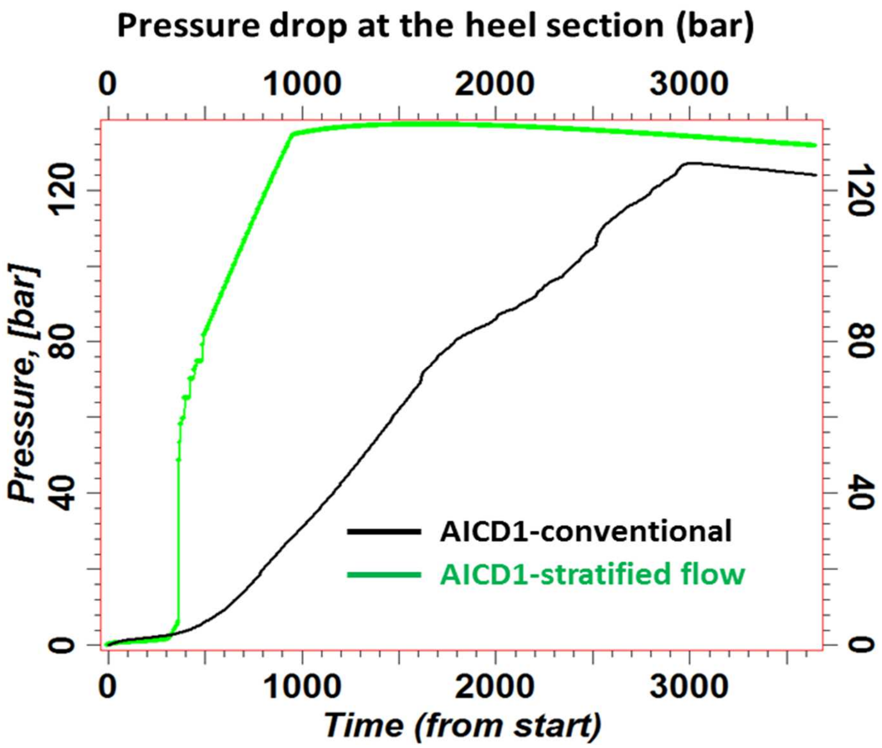

Figure 4-44: AICD2 individual valves performance exhibit large differences for the case of conventional wellbore model vs. the stratified flow model

4.4.7 ICD, AICD and AICV completions compared for water-influx behaviour

Figure 4-45 to Figure 4-49 illustrate further comparison was made (in model OW) between four completions scenarios: (a) 4AICVs with stratified flow, (b) 4AICDs with stratified flow, (c) upscaled AICD completion without stratified flow, and (d) Passive ICD completion. The impact of the completion option and the modelling method on water influx from the reservoir into the wellbore was examined to study the water encroachment and control at various points along the wellbore for the tested completions. All completions were designed to provide the same level of resistance for oil flow. The AICD and AICV completions are designed to provide the same reaction to 100% water flow.

Figure 4-45 and Figure 4-46 shows the water influx from the reservoir into the wellbore at the third and fourth simulation steps (i.e. after 3 and 4 months respectively). The water encroaches at the heel and the high permeability layer in the middle of the well. The ICD completion, of the same initial size, allow the water to flow with no restriction while different levels of water control were applied by the AFCD completions.

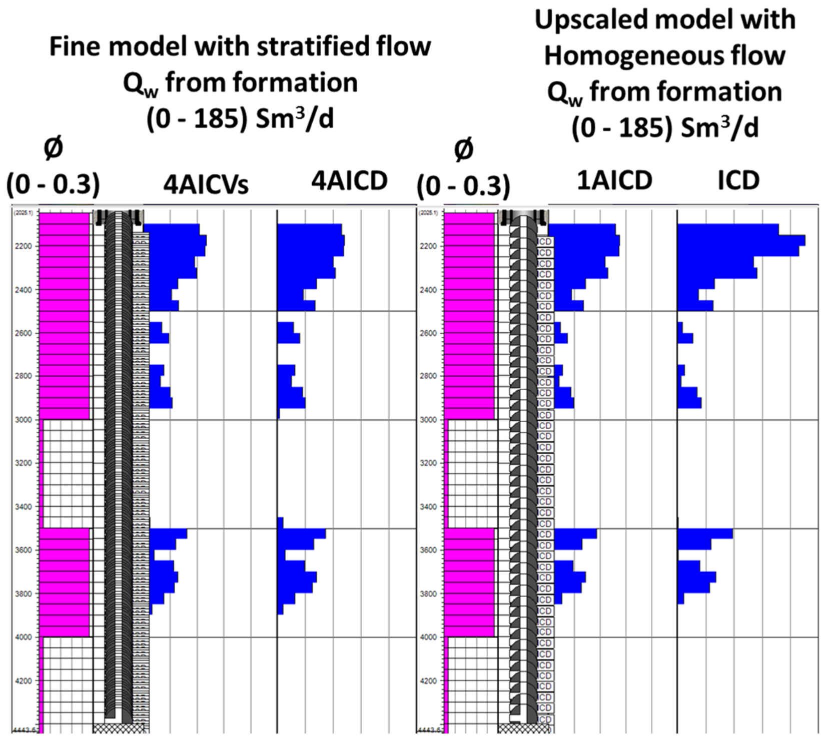

Figure 4-45: The water influx from the reservoir into the wellbore at the third simulation step (i.e. after 3 months) for AICV, AICD and ICD completions

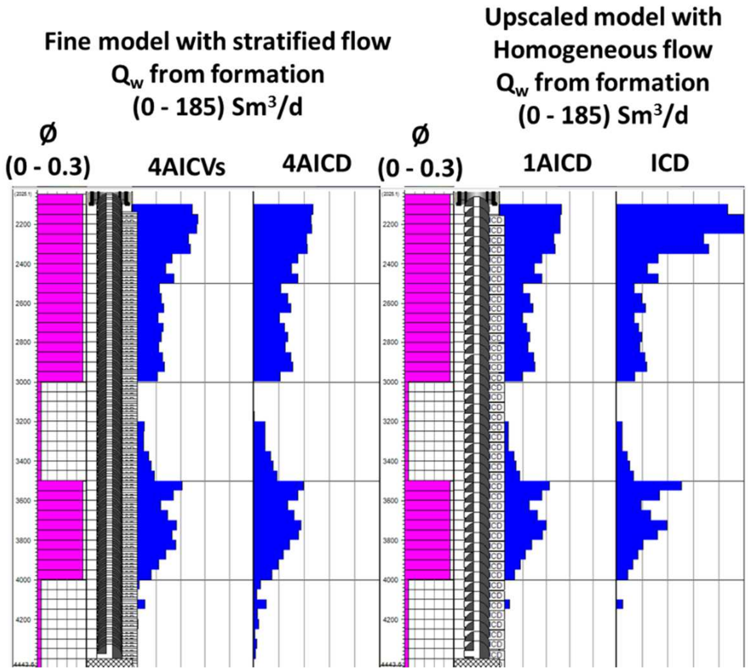

Figure 4-46: The water influx from the reservoir into the wellbore at the fourth simulation step (i.e. after 4 months) for AICV, AICD and ICD completions

In Figure 4-47 and Figure 4-48 after 30 and 100 months, respectively, most of the wellbore sections are producing water. The AICV-completion, show a very different performance than the AICD-completion that was designed to have the same initial and final responses to oil and water as the AICV completion does.

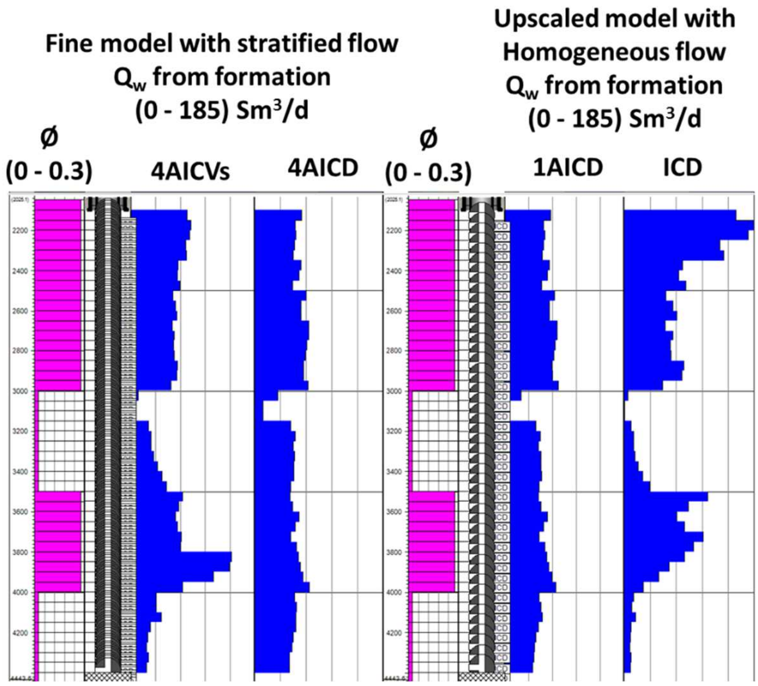

Figure 4-47: The water influx from the reservoir into the wellbore at the 30th simulation step (i.e. after 30 months) for AICV, AICD and ICD completions

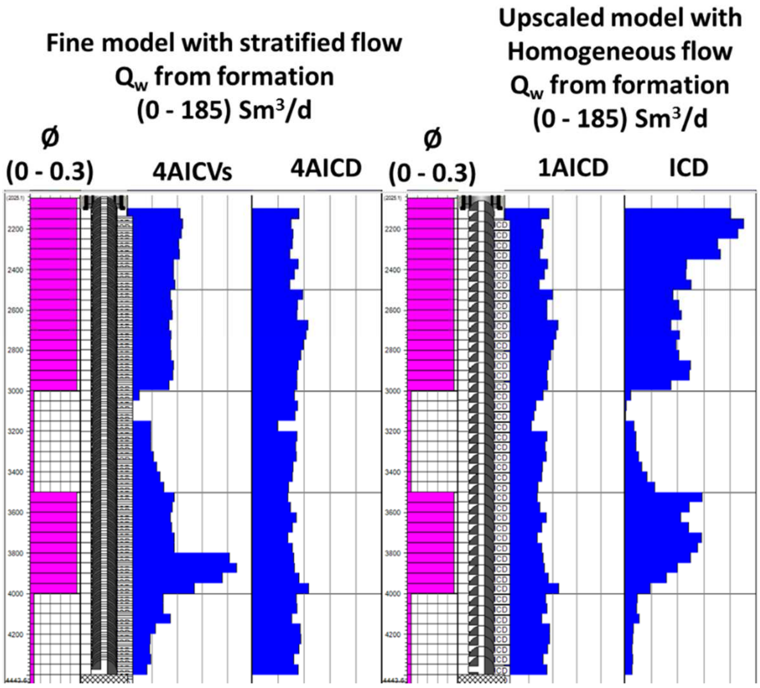

Figure 4-48: The water influx from the reservoir into the wellbore at 100 simulation step (i.e. after 100 months) for AICV, AICD and ICD completions

For the AICV-completion, several locations along the wellbore are shut almost completely. This has encouraged both oil and water to flow to other locations along the wellbore as depicted in Figure 4-49.

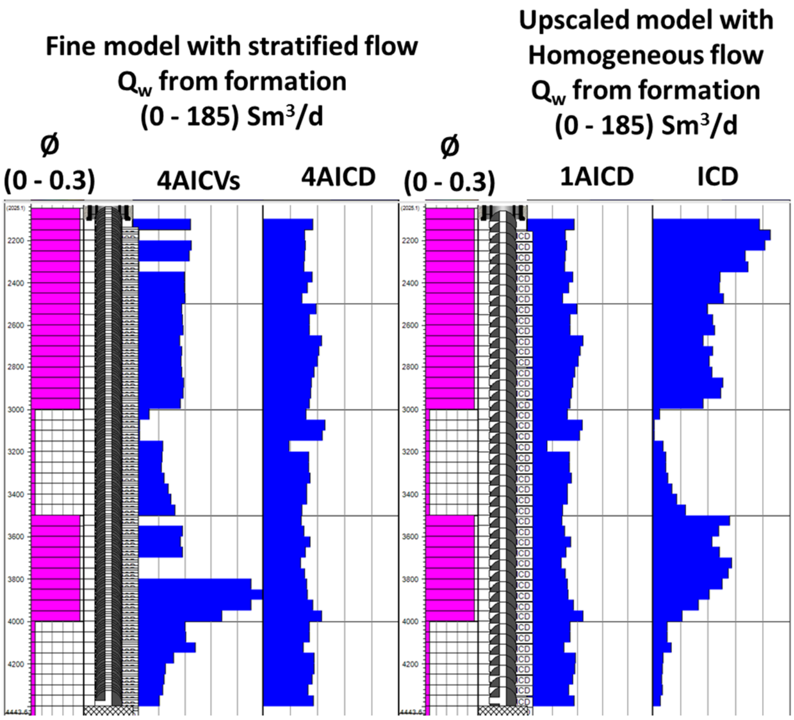

Figure 4-49: The water influx from the reservoir into the wellbore at the final simulation step (i.e. after 122 months) for AICV, AICD and ICD completions

In the figures discussed above, similar (minor differences) water influx performance was observed between the AICD cases (upscaled vs. stratified model). Whereas a considerable differences observed in the pressure response. An example pressure drop across one of the completion sections is provided in Figure 4-50. The BHP well performance with AICD completions modelled with and without stratified flow is provided in Figure 4-51. All the scenarios exert the same resistance to oil (initial pressure drop and BHP is exactly the same). However, considerable differences in completion performance upon breakthrough resulted. The AFCD optimisation is discussed in chapter (5).

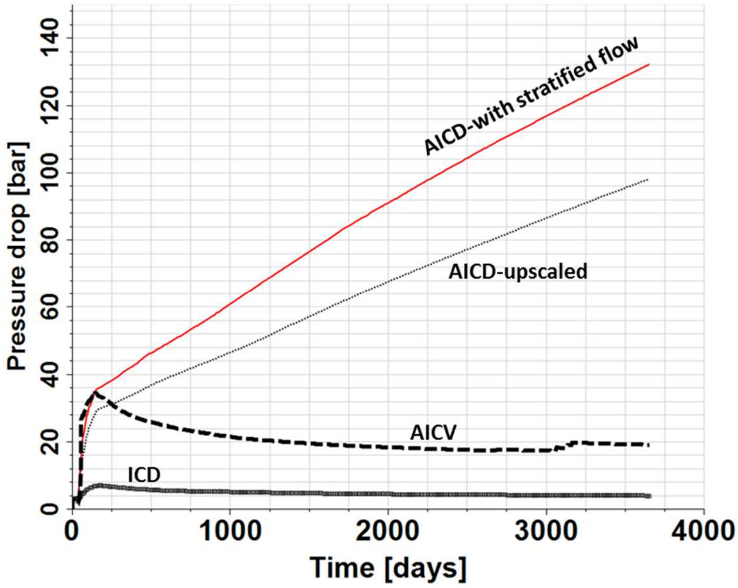

Figure 4-50: example pressure drop across once completion section for AICV, AICD and ICD completions

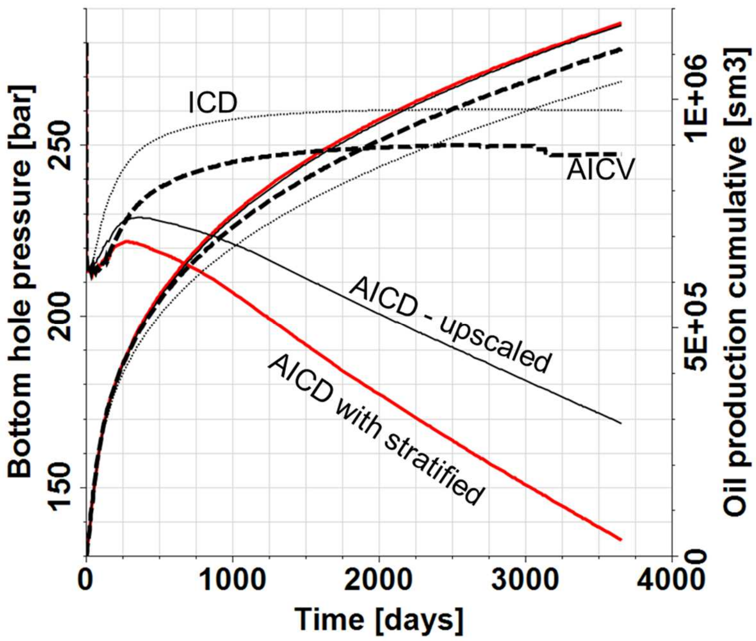

Figure 4-51: well performance (oil production and BHP) for AICV, AICD and ICD completions

4.4.8 *Discussion*

(1) A novel, extended, Multi-Segment Well (MSW) application has been developed to capture the impact of annular fluid segregation on (A)FCD performance in advanced wells. Initial work found that:

- The implementation of the methodology is simple with no extra computational problems being introduced in the case study performed. The simulation time was equivalent to a Fine wellbore model with no extra complications being observed for the modelled oil/water system.
- The model successfully replicated the AICV published performance.
- Passive inflow control devices show negligible sensitivity to fluid segregation. This may be due to the published flow performance model used by the industry.
- Autonomous flow control devices are sensitive to the fluid's distribution in the annulus with increased AFCD flow resistance being observed with segregated flow compared with the conventional "Homogeneous fluid flow" modelling approach.

(2) By considering stratified flow in the annulus, an improved representation of the hold-up, the multi-phase flow calculation and the properties of the fluid flowing through an FCD can be obtained. Hence a more precise modelling of AFCDs performance can now be envisaged. The methodology allows the engineers to investigate the advanced wells - close to reality - performance in real applications through an improved handling of wellbore models and their interaction with the reservoir in numerical simulation models to better represent the physics of the flow control process.

(3) An AFCD design that has one "shut-in" threshold applied in all sections of the wellbore must be optimised carefully before "permanent" deployment downhole. Especially for heavy oil fields, consideration for mobility ratio and outflow performance require tolerance to high amount of water production for a long production period. In some fields (with vertical wells), water zones are targeted so as to allow for enough pump submerge (e.g. the pump is over designed) to allow lifting the oil from the less productive zones. The resulting water production is more than 90%, with zones producing ~ 100% water cut were considered essential for the wells operation and economics. A recent AICV field installation [34] shows a case where AICV-completion has stopped the production

from the zone of 99% water (main contributing zone) potentially limiting the well's outflow performance.

(4) The optimum "intelligent" AFCD should "autonomously" capture both, (a) the improvement in oil production through unwanted fluid control and (b) allowing the good water/gas necessary for the well's outflow performance.

4.5 Discretised Wellbore for improved MPF in Undulating Wells

In the previous sections, we have shown how recent developments in the area of advanced well completions, and AICVs in particular, opened the door for new solutions; but has also presented complex modelling challenges. Proper engineering application of AFCD-completions, considering their designed sensitivity to the properties of the flowing fluid, necessitates a robust understanding of the downhole flow condition; namely the multiphase flow and the distribution of the various phases along the production well's length (see [94]).

In this section the assumption of horizontal well trajectory is evaluated against the "more realistic" undulating well trajectories.

4.5.1 Case study (4): Modelling the Performance of an Undulating Well

4.5.1.1 Model Description

An undulating well created in Model X2 {Figure 4-52} for this case study to evaluate the resulting wellbore performance when passive ICD-completion is installed compared with an active AFCD-completion.

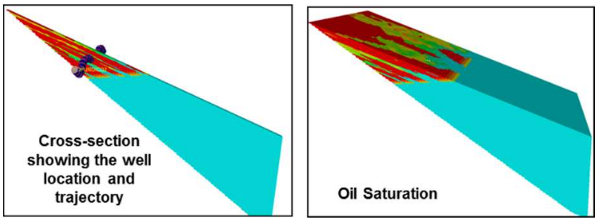

Figure 4-52: Model X2, 3D water saturation, with the undulating well depicted

Well-UN {Figure 4-52} was divided to 5 sections, depending on the angle of inclination, from heel to toe {Figure 4-53}. The software capability to capture the related multiphase flow physics discussed earlier {Figure 4-4} was investigated (next) in an open-hole completion (i.e. no (A)FCDs), before evaluating the (A)FCD-completion performance with an undulating wellbore.

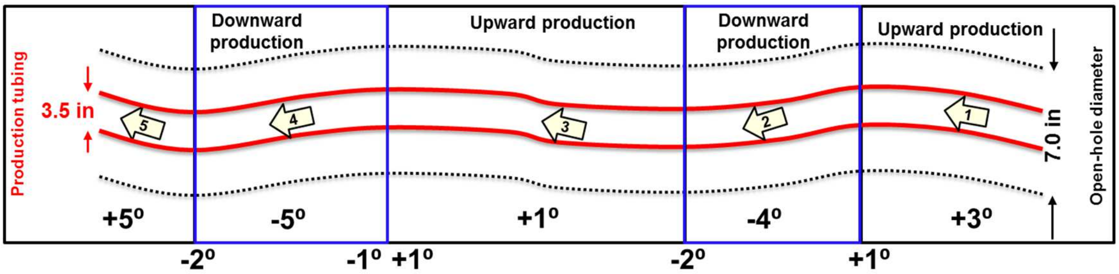

Figure 4-53: Well-UN divided to 5 sections from heel to toe depending on angle of inclination

4.5.1.2 Open-hole Completion Analysis

We first studied the fluid separation in the software by thoroughly evaluating the performance, on segment by segment basis, for fluid fractions/distributions (i.e. hold-up and water cut) as well as pressure drop across the completion.

4.5.1.2.1 Upward flow (Section 1)

Section 1 of the well points upward, i.e. the fluid is flowing upwards. The expected flow performance is for a higher velocity for oil (lighter, with a reduced flow area) and a slower velocity for the heavier fluid, e.g. water (accumulation with increased cross-sectional flow area). This is due to the addition of the slip velocity concept following the laboratory observation in Figure 4-4.

In Figure 4-54 concerning section 1 of well UN, each line represents either water cut or water holdup (red circles) for a segment in section 1. For different segments in this section of the well, the water holdup (red dotted lines) is completely different from the flowing water cut the solid black lines. The WC is calculated based on the flow rates of the fluids (oil and water); whereas, the W-HL is calculated based on the fluid volume at each segment. As expected the W-HL is greater than the WC because of the slippage discussed earlier.

The WC will be equal to the W-HL for any of well segment, if no slippage is assumed, e.g. if the well is assumed to be completely horizontal with homogeneous flow. By contrast, the WC is less than 5% and the corresponding W-HL is > 80% for the case modelled here. Wellbore undulations are then expected to have a significant influence on AFCD-completion performance due to the AFCD's sensitivity to the flowing fluid's properties.

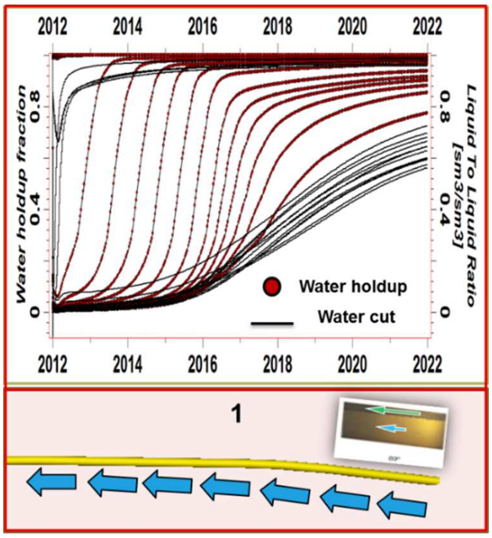

Figure 4-54: Section 1 fluid distribution with drift flux model used: Water holdup ≠ water cut for inclined sections

The drift flux model and the homogeneous model, in this case, produce the same WC. But the W-HL calculation is different, as expected {Figure 4-55}.

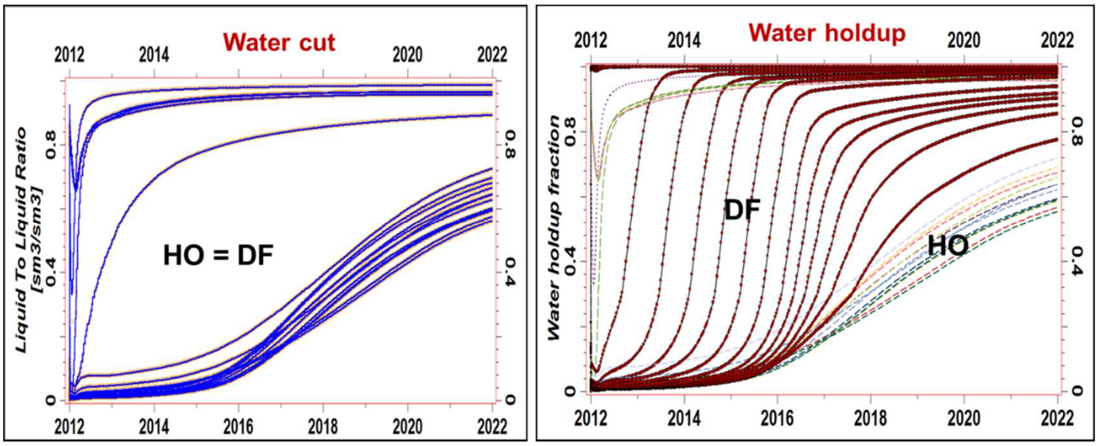

Figure 4-55: Drift flux vs. homogeneous models produce the same WC, BUT the Water holdup ≠ water cut for inclined sections

4.5.1.2.2 Downward flow (Section 2)

Section 2 is pointing downward. This angle of inclination corresponds to a higher velocity for the denser fluid due to gravity and a slower velocity for the lighter fluid. The same performance is observed in Figure 4-56.

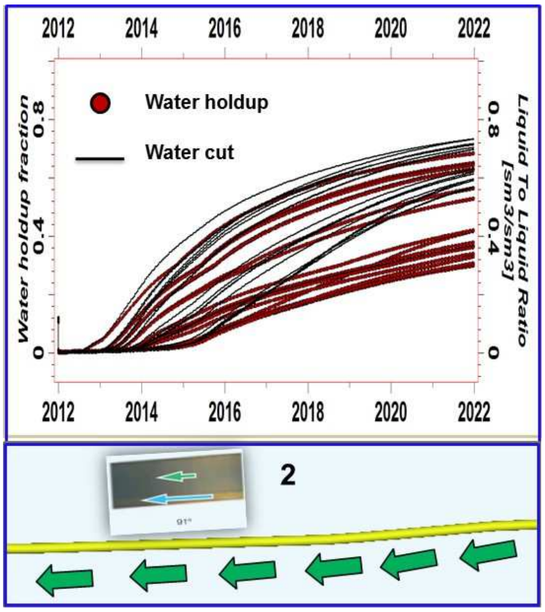

Figure 4-56: Figure 4-57: Drift flux model used: Water holdup ≠ water cut for inclined sections

4.5.1.2.3 Impact of Shutting the Well UN

The well UN was shut for one month to observe the MPF performance and the fluid fraction distribution, back flow etc.

The observation made is that, section 1 is fully saturated with water despite some sections within the wellbore producing oil as shown in Figure 4-54. Closing the well for one month, all the segments in section 1 have a W-HL =1 after one month {Figure 4-58}. This observation necessitates checking the well start-up especially when a very strict AFCD completion (e.g. AICVs) is installed (a similar problem was experienced during well clean-up by Nugraha, I., et al., 2016 [95] – see also [90]).

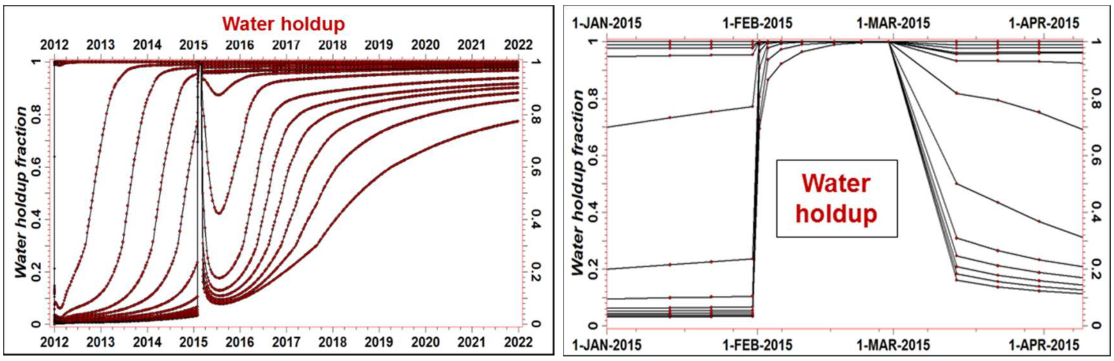

Figure 4-58: Well UN water holdup fraction for the segments in section 5

Crossflow was observed in section 2 where the fluids flow from segment 1 and reinjected in section 2 as shown in Figure 4-59. Please note, the AFCDs' injection performance (countercurrent/crossflow flow) is not published (the software calculations are based on reversing the flow sign).

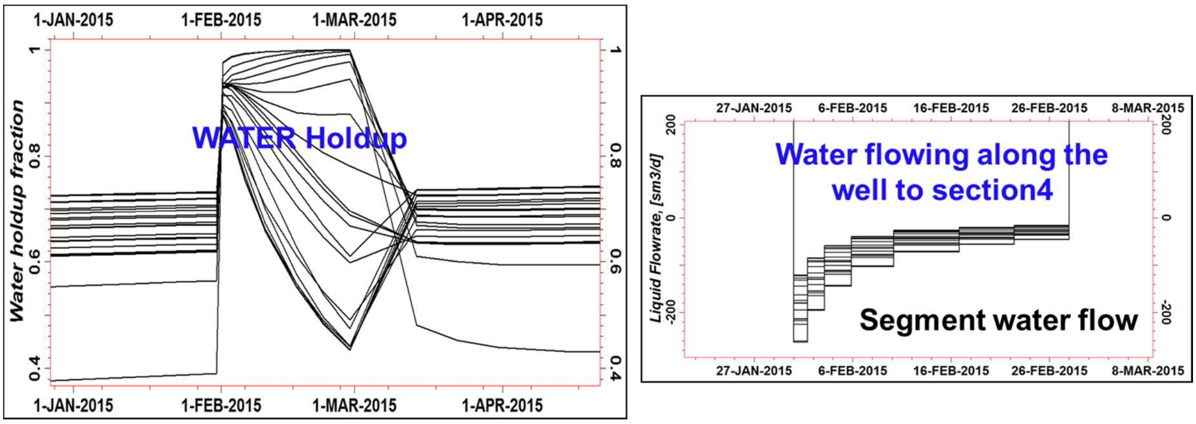

Figure 4-59: Well UN water holdup fraction and flow rates for the segments in section 2 showing the fluid flowing from section 1 and reinjected in section 2

4.5.1.3 Passive FCD-completion performance in an undulating trajectory

Considering an ICD-completion that is passive (i.e. viscosity independent), all the parameters investigated {Figure 4-14} (ICD-completion, Trajectory, well segmentation, and multiphase flow) have been found to have a negligible impact on the total well performance {Figure 4-60}.

This results shows that assumptions made when simulating a passive FCD have a negligible effect on the results predicting the FCD flow (if assumed to be independent of Re).

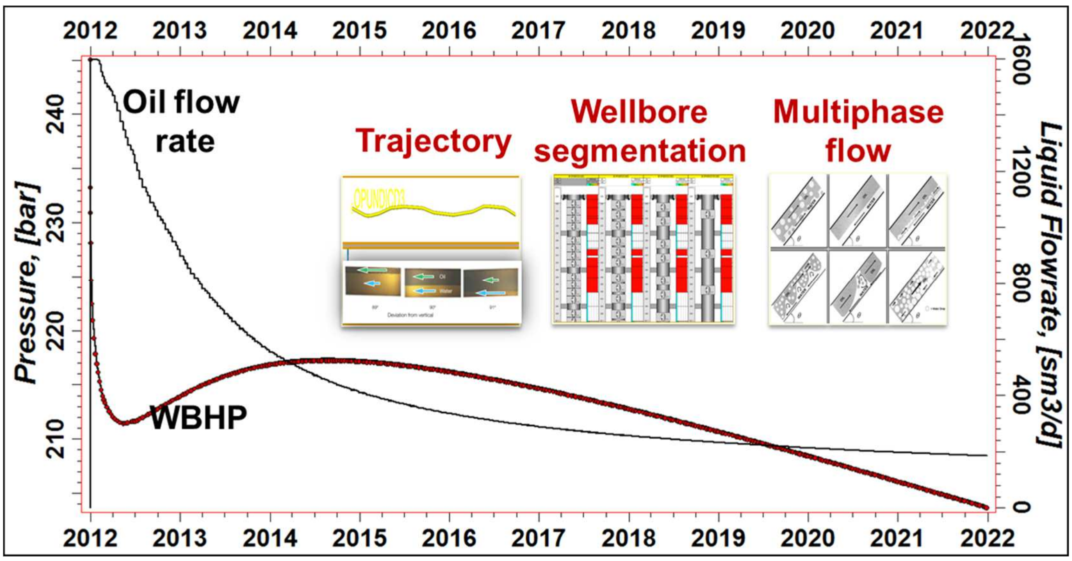

Figure 4-60: the impact of well trajectory, well segmentation and multiphase flow on ICD-completion performance

4.5.1.4 AFCD-completion performance in an undulating trajectory

AFCD-completion, as expected, exhibit a considerable difference to the passive ICDs when modelled in an undulating well trajectory. The differences in fluid distribution discussed in the open-hole modelling, results in varying pressure drop and rates when AFCDs are installed in the completion. This variation in performance depends considerably on the modelling approach and parameters such as: the AFCD performance (restriction level), the number of valves and the AFI modelled. In the analysis provided below, the conventional annulus flow modelling approach is used (i.e. no explicit fluid separation). The drift flux model is used for capturing the fluid slippage and fraction distribution in the undulating annulus.

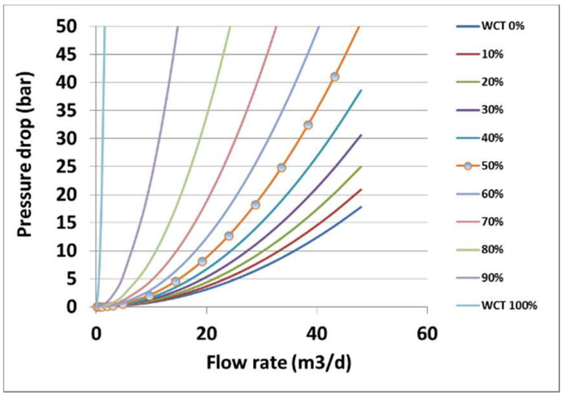

X exponent	2
Y exponent	1.4752
a_{AFCD}	0.0173

Figure 4-61: AFCD performance and modelling parameters

4.5.1.5 The impact of the number of valves and the packer distribution

4.5.1.5.1 Fine vs. upscaled wellbore model with full AFI

First we examine the commonly used practice of wellbore scaling. Full annulus isolation is assumed, with one segment represents 4 AFCDs compared with the case where two segments are placed between the backers each of which represent 4 AFCDs as depicted in Figure 4-62.

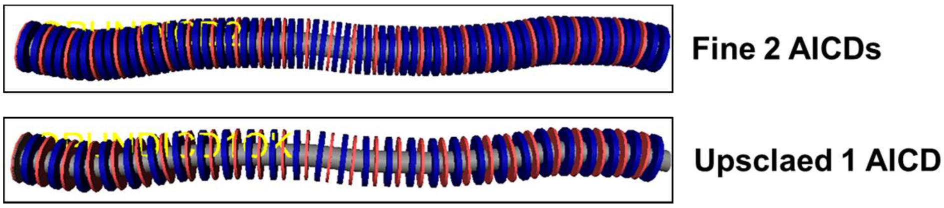

Figure 4-62: Fine vs. upscaled wellbore model with full AFI

The fine wellbore model allow a more detailed calculation encouraging the fluid separation and slippage effects to be captured (see for example Figure 4-54). Hence, a considerable difference in the wellbore pressure performance is observed between the upscaled and the fine wellbore model when AFCD-completion is installed {Figure 4-63}. Less difference in the well production performance results in Figure 4-64. Hence similar fluid production can result but with higher pressure loss across completion once more MPF effects are captured when modelling AFCD-completions.

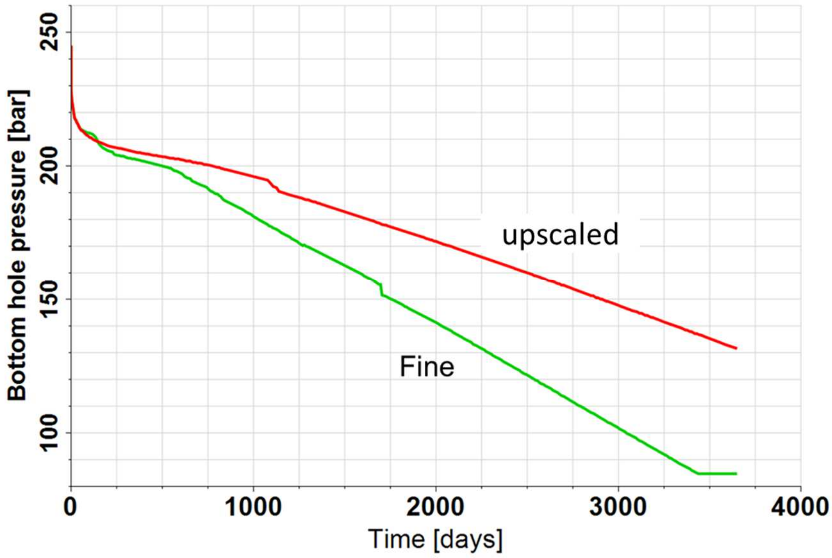

Figure 4-63: BHP for the Fine vs. upscaled wellbore model

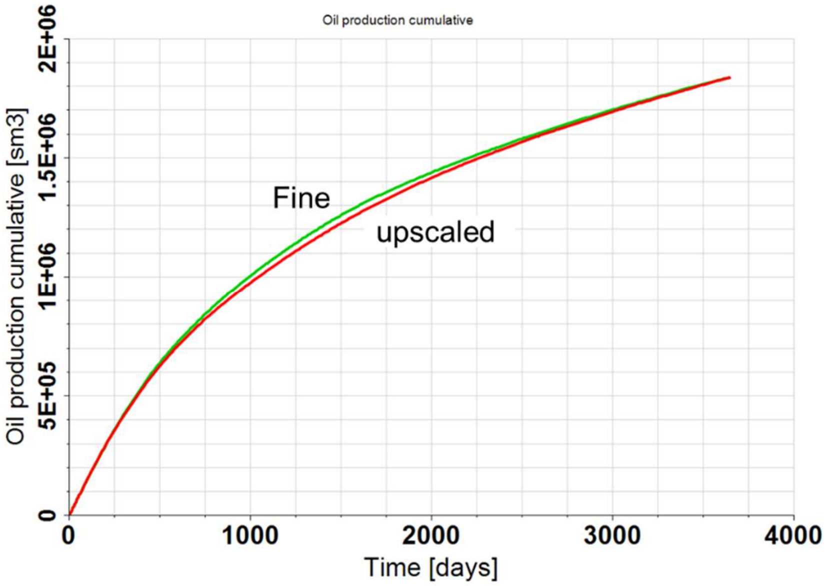

Figure 4-64: oil production for the Fine vs. upscaled wellbore model

4.5.1.6 The impact of modelling an undulating well as a horizontal well

In this section, we test the assumption of modelling an undulating well completed with AFCDs as a horizontal well. The connections and transmissibilities are preserved to ensure similar influx from the reservoir. The well inclination, however, has been set to be horizontal by fixing the depth of the wellbore segments to a specific value such that the wellbore model calculations are based on a horizontal trajectory while the influx from the reservoir is maintained.

4.5.1.6.1 Upscaled wellbore model (1 segment represents 4 AFCDs)

We start with the upscaled wellbore model where 25 AFCD segments are used to represent 100 devices with full annular isolation {Figure 4-62}. The results in Figure 4-65 shows, an expected, small difference (minor) between the two scenarios (horizontal vs. undulating well trajectory). Minor differences observed at the valve level as well (e.g. water flow rate through the valve at the heel Figure 4-66). The one valve (scaling) with full annular isolation behaves as a fully homogeneous model and does not allow the fluid separation to take effect in the wellbore model due to averaging in a large scale (small number of nodes – may be one every 50 m). Therefore, little difference was expected.

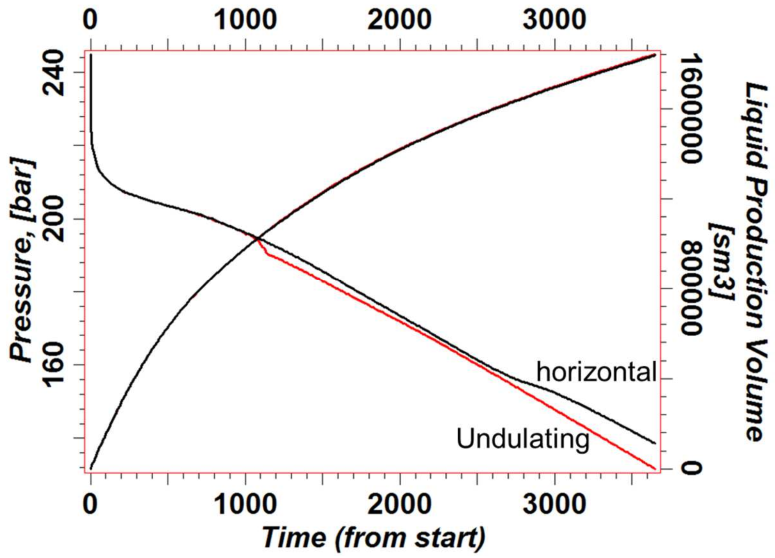

Figure 4-65: the upscaled wellbore modelled as a horizontal well with no undulation

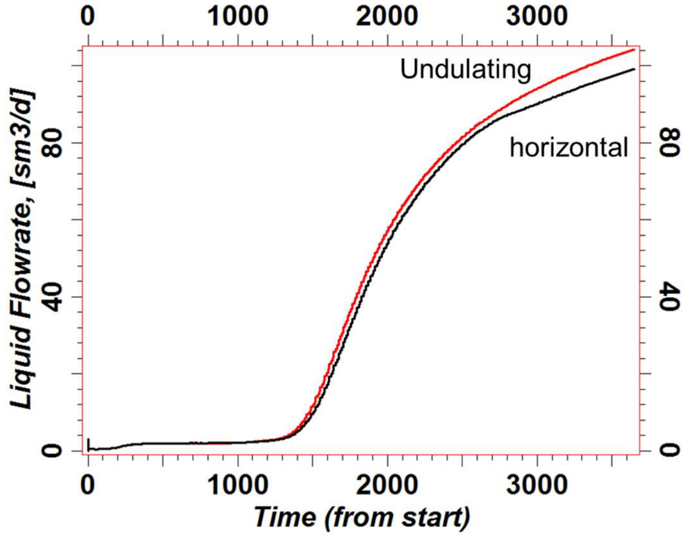

Figure 4-66: water flow rate through the valve at the heel

4.5.1.6.2 Fine wellbore model (1 segment represents 4 AFCDs)

As discussed above, a fine model exhibit different results since it allows modelling the fluid separation and slippage in a finer scale (multiple nodes – one every 25 m). Hence a greater impact on modelling results were also observed when such a fine wellbore is modelled as a horizontal well were the impact of the MPF was stopped as discussed earlier {Figure 4-67}.

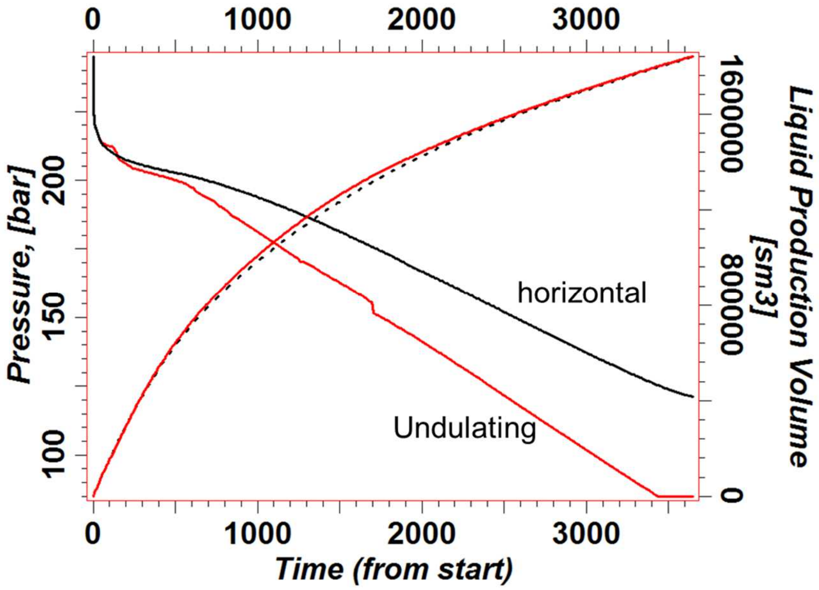

Figure 4-67: the fine wellbore modelled as a horizontal well with no undulation

It is important to realize that, once an AFCD completion is installed, the direction of flow in the annulus will depend on the pressure distribution and the influx points along the wellbore. The observations shown in the open-hole completion may reverse because the annular fluid may flow in opposite direction (the toe direction), following the least flow resistance. The MPF phenomena (upward flow or downward flow) discussed earlier in section 1 and 2 of the open-hole well model may thus reverse. To summarise, various effects occur during simulation and in real life that impact the AFCD response and the resulting well performance have been studied. Interactive well/reservoir modelling is the key technique that captures these phenomena. However, in all modelled scenarios, additional pressure drop across the AFCD-completions always resulted with adding more details (e.g. stratified flow, well trajectory, upscaling, etc.). This observation must be accounted for during the design and installation stages.

4.6 Conclusion

The MPF in the wellbore is very complex. The AWC's valves are expected to undergo a series of varying phases flowing with different percentages between 100% oil to 100% gas (or) water to mixture. Such flow combinations are expected to pass thorough the valve at a relatively short time scale (e.g. minutes) of a MPF resulting from the varying, e.g., well trajectory, pressure drops (due to valves' reaction), rates along the well and influx from the reservoir (phases and rates).

Capturing such complexity require a sophisticated detailed calculations (e.g. Computational Fluid Dynamics (CFD)). However, within the context of reservoir modelling, the wider picture is required. The reservoir simulation is not "normally" detailed, as such, in terms of simulation time (normally months), and in terms of capturing the spatial reality surrounding the wellbore as well as deep in the reservoir (geological uncertainty). The importance of coupled well/reservoir modelling was discussed in chapter 3.

The multiphase flow is greatly simplified, in the coupled well/reservoir modelling tools available today. This is due to the assumption that the fluids behave as a homogeneous mixture whose properties were averaged (volume weighted) from the individual phases' properties. The currently used AFCD performance modelling approach, that was suitable enough for a passive FCD, is physically controversial for modelling phase selective FCDs therefore is recognised as needing update.

Engineering data provided by Production Logging Tools (PLT) in a real well or by experiments in the laboratory, have indicated stratified multiphase flow to be the most frequently encountered flow environment in horizontal and highly deviated wellbores. Considerable differences in phase velocities and holdup values resulting from small ($\pm 1^0$) changes in wellbore inclination from the horizontal have been observed. A so-called horizontal well is almost never actually horizontal. Several challenges can hinder the originally planned trajectory resulting in a shorter well, varying inclinations and perhaps different target (sand unit) in some cases.

The physics above should to be included in the modelling workflow. It has a considerable impact on the predicted performance of the AFCDs behaviour. The problem is further exacerbated by accumulation of the denser fluid at low points and the lighter (e.g. gas) at the high points of the well trajectory.

The analysis of the impact of traditional wellbore segmentation and MPF modelling on AFCDs when a stratified flow environment exists shows that:

a) The pressure drop across the AICD increases and the rate decreases as the device's response to water becomes more restrictive due to stratification.
b) The total flow rate for segregated annular flow is lower than when modelled with homogeneous annular flow (except for fast MPF performance where MPF parameters can be calculated (iteratively) that allow for a similar performance for both cases, i.e. one specific MPF performance matching the whole "WC" range for both homogeneous and stratified flow).
c) A considerable difference in the system performance (flow rate) observed at various WWC for the MPF designs applied (slow, linear and fast).

Equations provided (e.g. Equation 4-4) which incorporate both, the improved single phase performance formula {Equation 3-18} and a MPF expression that has been found to match data generated during testing AFCDs in a multi-phase flow loop.

Calculations have shown that a fast MPF performance for AFCDs is more likely to occur downhole (compared with slow and linear), mostly influenced by fluid stratification/segregation in the annulus. The current industry practice of assuming simple values, e.g. (1), for the homogeneous mixture parameters is very simplistic and can lead to misleading simulation results and, therefore, completion designs. The methodology presented here facilitates incorporating the MPF performance within the current simulators capabilities while capturing the fluid stratification effects.

A novel, extended, Multi-Segment Well (MSW) application has been developed to capture the impact of annular fluid stratification on (A)FCD performance. This model, was successfully validated against published AICV performance. It can be used to identify the optimum AFCD performance (e.g. AICV shut-in threshold) for each application.

(1) The method allowed answering different completion optimisation questions (within the context of well and reservoir interaction) as well as testing various effects, scenarios and concepts.

(2) The studied examples have shown that an autonomous reaction potentially improves the production. However, each AFCD type (available today) provides a fixed performance/resistance for unwanted fluids' inflows (or a fixed shut-in threshold, e.g., for AICVs). The (wider) optimum "intelligent" AFCD is ought to capture both, (a) the improvement in oil production through optimal unwanted fluid control (case specific) and (b) allowing the good water and (or) gas necessary for the well's outflow performance [35].

Taking stratified flow into account in a coupled well/reservoir simulation (considering well trajectory, well segmentation, and multiphase flow): does not impact the results obtained when passive inflow control devices present in the well. On the other hand, the results deviate considerably when AFCDs are modelled in comparison with the conventional "Homogeneous fluid flow" modelling approach.

Chapter 5 AFCD Optimisation and Uncertainty Analysis

Several ICD completion design methods are available for passive FCDs (ICDs) [6, 14, 19]. ICD completion design involves optimizing the strength and type of these devices along the wellbore. There is no an AFCD completion optimisation workflow widely adopted yet. The AFCD completion offers an extra degree of freedom by adding a phase-selective functionality to the passive performance of an ICD. This chapter offers an insight into how and why such completion can improve well production, and what the optimal AFCD completion design may look like following the discussions on chapters 3 and 4. The oil recovery for various AFCD functionalities have been examined for different types of reservoirs.

5.1 Introduction

The parameters with the greatest influence on the ICD completion design are the well's productivity index (both its absolute value and its specific value as a function of the location along the wellbore), the length of the completion, the targeted drawdown or production rate and the properties of the flowing reservoir fluid (density and viscosity) [96]. The questions to be addressed here are when, how and which type of FCD can optimize production [97].

ICD completion design involves optimizing the strength (Flow Area) and type (e.g. Nozzle) of these devices and their distribution along the wellbore. Several ICD completion design workflows have been developed. However, an AFCD completion imposes an additional challenge for the design by adding an extra active response to the otherwise passive performance of the ICD. Al-khelaiwi and Davies, 2010's workflow for the ICD completion design optimization {Figure 2-16} has been extended to account for AFCD reactive control [39].

The understanding developed from the completion performance of these "hypothetical" AFCDs indicates what an optimal AFCD-completion design would be, and how it compares with other FCD-completion designs.

5.2 AFCD optimization workflow

We have adopted the "parametrized AFCD-equation" discussed in Chapter 3 (Section 3.3.2). These two parameters, (1) the area of the imaginary (nozzle) ICD open to 100% oil and (2) the diameter of the imaginary ICD open to water/gas, are used to describe the AFCD performance for all FCD designs (Workflow (1) is provided in Figure 3-8). The

AFCD modelling approach presented will be used to evaluate the feasible AFCD designs by systematically varying the 2 parameters (the AFCD oil flow areas and the AFCD water/gas flow areas) in a commercial reservoir simulation of several geological models accounting for different well and reservoir conditions. This simplification of the device's mode of operation, allows investigating the viability of controlling unwanted fluid production at the level of the individual completion joint for different applications or to compare the AFCD's performance with the equivalent ICD or other form of FCDs. It allows for testing the concept of AFCD in terms of two arbitrary diameters. Hence, optimised AFCD performance can be investigated on a wide range of AFCD-hypothetical designs that are not necessarily restricted to the currently available devices capabilities. The nearest existing devices can be identified once the optimum device performance have been. Furthermore, it can be used as a tool/approach to help the designers pioneer new AFCD designs that allow changing the response to oil and unwanted fluid at the wellsite.

We will start with ICDs where the oil and water/gas flow areas are the same, and then change the AFCD restriction level between tolerant and restrictive in order to illustrate the impact of the two parameters explained in Section 3.3.2. We will also assume zonal isolation at every joint. This latter assumption allows ignoring the annular flow regime effects for the sake of "pure" AFCD design optimisation in this study.

Workflow (3) described in Figure 5-1 has been implemented on several models accounting for different well and reservoir uncertain conditions.

The optimization setup applied, is as follows:

1. First select an ICD nozzle size from the discrete 12 standard sizes of nozzles in Table 3-1.
2. Define the number of AFCDs / joint. We used a maximum of four AFCDs per joint in this study. This will define the total area open for flow across each 12 m joint.
3. Define the AFCD open diameter when exposed to 100% unwanted fluid. 12 positions where selected for this analysis: 0.1, 0.2, 0.3, 0.4, 0.5, 0.6, 0.7, 0.8, 0.9, 1.0, 2.0, and 3.0 (mm). The optimizer can select one of these values as an equivalent nozzle diameter that best matches the reactive control built on a commercially available AFCD at 100% unwanted fluid flow.
4. Use the selected values in points 1 to 3 in the workflow (1), provided in Figure 3-8, to find the appropriate parameters which generate the performance of an AFCD with the selected specifications.

5. Define the number of joints per segment in the wellbore model (segment length/12 m joint). Note that, there are limitations for AFCD completion optimization for the number of AFCD joints to be installed for a certain length of the wellbore, given each AFCD joint is 12 m long. Similar challenges were faced by (Least, B., 2013) in Ecuador where the AICD number per 12 m joint was doubled based on the optimum completion design.
6. Annular Flow Isolation (packers) are distributed as required throughout the completion [84].
7. This study repeats steps 1 - 6 for several reservoir models to address uncertainty in the reservoir description. The search domain results in 12 (flow area/joint) x12 (flow area at breakthrough) x4 (joints per 50 m completion length) cases for each sensitivity analysis, a total of 576 simulation runs. Therefore, the results, discussed below, offer the complete picture of the impact of any design of the sandface flow control completion on the oil recovery. This information can be used to understand the impact of sandface flow control, select the appropriate control and the corresponding AFCD type and specification for a given reservoir model. It will offer a valuable insight to the engineers designing the wells and their completions.

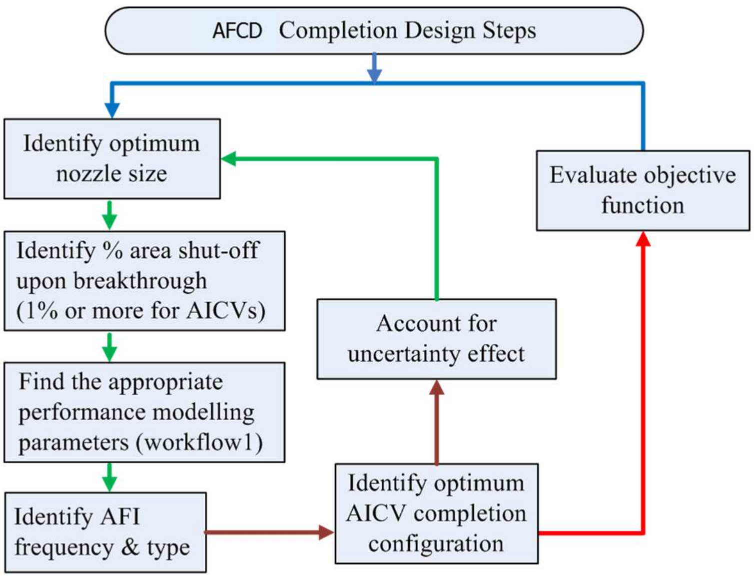

Figure 5-1: Workflow (3), AFCD optimization

5.3 Impact of AFCD-completion performance on oil recovery efficiency

Five reservoir models have been used to investigate the impact of autonomous downhole control on field production. The global optimum solution for the given production constraints and the selected completion options was identified by use of a full factorial experiment that considered all possible combinations of variables to investigate the complete search space as discussed above.

5.3.1 Reservoir models description

The chosen reservoir models are representative of a wide range of the challenges found in heavy oil production with FCD completions.

The models cover the following cases which are representative of the majority of reservoir challenges found in heavy oil production where FCD completions are routinely employed:

- Model 1 and 2: Moderate heterogeneity.
- Model 3: Compartments with a sealing fault.
- Model 4: High permeability variation (high permeability streaks, super K zones, etc.).
- Model X2 described in chapter 3.

Reservoir models 1 to 4 employed the following production and wellbore constraints during optimization process:

1. Each FCD joint is 12 m long and may have up to 4 nozzles.
2. FCD maximum open to flow diameters considered are similar to the Nozzle sizes as per Table 3-1.
3. Each wellbore segment (50 m) can have up to four joints.
4. Packers are located between all wellbore model segments, i.e. annular flow between the segments is not allowed.
5. Flow rate is 3000 (Sm^3/day).
6. Well length (2300 m).
7. 100 bar minimum flowing bottom whole pressure (BHP) limit.

Table 5-1: Reservoir Model 1 to 4 general properties

Variable	value	Units	Variable	value	Units
			Fluid properties:		
Geometry:			Oil density at reservoir conditions	990	Kg/m^3
			Oil dynamic viscosity at reservoir conditions	90	cp
Length (x direction)	4700	M	Bubble point pressure	70	bar
Width (y direction)	1000	M	Solution gas oil ratio (GOR)	5	Sm^3/Sm^3
Height (z direction)	260	M	Water density at reservoir conditions	1000	Kg/m^3

Oil column	60	M	water dynamic viscosity at reservoir conditions	0.5	cp
Depth of OWC	2260	M			
Grid blocks in x direction	92	-	Well dimensions:		
Grid blocks in y direction	26	-	Well length	2300	m
Grid blocks in z direction	50	-	Casing OD	7.0	in
			Pipe OD	5.5	in
			Pipe ID	5.0	in

Table 5-2: Reservoir Model 1 to 4 description

Model 1 has moderate heterogeneity with simplified deposition Horizontal permeability Minimum=100 md Maximum 1000 md Kv/Kh = 0.1	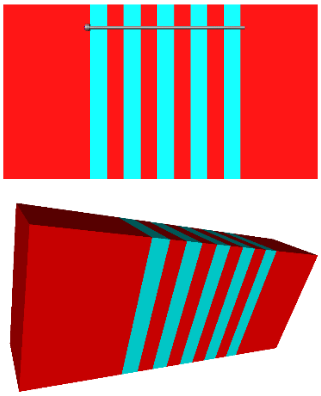
Model 2 has moderate heterogeneity with more realistic deposition Sand (1): Horizontal permeability Minimum 400 md Maximum 1000 md Mean 700 Standard deviation 300 Random distribution Kv/Kh = 0.5 Sand (2): Horizontal permeability Minimum 0.1 md Maximum 300 md Mean 150 Standard deviation 140 Random distribution Kv/Kh = 0.5	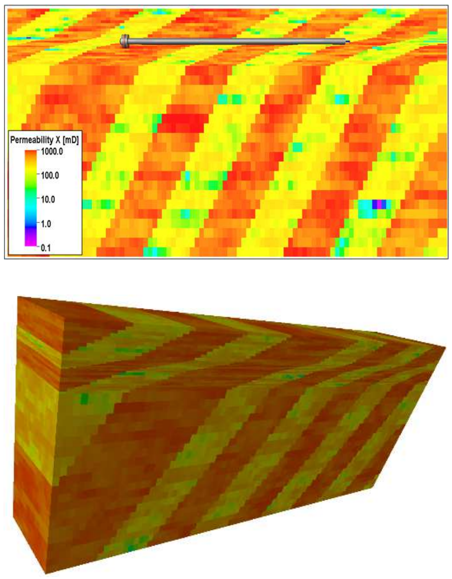

Model 3 is similar to Model 2 with flow barrier in the middle of the well Sand (1): Horizontal permeability Minimum 400 md Maximum 1000 md Mean 700 Standard deviation 300 Random distribution Kv/Kh = 0.5 Sand (2): Horizontal permeability Minimum 0.1 md Maximum 300 md Mean 150 Standard deviation 140 Random distribution Kv/Kh = 0.5	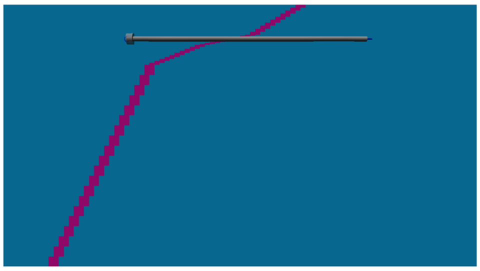 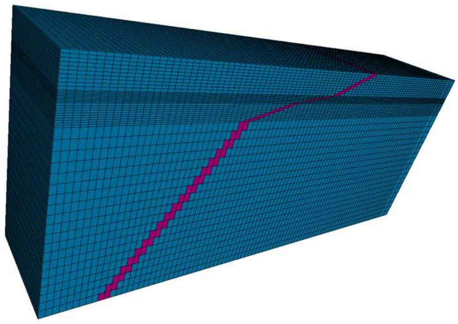 Fault location with (0) transmissibility
Model 4 with extreme permeability variations (high permeability streaks, super K zones, etc.) Sand (1): Horizontal permeability Minimum 500 md Maximum 10000 md Random distribution Kv/Kh = 0.2 Sand (2): Horizontal permeability Minimum 0.1 md Maximum 300 md Mean 150 Standard deviation 140 Random distribution Kv/Kh = 0.5	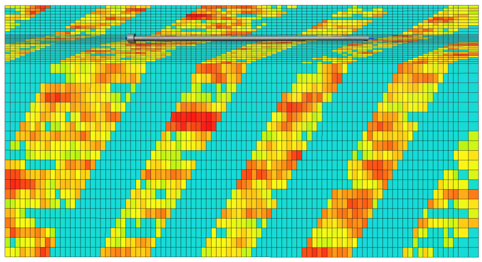 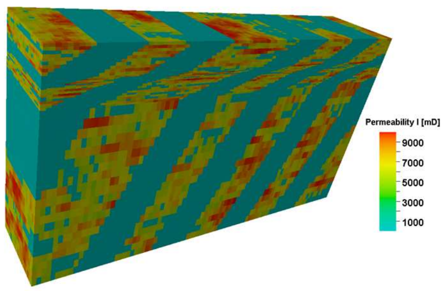

A description of the models used in this analysis is provided in Table 5-2. A full factorial experiment is performed to consider all possible combination of variables to investigate the whole search space. This allows the identification of the global optimum solution that considers the defined production constraints and the selected completion options.

5.3.2 Results and Discussion

Reservoir model 1 results are discussed in detail below. Models 2, 3, 4 and 5 showed conceptually similar results.

Figure 5-2 represents a 3D-response surface of the cumulative oil production versus the equivalent nozzle size (initial area = area open to 100% oil flow) and the equivalent shut-in diameter for a well completion configuration based on a constant FCD strength and number of joints per wellbore segment (see Appendix 7). Note that we introduce an additional variable – the frequency of AFCD installation. The wellbore segment in the model was 50 m long, and can host from 1 to 4 (AFCD) joints/segment. A similar 3D response surface was observed for all models studied.

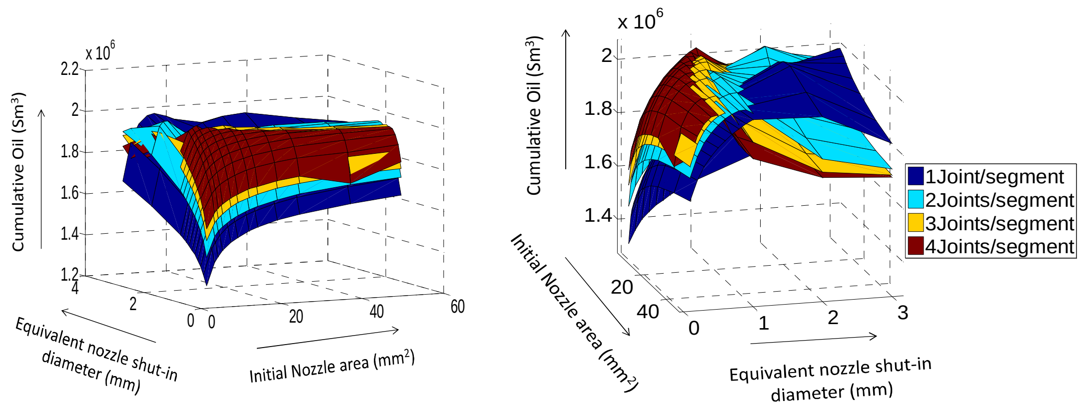

Figure 5-2: Model (1) cumulative oil production response surfaces

As expected, the "ridge" of optimum AFCD parameters on the response surface moves towards larger area - less restrictive, direction when the number of AFCDs per segment is reduced (i.e. from 4 AFCD joints/segment to 1 AFCD joint/segment) - while maintaining the optimum cumulative oil production. This implies that the optimum completion performance can be achieved by several combinations of the AFCD's oil inflow area and the AFCD placement frequency, i.e. the operators can sometimes still achieve the optimum recovery by changing the AFCD placement frequency even if the oil inflow area per device cannot be changed at the wellsite. We selected the "4 AFCD joints/segment" option as a typical example for discussing the response surfaces in detail.

The response surface shows that, once the flow area is large enough, the pressure drop across the AFCD is negligible compared to the reservoir pressure drop. Hence further increase in the area makes little difference. This is observed as a "ridge" extending along X-axis once the X is larger than 10 mm^2. The impact of the shut-in diameter is not intuitive – the maximum separates the control of "good water" from the "bad water", meaning lower water rates should not be restricted so as not to hinder oil production (good water), whereas higher water levels deteriorate the well inflow performance and have to be restricted (bad water). The AFCD restriction rate in reaction to water rate has to be selected carefully – a full shut-in, or stopping the inflow, is not the optimum solution.

It has been found that the Figure 5-2 response surface can be arbitrarily divided into 7 regions {Figure 5-3}. Each region allows a different AFCD interaction with the reservoir, as discussed in detail below. Example AFCD performance plots, where (%) curves refer to WC are also provided to help understand how restrictive the performance of each AFCD designs in the various regions.

Figure 5-3 is a series of detailed illustrations of the surface corresponding to model (1) with 4 joints per wellbore segment. The response surface can be divided into several regions which show a different classes of AFCD interaction with the reservoir.

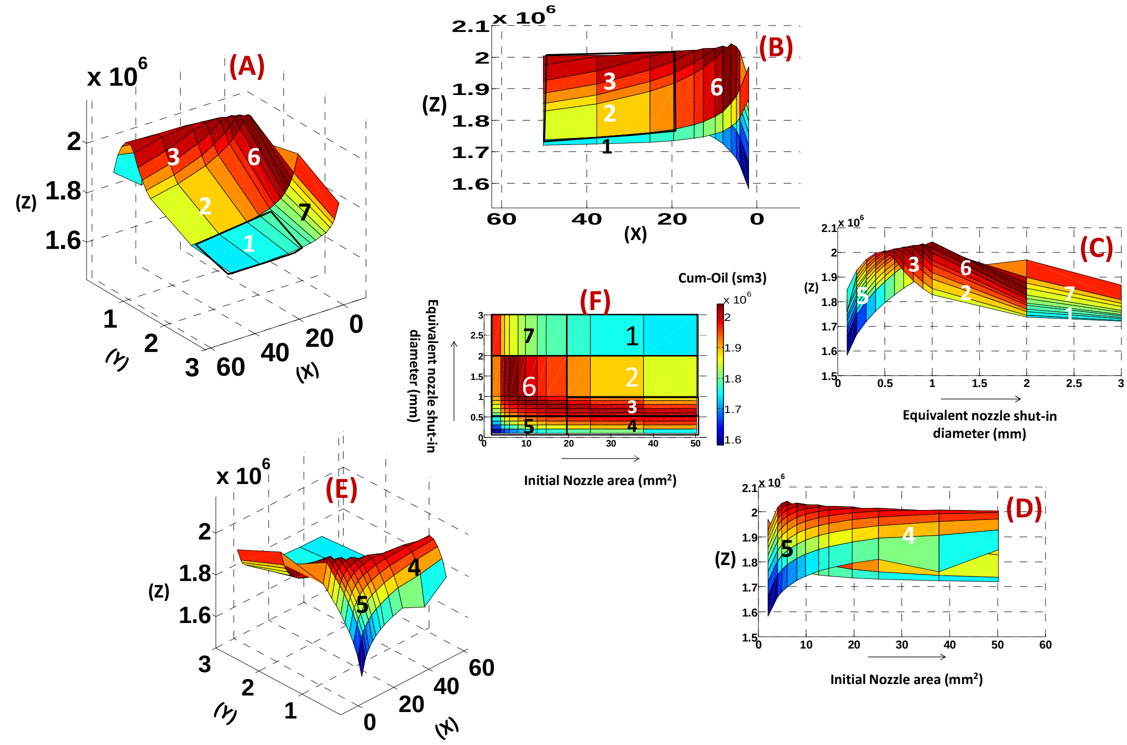

Figure 5-3: Model (1), cumulative oil production response surface (4 joints per wellbore segment). X = initial area open for flow (mm2), Y = the equivalent shut-in diameter (mm), and Z = cumulative oil production (sm3)

5.3.3 AFCD Performance Regions 1, 2 and 3

For discussion, we map several regions (1 – 7) on cumulative oil production response surfaces. Each surface represents a particular design which reflects the number of devices used per wellbore segment. The AFCDs' performance in regions 1, 2 and 3 is characterized by a large initial area Figure 5-3 "a" and "b". Such a device provide a reduced pressure drop for oil flow with a low percentage of water flow {Figure 5-4}. A lower degree of flow equalization is obtained along the length of the completion. An earlier water breakthrough is thus expected. This can occur either opposite high permeability layers (heterogeneous reservoir) or at the heel of the well (homogeneous reservoir). The AFCD's reactive performance in region (1) applies a small level of resistance to water with no improvement in the well performance being observed.

A device with a moderate resistance to the flow of water (region 2) shows an increased oil production {Figure 5-3 "a" and "b"}. However, a device that imposes a greater restriction to flow after breakthrough of the unwanted fluid (region 3) results in a greater increase in oil production, as illustrated in Figure 5-3 "a and c" by the sharp increase in the slope of the cumulative oil production.

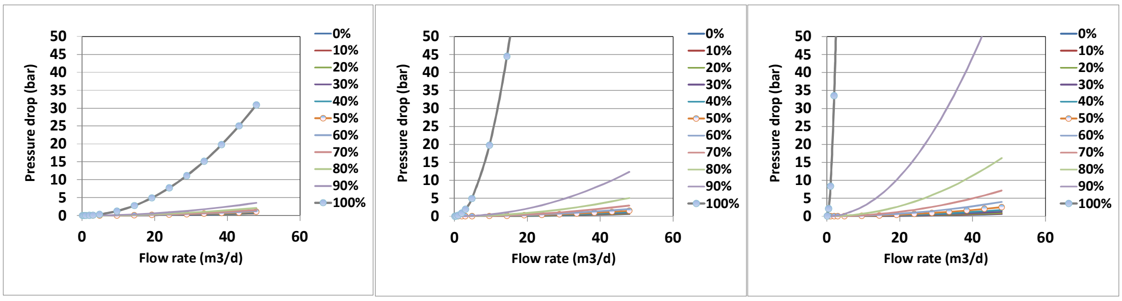

Figure 5-4: examples for AFCD performance from region (from left) 1, 2 and 3 (percentages values refer to the water-cut).

5.3.4 AFCD performance Regions 4 and 5

AFCD performance in region 4 {Figure 5-5} is characterized as "very water restrictive". The AFCD imposes a high pressure drop at small percentages of water-cut; restricting the production of both oil and water. Field experience and the typical shape of the relative permeability curves teach that efficient oil recovery can require a tolerance to higher levels of water production. The situation is further complicated if a small initial nozzle size is selected as indicated by the negative slope shown in Figure 5-3 "d" and "e".

This latter effect is further pronounced in region 5. This region is characterized with a small initial area and a very restrictive reaction to unwanted fluids, Figure 5-3 "e". As one would expect, region 5 results in the lowest oil recovery due to the very high pressure drop across the completion required for oil flow. This high pressure further increased rapidly once water production starts, as illustrated by the example AFCD performance in Figure 5-5.

The well's productivity index is one of the most influential parameters for the ICD completion design – both its absolute value and its variation as a function of the location along the wellbore. Its value is greatly impacted by the type and configuration of the installed completion. A good practice is to design the well for a higher Productivity Index (PI), allowing more production if the PI value is a greater than expected. Similarly, including a sliding sleeve device into the completion allows bypassing the AFCDs if the well's PI turns out to be smaller than that expected, e.g. Least, B., 2013 [45].

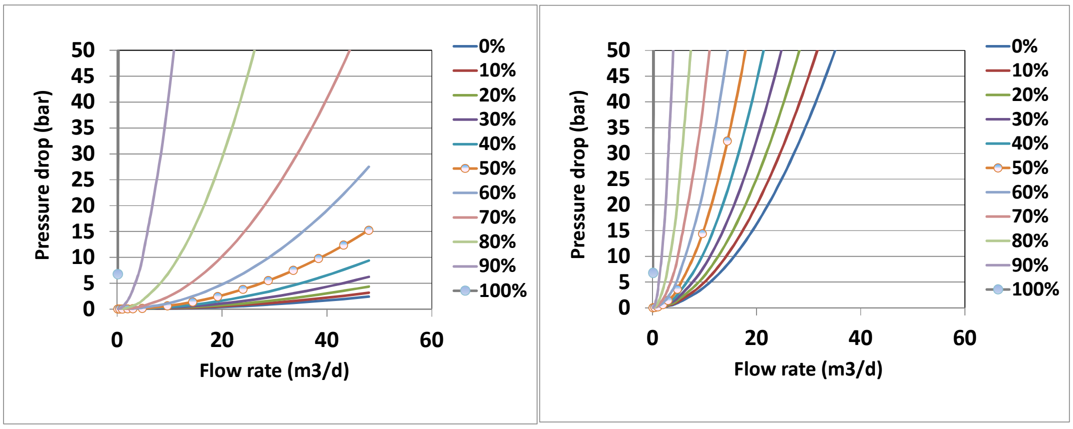

Figure 5-5: examples for AFCDs' performance from region (from left) 4 and 5 (percentages values refer to the water-cut).

5.3.5 AFCD Performance Region 6

Region 6 contains the global maximum production (the optimal completion scenario) for this particular model and production constraints. The AFCDs' performance is optimized by both (1) The AFCD's initial area, as shown by the slope in Figure 5-3 "b" and (2) the AFCD's reactive control, as shown by the improved oil production caused by its optimal restriction of water after breakthrough for each nozzle size, see the slope of cumulative production vs. equivalent shut-in diameter in Figure 5-3 "c". This analysis showed that model (1) required an initial level of flow equalization followed by a further increase after water production had started. This can also be inferred from the comparison between AFCDs performance in region 6 (the optimum), Figure 5-6, and the performance in the other regions illustrated above.

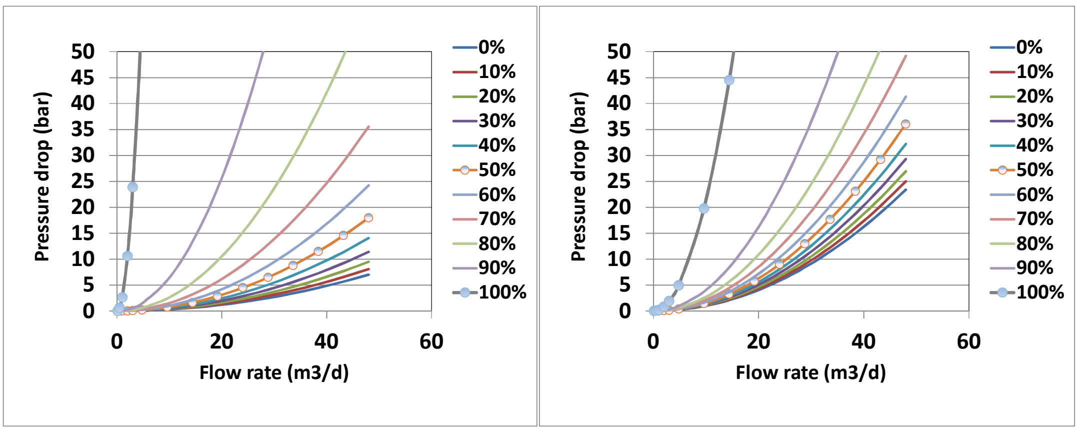

Figure 5-6: Two examples for AFCDs' performance from region 6 (percentages values refer to the water-cut)

5.3.6 *AFCD Performance Region 7*

The AFCD performance in region 7 combines a small initial flow area with a small restriction of water. The initial increase in oil production is achieved due to a more uniform inflow and so delayed water breakthrough; but, when compared with regions 3 and 6, a reduced level of oil production is recorded after water breakthrough since the watered zones are not effectively controlled. Figure 5-7 shows the corresponding AFCD performance – response to oil is restricted, while the response to water is relaxed, bringing the performance curves in a narrow window between the two. This relates to the ICD performance. It's clear to see that an ICD completion has a lower efficiency than one completed with AFCDs.

Region (7) has been excluded from further analysis since it contains a few cases for which the pressure drop across AFCD reduces after water breakthrough. This impractical performance is derived from a combination of the imposed model constraints and the workflow's conditions leading to a higher area at breakthrough than the initial nozzle size.

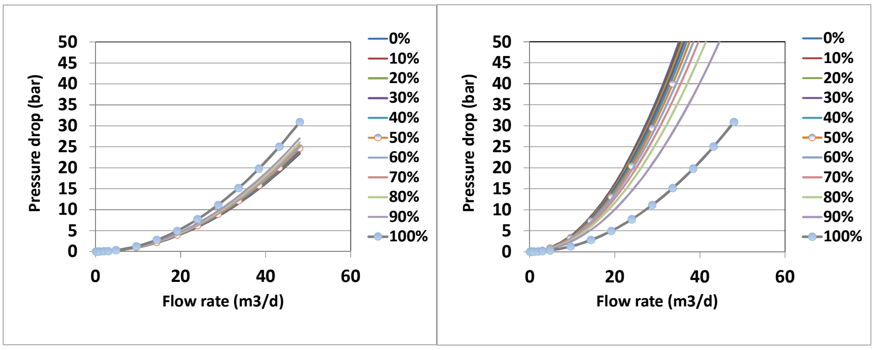

Figure 5-7: Two examples for AFCDs' performance from region 7 (percentages values refer to the water-cut).

5.3.7 *Results from Model (2)*

It is known that a higher degree of equalization is achieved by a higher restriction. However, based on the results obtained from regions 3 and 6 in model (1), we can observe that "an optimum development strategy does not always require complete uniformity of inflow that an ICD can provide" [98]. This fact is more obvious in model (2); Figure 5-8 shows the highest levels of oil production is (again) achieved by completions in regions 3 and 6, with the global optimal solution located in region 3. This model's higher level of geological heterogeneity results in the production optimization being more influenced by the degree of the control after water breakthrough rather than initial (oil only) flow equalization. This can be deduced from the values and the gradients of the relevant slopes in Figure 5-8. This observation implies that, AFCDs can deliver more value in reservoirs with high degrees of heterogeneity and uncertainty.

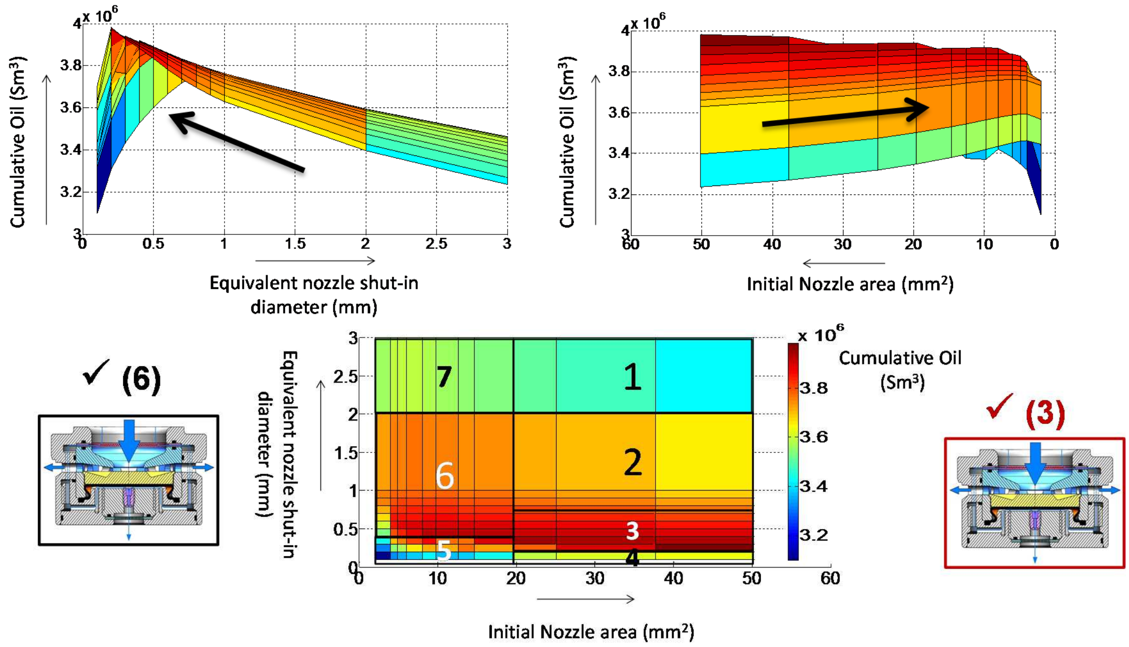

Figure 5-8: Model (2), cumulative oil production response surface (4 joints per wellbore segment). Region 3 control behaviour can only currently be delivered by AFCDs. AFCD can still play an important role region 6.

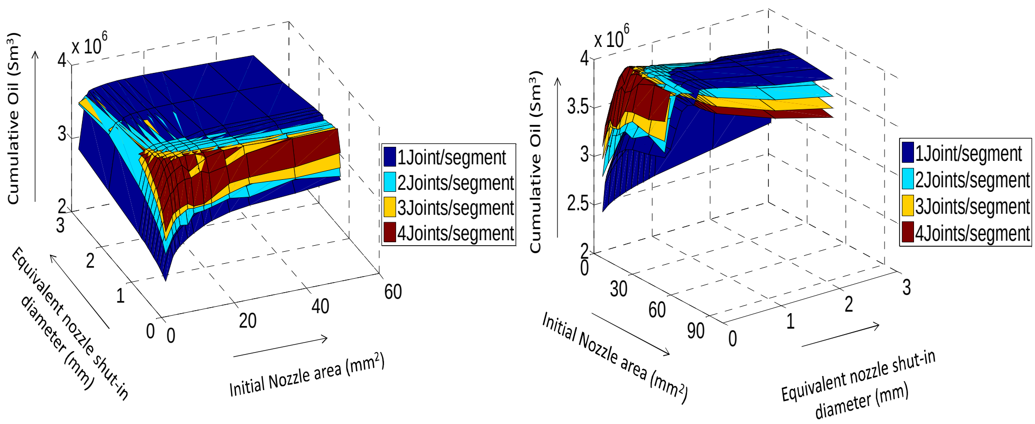

Figure 5-9: Model (2) cumulative oil production response surfaces

The response surfaces in Figure 5-2 and Figure 5-9 show that completions with 1 joint per wellbore segment deliver a higher production of oil at low levels of AFCD reactive control under the defined constraints. This is due to the small total area installed and the consequent flow equalization. The condition is reversed when a device with high levels of autonomous reactive control is installed. The AFCD completion allows more production with larger (base) nozzle size and with a greater number of joints per wellbore segment for both models 1 and 2. This is specifically true for AFCDs that impose a greater restriction to flow at water breakthrough. However, if a very sensitive AFCD is installed both water and oil will be stopped. This was also observed earlier in model 1, region 4 {Figure 5-3}.

The analysis of this model's performance shows that oil production is mostly influenced by the control of water flow after breakthrough. The global optimal solution falls in region 3 with a large initial area open for oil and a high level of water control after breakthrough {Figure 5-10}.

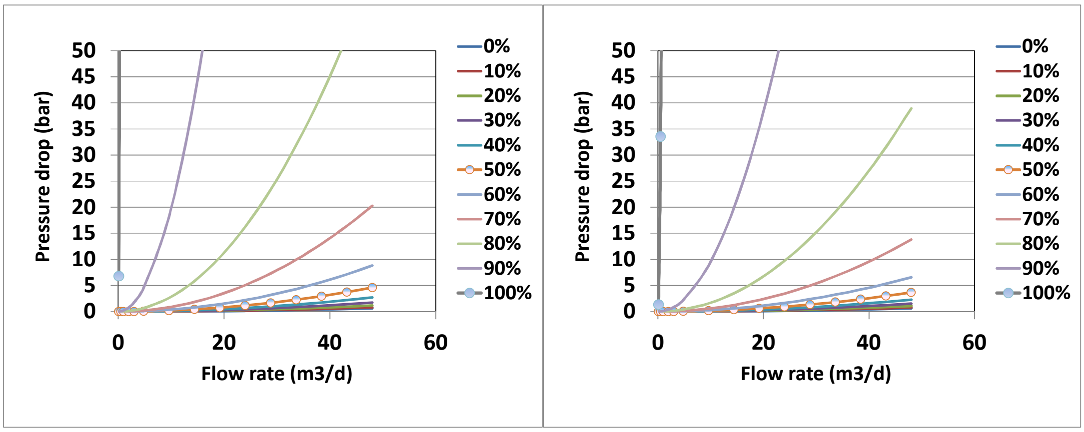

Figure 5-10: Two examples for an optimized AFCD performance from region 3 (model 2) (percentages values refer to the water-cut).

5.4 Comparison of AFCD optimal solutions

Figure 5-11, the top surface for all models with 4 joints per wellbore segment, shows that:

- The addition of an optimized active module (AFCD) to the AWC results in an improved well performance for all the models, Figure 5-12.
- Different levels of improved production are achieved with various combinations of water flow restriction and initial areas open for oil flow.
- AFCD performance in region 3 has a high initial area with a reasonably high level of AFCD restriction to water flow.
- A region 6 AFCD has a greater degree of initial flow equalization with a (relatively) moderate levels of restriction at breakthrough.
- The optimum solution (highest cumulative oil production) is most commonly found in regions 3 or 6 depending on the level of heterogeneity and the model's complexity. Note that Optimisation of "Net Present Value" rather than cumulative oil production will favour completions that increase early production while high water handling costs will favour water restrictive completions.

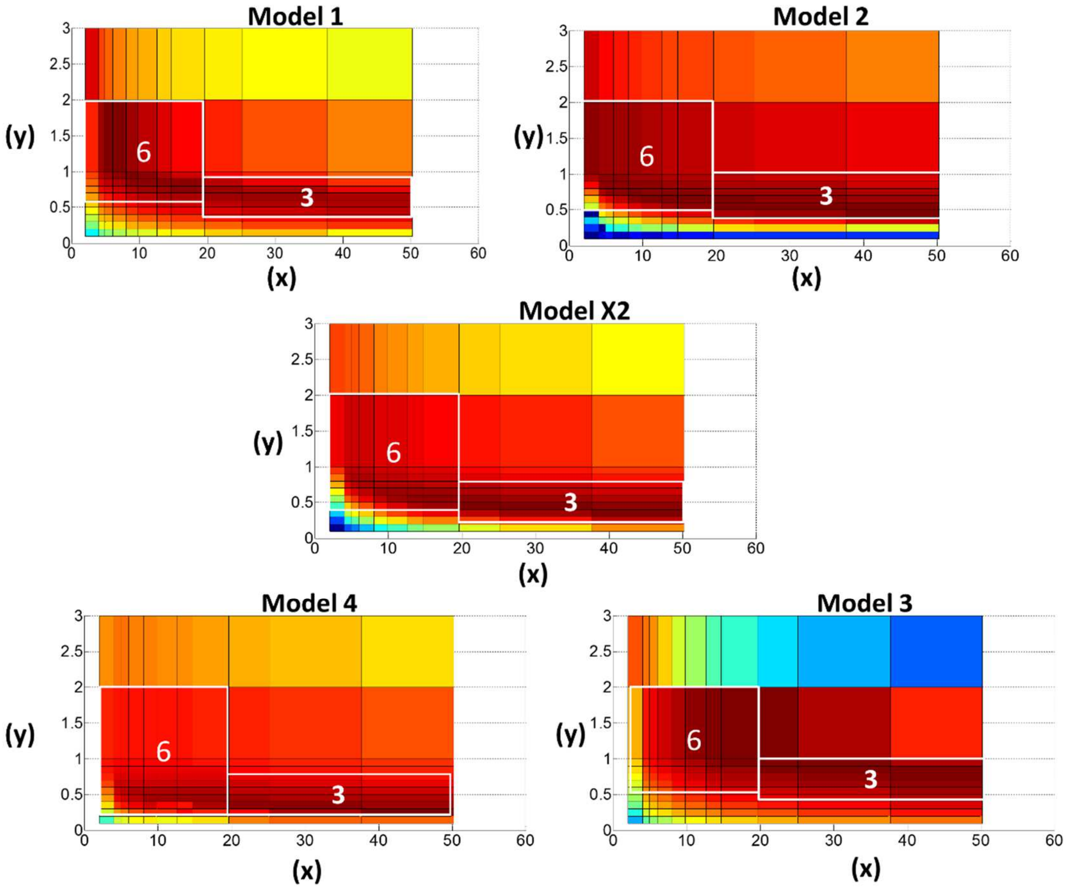

Figure 5-11: analysis of the top view of the 4 joint/segment response surface for all models. The colours represent the value of the cumulative oil production (blue is the lowest and dark red is the highest). X = initial area open for flow (mm2), Y = the equivalent shut-in diameter (mm), and Z = cumulative oil production (sm3)

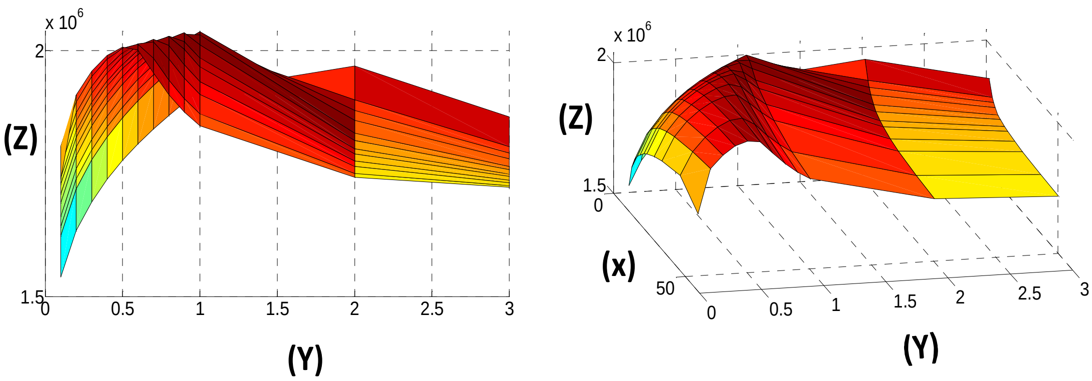

Figure 5-12: Model (1), cumulative oil production response surface (4 joints per wellbore segment). X = initial area open for flow (mm2), Y = the equivalent shut-in diameter (mm), and Z = cumulative oil production (sm3)

- Increasing the number of FCD-joints/wellbore segment may improve the production. A clear trend is again observed {Figure 5-13 **results from Model X2**}. The optimum solutions is moving toward region 3 and 6 (as discussed above) as the number of joints increases. The incremental oil production in the tested model improves rapidly for response surfaces with 1 to 4 (joints per segment); but only slowly thereafter. The number of joints/wellbore segment should also be optimized by monitoring the resulting well productivity index from the selected completion string.

- The optimum AFCD design changes when designing the number of AFCDs per joint, where the optimum production values are close together. It is thus possible for the completion to exhibit a suboptimal performance by installing an incorrect number of AFCDs per joint. Note that this is more likely to occur with AFCDs, because their performance covers a larger range of possible conditions (for region 3 and 6).

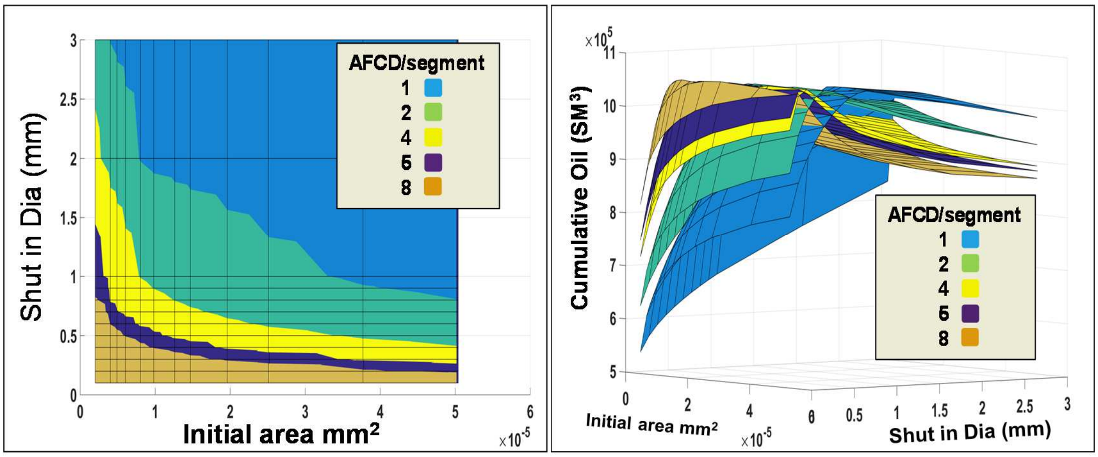

Figure 5-13: cumulative oil production response surface, number of joints/segment sensitivity (Model X2)

5.4.1 Comparison of AFCD vs ICD performance

Figure 5-12 suggests that the global optimum solution is an AFCD completion with 4 joint/segment and with 1 mm equivalent shut-in diameter for model (1). These cases are plotted in Figure 5-14 “left” against the performance of an ICD completion and similarly for model (2) in Figure 5-14 “right”. The cases with minimum and maximum water resistance have also been included. We can see the non-linearity in the results from the shape of the AFCD response surfaces (with equivalent diameter of 1.0 and 3.0 mm). AFCD (1 and 3) provide a similar cumulative oil performance to the analogous ICD completion scenarios for model (1). AFCD (1) shows a distinctly better performance than the ICD completion - the ICD completion requires a greater restriction to improve the production. When optimised, AFCDs indeed are the next generation FCD even compared to the recent, ICD-based, AFCDs.

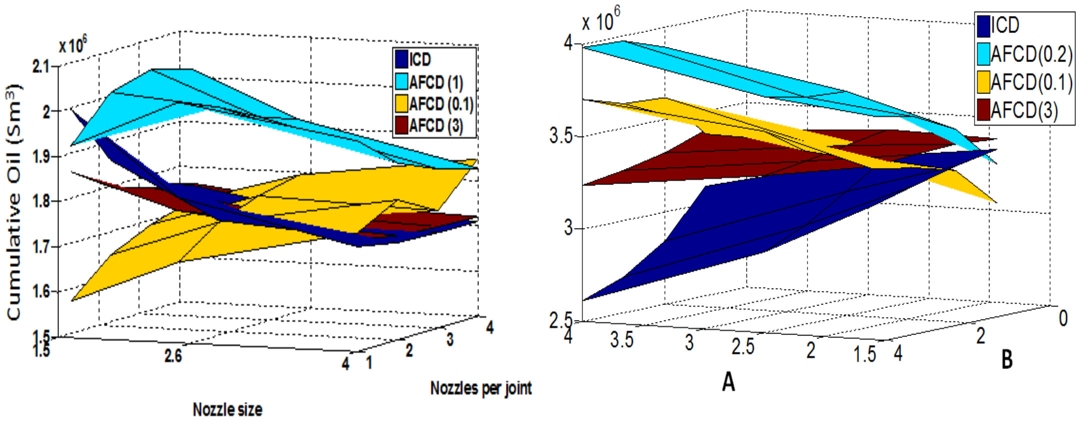

Figure 5-14: Model (1) - left, AFCD 4 joint/segment with 1 mm equivalent shut-in diameter (AFCD 0.1 mm), (AFCD 1 mm), (FCD 3 mm) compared with the equivalent ICD completion design. Same for model (2) – right. B = Nozzle size and A = number of nozzles/joint, A and B defines the initial area/12 m joint

Figure 5-15 compares the ICD completion scenarios with the equivalent AFCD completion for model (1). The ICD completion often demonstrates similar, and sometimes better, performance than the equivalent AFCD completion. An optimized AFCD (with a 1.0 mm diameter by-pass) gave the best result. Analysis of model (1) results showed that the cumulative production was more sensitive to the initial oil flow equalization than the late time water shut-off behaviour.

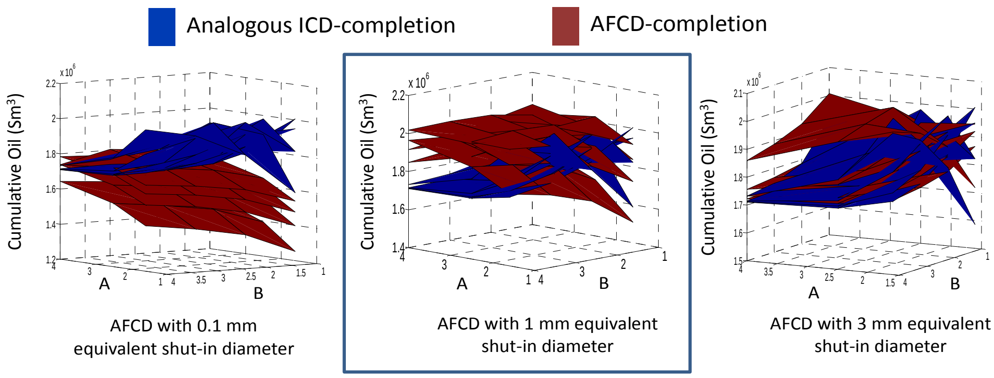

Figure 5-15: Model (1), 3 AFCDs' performance with four surfaces (1, 2, 3 and 4 joints/segment) compared with the equivalent ICD completion designs. Axis B = Nozzle size and Axis A = number of nozzles/joint, A * B equals the initial area/12 m joint.

The completions' performance in Model (2), with its increased level of reservoir heterogeneity {Figure 5-16}, showed that AFCDs with various restriction levels achieve a better production than the analogous ICD-completions. AFCD-completions with a high initial area performed best. The global maximum {Figure 5-8} is obtained with a 0.2 mm AFCD (= an equivalent diameter of 0.2 mm). Almost 50% increase in oil production was achieved compared with the same passive completion specifications; see also Figure 5-14 "right".

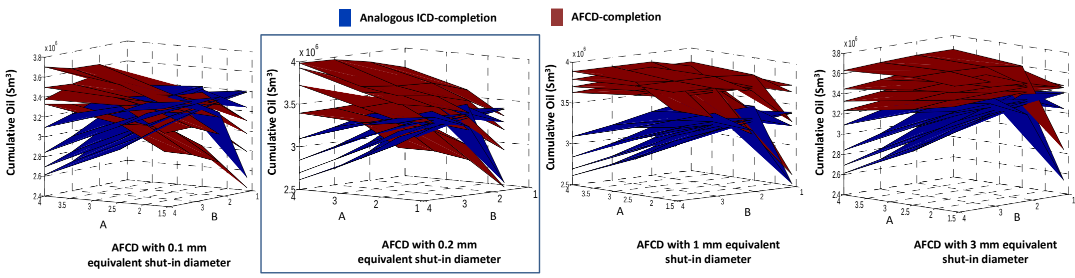

Figure 5-16: Model (2), 4 AFCDs' performance with four surfaces (1, 2, 3 and 4 joints/segment) compared with the equivalent ICD completion designs. Axis B = Nozzle size and Axis A = number of nozzles/joint, A * B equals the initial area/12 m joint.

5.5 Key learnings from the AFCD optimization study:

1. An ICD completion may require a high level of flow equalization to improve the production, while an optimized AFCD completion allows for greater oil production with higher initial area open for flow. This has a direct impact on the well's Inflow Performance and early life oil production.
2. An optimized AFCD provides greater flexibility to deal with the reservoir uncertainties. An ICD completion is forced to always restrict the flow delaying the breakthrough of unwanted fluids. It is therefore more sensitive to uncertainty.
3. A full factorial design was used to (i) investigate the whole search space, (ii) understand the structure (shape) of the objective function, and (iii) identify the global optimum solution for the AFCD completion design. It is recognised that this approach is not computationally feasible when designing intelligent wells in a real-full field model. Optimization algorithms will be required to maximize the objective function in such cases.
4. This work has illustrated the manner in which an AFCD completion can be designed to provide greater flexibility and improved production performance with greater added value than the equivalent passive ICD completion. However, the effectiveness of the chosen AFCD completions depends on detailed knowledge of the well candidate as well as completion planning and design. The results from this study can be used to guide and speed up the AFCD completion optimization process:

   A. Regions 3 and 6 from the scenarios studied provided the optimum production. They correspond to installing an AFCD with a (mainly) reactive production approach or a proactive-reactive approach respectively (when translated into the appropriate AFCD or AICD performance).
   B. The search space can be limited to regions 3 and 6. This reduces, when optimising

a completion design, the optimization cost by more than 50% compared to searching the whole response surface. The general trend observed for the objective function also aids steering the optimisation process.

C. The observed objective function response surfaces are smooth. This important results allow use of fast, gradient-based optimization techniques for finding the global maximum solution.

D. Point (C) above is true when optimizing a single response surface. It is therefore recommended to optimize the AFCD performance with respect to a constant number per joint (though it is recommended to check that the response surface is smooth). An alternative approach for AFCD design: the same conclusions apply when it is necessary to optimise the number of joints for a constant AFCD performance.

E. Designing the AFCD completion for the maximum expected well Productivity Index (PI) has the advantage that the completion design will have the capacity to benefit from any "upside" in the reservoir uncertainty. This unlocking of extra value can be done confidently, particularly when operating in a high cost offshore environment, due to the AFCD's reactive response to unexpected production of water or gas.

5.6 Impact of Reservoir Uncertainty on AFCD-completion design robustness

In Model X2, the selected optimum AICD design {Figure 3-86 and Table 5-3} is used for investigating the impact of a (purposely) built uncertainty (e.g. a sealing fault crossing the well, varying permeability distributions etc.) added to model X2. Eight models in total are used in this study as detailed in Table 5-4 and described in Figure 5-17, Figure 5-18 and Figure 5-19.

Table 5-3: Model X2 selected optimum AICD design parameters

a_{AICD}	y	x
0.1337	2.5	2

Table 5-4: High uncertainty level modelled

Model X2	Is the base case.
Model R1	Same as model X2 with a fault introduced near the heel section crossing the entire sector model {Figure 5-17}
Model R2	Same as model X2 with a fault introduced in the middle of the sector model {Figure 5-17}.
Model R3	Model X2 permeability multiplied by 2 {Figure 5-18}
Model R4	Model X2 permeability multiplied by 3{Figure 5-18}
Model R5	Model X2 permeability multiplied by 4{Figure 5-18}
Model R6	Model X2 permeability multiplied by 0.5{Figure 5-18}
Model R7	Permeability distribution changed {Figure 5-19 }

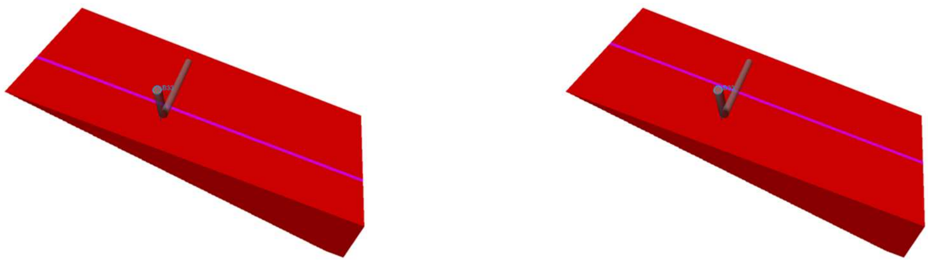

Figure 5-17: Faults introduced in mode X2 for the Cases R2 and R3

With the oil production set as the main objective, first the probability distribution function (normal) was generated for the open-hole, the selected AICD, and the equivalent ICD completions. In Figure 5-20, the equivalent ICD size introduces minimal resistance and hence almost a similar performance to open-hole completion is obtained. On the other hand, the AICD reacts to water influx within the wellbore improving the oil from less affected sections. As a result significant oil production obtained with AICD-completion. This example shows the AICD-completion potential of targeting high oil production initially (valuable early oil) while still being able to control the inflows of unwanted fluid upon breakthrough. Next, this performance is compared against passive ICDs which target high level of equalization.

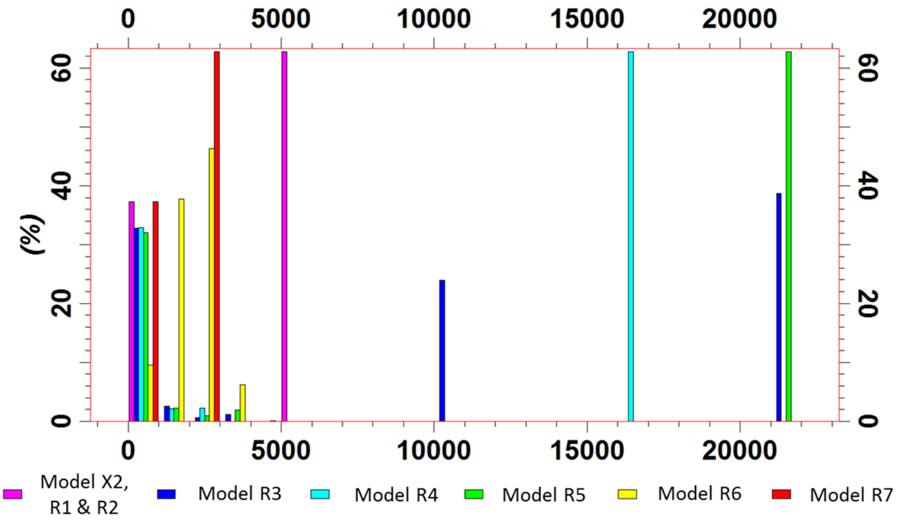

Figure 5-18: permeability distributions generated for the uncertainty study

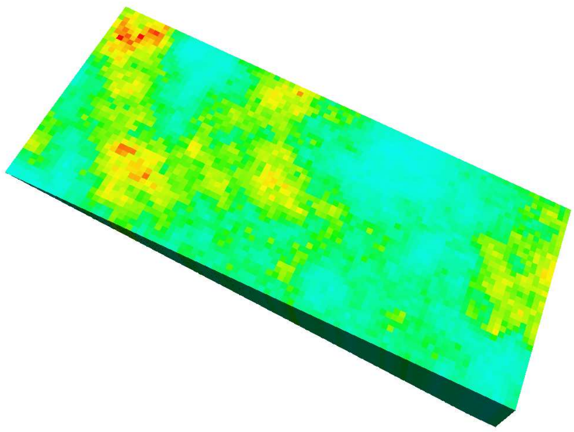

Figure 5-19: Permeability distribution for model R7.

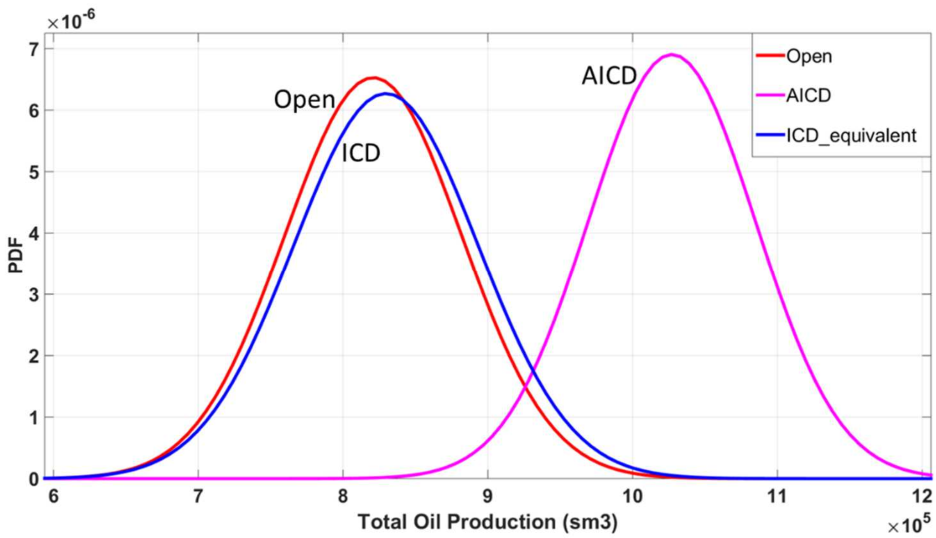

Figure 5-20: Total oil production pdf for open-hole, AICD and equivalent ICD completions in well X2

ICD2 and ICD3, with more flow equalization, were also tested in comparison with the selected AICD design in Figure 5-21. A stricter ICD design does improve the oil production on the consequence of higher pressure losses across the completion as discussed in chapter 3. Yet AICD-completions exhibit a superior performance in both inflow (oil gain) and outflow performance (BHP).

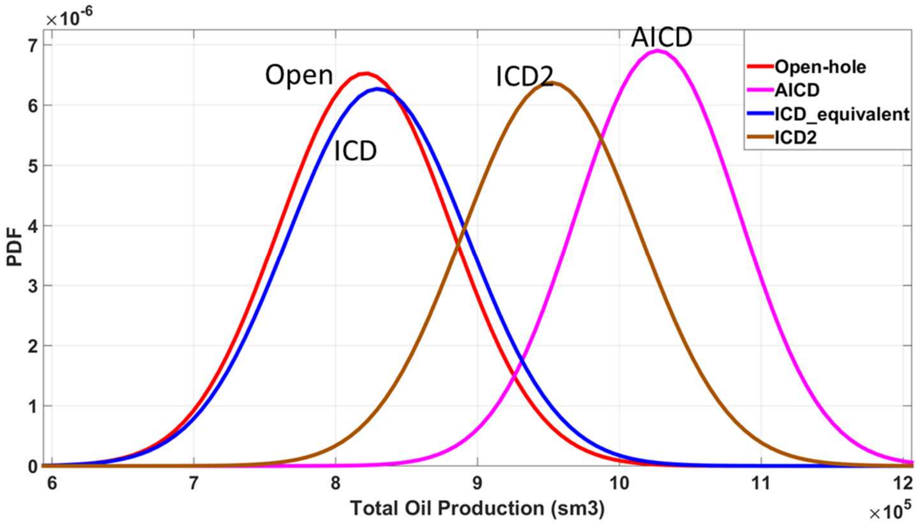

Figure 5-21: Total oil production pdf for open-hole, AICD, equivalent ICD and a stricter ICD2 completions in well X2

The results above show that, the ICD completion can be designed with different objectives. Not only to rectify the HTE, but also to control the high PI zones to allow for more oil in the long term. AICDs on the other hand, have different objectives. They are used mainly to control the unwanted fluid upon breakthrough. However, they can still be used to apply the necessary initial control and designed to provide a targeted unwanted fluid control.

Figure 5-20 and Figure 5-21 give examples of the different ICD/AICD responses. The examples considered show that it is important to consider both the AFCD's oil-restrictive and water-restrictive performance. The latter increases in importance as the formation's heterogeneity increases (several models tested for AFCD optimisation in chapter 5). This methodology can thus be used by well completion engineers when selecting and optimising the downhole flow control completion, including the autonomous inflow control valves (AFCDs).

Further studies similar to section 3.8.3.4.2 have confirmed the conclusion that an AFCD completion with autonomous reaction to an unfavourable phase increases robustness of the design in most cases. However, the designs should always consider well deliverability (inflow/outflow) at later life when unwanted fluid breakthrough and pressure depletion prevail.

5.7 Impact of MPF uncertainty on AFCD-completion performance and value prediction

The accuracy and reliability of the AFCD and AFCD-completion modelling (jointly with the reservoir model) is still open for debate. It is important to recognise this problem, and its potential impact on, e.g., the AFCD-completion design workflow or field production prediction, on a case-by-case basis (further discussion in chapter 4). Some elements of this analysis are explained in this section.

5.7.1 Impact of Standalone MPF on the AFCD-completion Performance Forecast

The impact of the annular MPF effects on the AFCD-completion optimisation results have been studied (chapter 4). The mixture properties of one AFCD design has been changed to investigate the impact of possible changes on the MPF on the order of optimisation following the discussion above.

Figure 5-22 gives an example showing the results of changing the mixture properties definition (see section 4.2.3). It was observed that the multiphase flow as applied here does not impact the optimisation sequence but rather the magnitude of the response parameter studied (at this stage NPV response is presented). The same finding is observed in different AFCDs designs {Figure 5-22}.

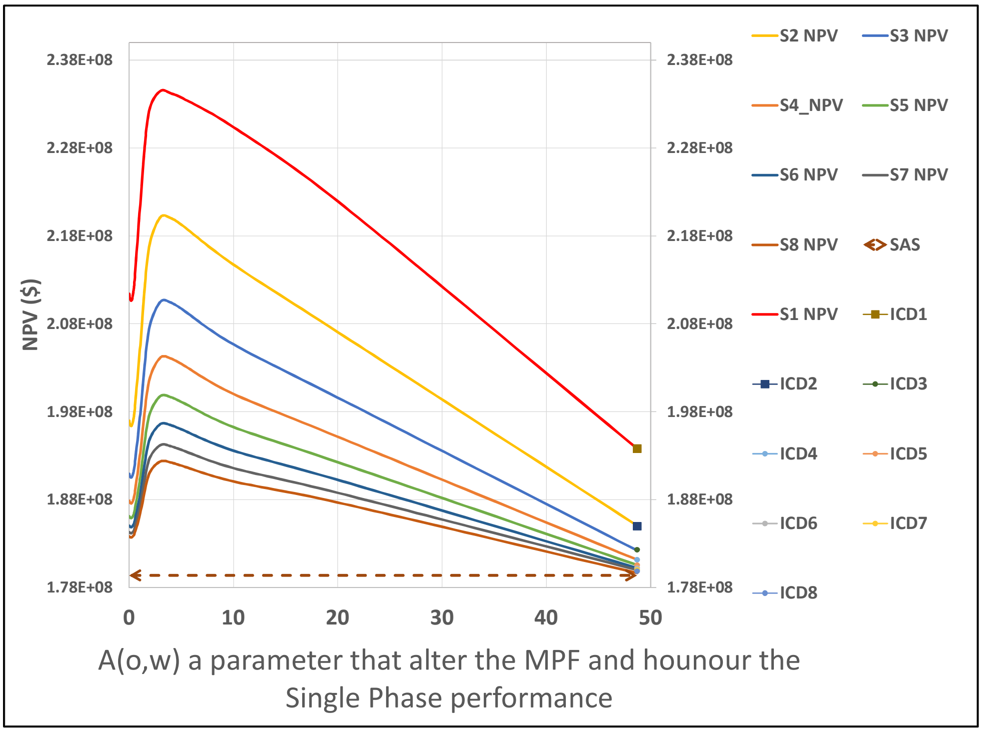

Figure 5-22: Sensitivity of the multiphase flow impact on the objective function

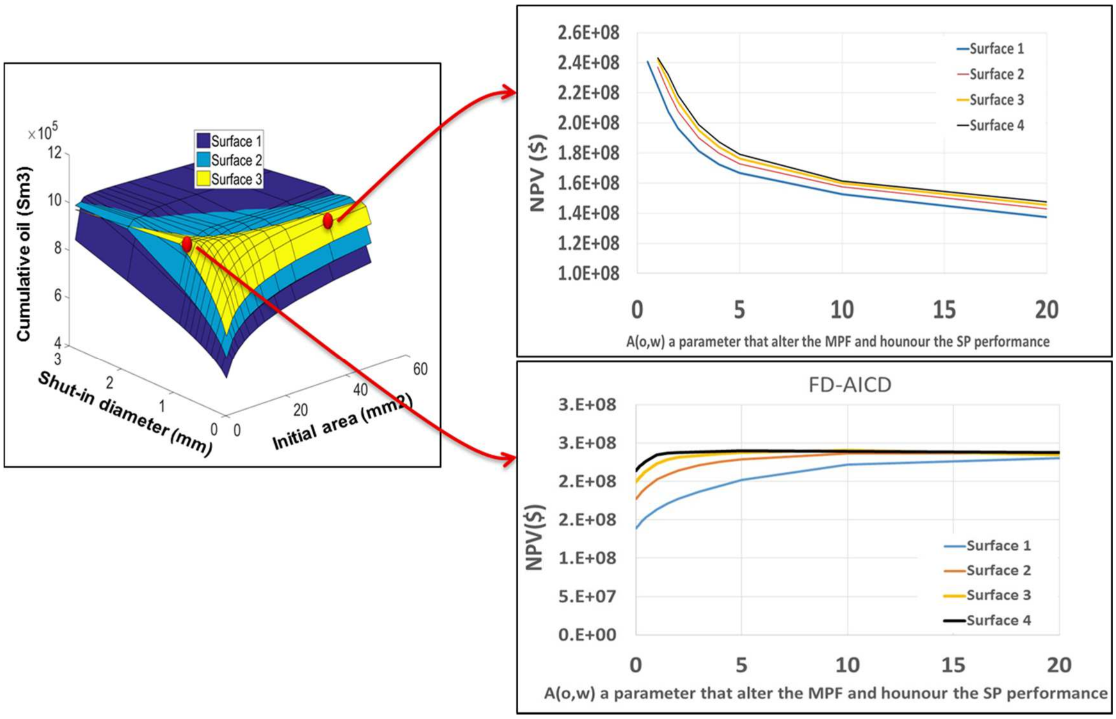

Figure 5-23: Sensitivity of the multiphase flow impact on the objective function

This means that although the engineers using this approach will be able to find the appropriate AFCD-completion design, they may not be able to evaluate its benefit correctly, which jeopardises the field development objectives and questions the asset's value. A complete solution that incorporates the stand-alone AFCD multi-phase flow and annulus flow model is required as discussed in in chapter 3 and 4. The recommendation for inclined and undulating sections of the well, is to capture them in a discretized annulus simulation which matches the actual wellbore geometry as near as possible.

5.7.2 Impact of the AFCD performance model

Here we present an example of different approaches to modelling FD-AICD range 3B device (Least, B., et al 2012). As discussed before, Equation 3-18 describing an AFCD performance can be incorporated as a tabulated input to the reservoir simulation. This approach is used to compare AFCD completion performance described by either Equation 3-12 or Equation 3-18 in the reservoir model 2. Applying these equations in reservoir model (2), the two performances in Figure 5-24 can be achieved.

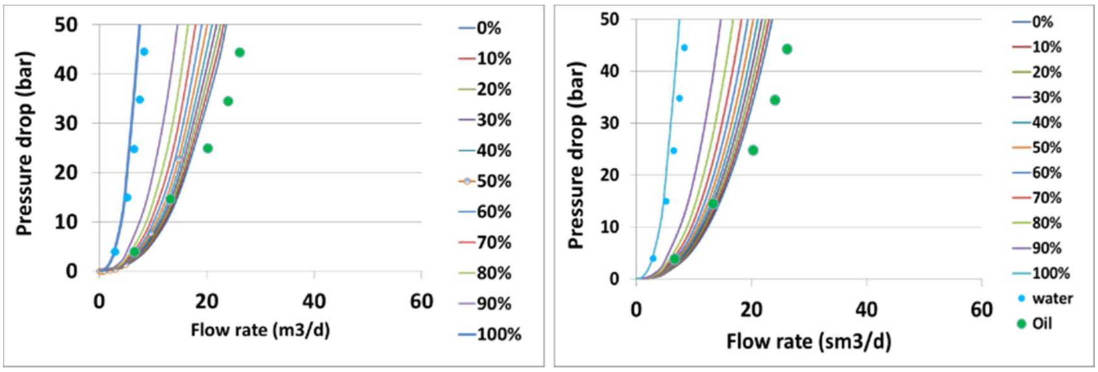

Figure 5-24: Matching the data provided in (Least, B., et al 2012) using equation (1) – left, and equation (6) right.

The two performances modelled in Figure 5-24 look quite similar. The simulation results obtained applying both methods are consequently very similar. Figure 5-25 shows the MPF sensitivity applied in model (2) using the two approaches. The difference observed on average is less than (0.1%) for all the cases performed employing different completion scenarios. Equation 3-12 worked well in this case (for the modelled fluid). The parameters (a_{AICD}, x and y) have to be derived using workflow (1) for each application with different fluid properties. This means that the multi-dimension in Equation 3-12 was redundant – in fact a better performance for single phase flow data is achieved with the 2-parameters of Equation 3-18.

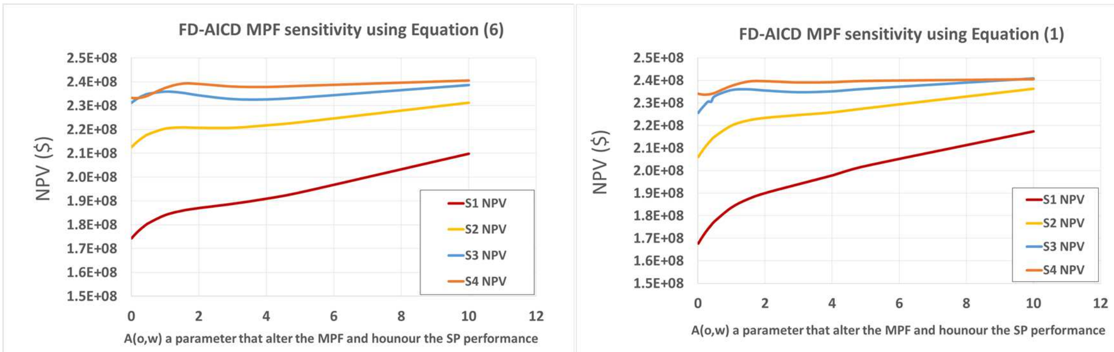

Figure 5-25: Sensitivity of the multiphase flow impact using equation (1) and (6) on model (2).

5.7.3 The Impact of the Grid Scale on AICD-completion Results: Light oil and gas

The objective of this case study is to assess the performance of specified AFCD models and parameters to determine how sensitive the performance of a sector model, extracted from a real field application, is to the variations in the AFCD model and/or the description of the near wellbore grid scale. The impact of the grid scale together with varying AFCD designs on the model's results and efficiency (simulation time) is evaluated. Optimization of an AICD completion has also been performed. The AICD performance was modelled using Equation 3-12 in ECLIPSE.

5.7.3.1 *Fine Model Description*

The area around the wellbore was divided into 6 divisions depending on its proximity to the well. This step is made to allow for a somewhat logarithmic-like LGR distribution in an attempt to capture the natural gas coning development more accurately. A Matlab routine was built to generate the LGR input files at various levels of refinement {Figure 5-26}.

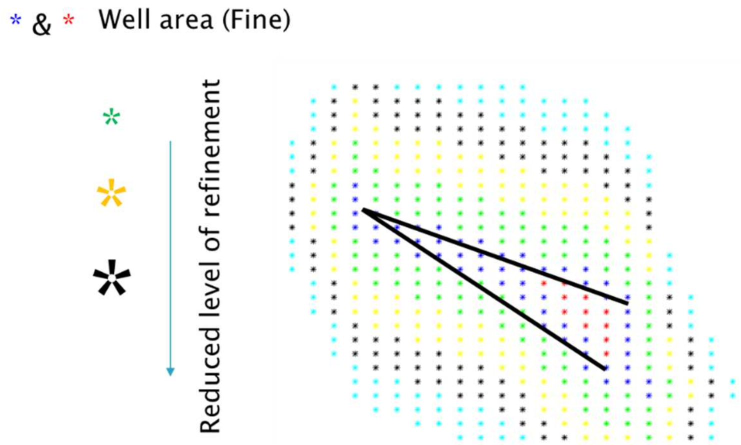

Figure 5-26: Model-X LGR sections to allow for logarithmic like distributions

Six fine models were developed with the description provided above. The original, equal-size cells were divided into (2x2, 1x1), (3x3, 2x2, 1x1), (4x4, 3x3, 2x2, 1x1) etc. starting from the wellbore segments and subsequently moving outwards. All the refined cells were also divided into 2 in the vertical (Z) direction in all cases.

5.7.3.2 *AWC performance*

Three completions were tested on the fine model:

1) Standalone screen completion (SAS). This represents a case with an open hole with no pressure loss along the completion aside from the friction losses on the main production pipe (heel toe effect – HTE).
2) AICD-completion. Two AICD designs were tested:
   a) AICD-1. The performance of AICD-1 is based on the (RCP) valve performance received via personal communication with one of the main companies involved in AFCD technology. It was based on their flow loop tests. This is considered to be the base case in this study.
   b) AICD-2. This is a hypothetical AICD design generated synthetically utilising the workflow1 provided in Figure 3-8. It has been made with a (relatively) aggressive resistance to gas.

The main difference between the two AICD models is the remaining flow diameter after breakthrough. AICD-1, with the larger flow diameter allows a higher gas production flow rate compared to AICD-2 {Figure 5-27}. This can be explained by the fact that the mixture density and viscosity have an opposite effect with the increase in gas fraction in Equation 3-12, as opposed to the oil-water flow situations. This is especially pronounced when the value of y is less than 1 (see Equation 3-12).

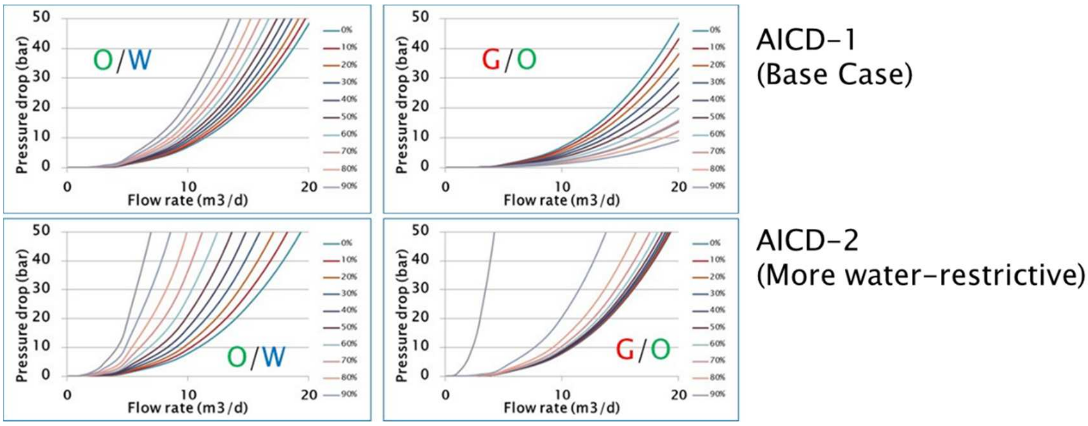

Figure 5-27: Model-X LGR sensitivity, AICD performance (two phase flow)

Figure 5-28 shows the cumulative oil production for Standalone screen (SAS) vs. AICD-1 completions. LGR resulted in a higher oil production. This can be linked to the changes observed in the saturation map – the smaller grid size in this case allows an improved sweep and increased oil recovery.

The AICD-1 completion has an increased oil recovery, with the relative oil production gain (4%) being almost independent of the grid resolution. However, the absolute oil recovery {Table 5-5}, a value which will affect the economic calculations, shows an 8-21% increase depending on the size of the model grid cell refinement.

Table 5-5: Model-X Oil gain statistics

SAS	NO LGR	LGR distribution					
		211	321	432	43211	54321	654321
	2.2E+06	2.4E+06	2.5E+06	2.6E+06	2.6E+06	2.6E+06	2.7E+06
	Relative FOPT (%) increase to SAS/no LGR	9.3	14.0	17.4	17.4	19.6	21.1
AICD	NO LGR	LGR distribution					
	2.3E+06	2.5E+06	2.6E+06	2.7E+06	2.7E+06	2.7E+06	2.8E+06
	Relative FOPT (%) increase to AICD/no LGR	8.6	13.6	16.8	16.8	19.3	21.2
AICD vs. SAS	Relative FOPT (%) increase to SAS with LGR						
	4.6	4.0	4.3	4.1	4.0	4.3	4.7

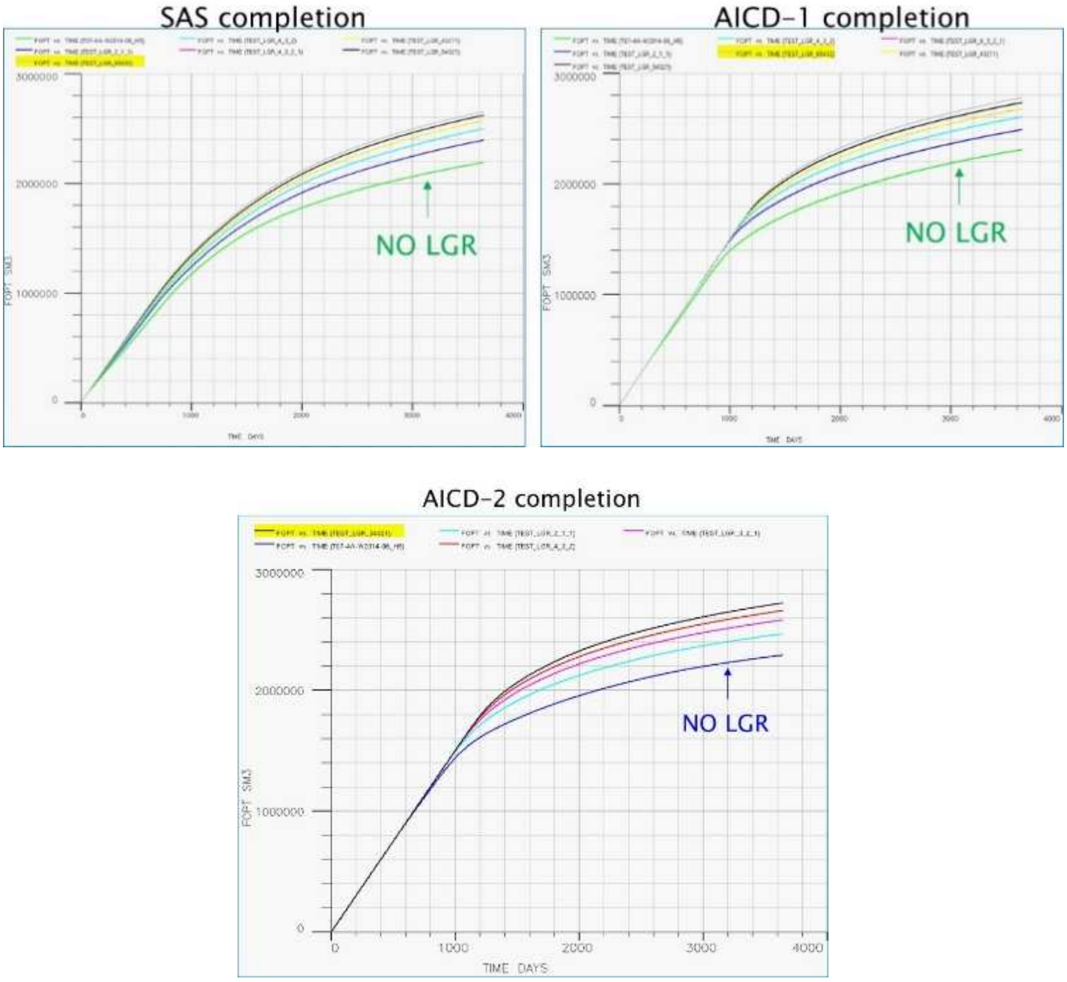

Figure 5-28: Model-X Cumulative oil production, Standalone screen (SAS) vs. AICD-1 and AICD-2 completions

5.7.3.3 AICD Optimisation Study

In this section the results for the optimization of the number AICDs/joint for the AICD-1 model (base case) are presented. This study was performed with the reservoir model-X with no LGR and the results are then applied on the created LGR models to re-evaluate the grid resolution impact.

5.7.3.3.1 The AICD-1 (base case) model

The AICD-1 (base case) multiphase performance allows for a higher gas production flow rate. The AICD-1 parameters {Equation 3-12} result in the AICD pressure drop being more relatively sensitive to water than gas production {Figure 5-27}. This behaviour of the AICD-1 model is thus more restrictive to water rather than gas flow. In fact, multiphase (Gas, Oil and water) flow with increasing gas production at constant water production reduces the pressure drop across the AICD {Figure 5-29}.

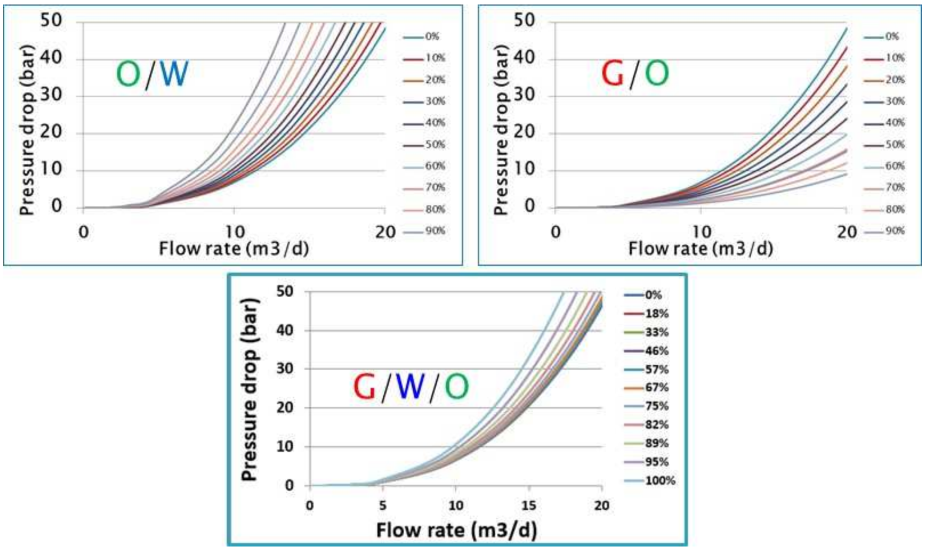

Figure 5-29: AICD-1 (base case) multiphase performance analysis. The (%) represents the summation of unwanted fluid fraction (see Table 5-6)

Table 5-6: Multiphase flow calculations used to produce the G/W/O multiphase performed curves in Figure 5-29 as would be applied in the simulator using Equation 3-12

Annulus fluid fraction											
OIL fraction	1.00	0.82	0.67	0.54	0.43	0.33	0.25	0.18	0.11	0.05	0.00
water fraction	0.00	0.09	0.17	0.23	0.29	0.33	0.38	0.41	0.44	0.47	0.50
gas fraction	0.00	0.09	0.17	0.23	0.29	0.33	0.38	0.41	0.44	0.47	0.50
Unwanted fluids fraction	0.00	0.18	0.33	0.46	0.57	0.67	0.75	0.82	0.89	0.95	1.00

The above AICD-1 performance has been used for the study to optimise the number (1, 2, 3 or 4) of AICDs/joint. The well inflow performance for all these cases showed a small change in the water and gas production with negligible effect on the oil production {Figure 5-30 & Table 5-7}.

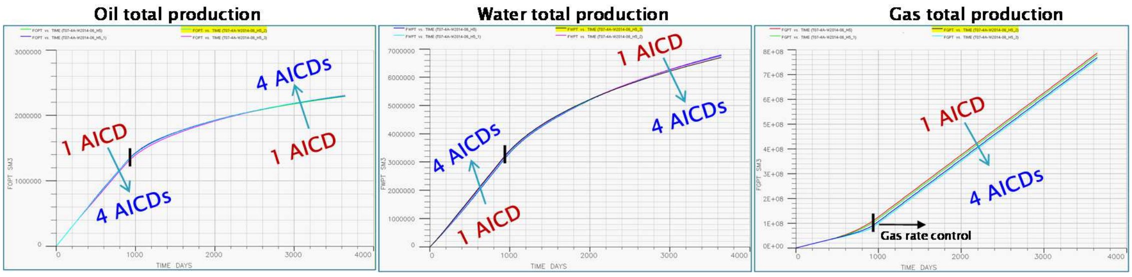

Figure 5-30: AICD-1 optimisation total well performance

This relatively unchanged reservoir inflow performance was achieved despite a significant reduction in the well's bottom-hole pressure {Figure 5-31} for the 1 AICD/joint completion.

Table 5-7: AICD-1 optimisation total well performance

1 AICD (as base case)	2 AICDs	3 AICDs	4 AICDs
FOPT differences (%)	⬆0.33	⬆0.56	⬆0.73
FWPT differences (%)	⬇– 0.31	⬇–0.52	⬇–1.3
FGPT differences (%)	⬇– 0.94	⬇– 2.33	⬇–3.2

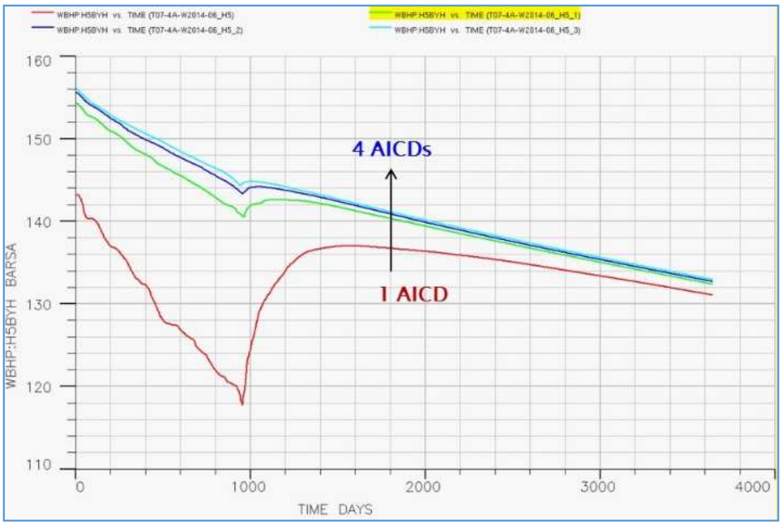

Figure 5-31: AICD-1 optimisation bottom-hole pressure, well performance

A detailed performance analysis at the lateral, segment and reservoir levels for AICD-1 model showed that, at earlier times, less water was produced for completions with a lower number of devices/joint {Figure 5-32}. This occurred despite the very early water breakthrough due to the small distance between the well and the oil-water contact.

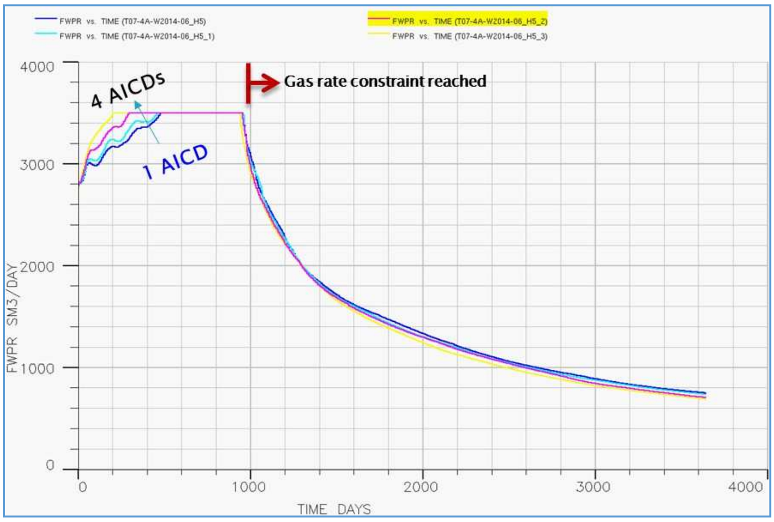

Figure 5-32: Model-X, AICD-1 water production rate for 1,2, 3 and 4 AICDs/joint

The gas production, unlike the water production, increased with a reduced number of AICDs/joint {Figure 5-33}.

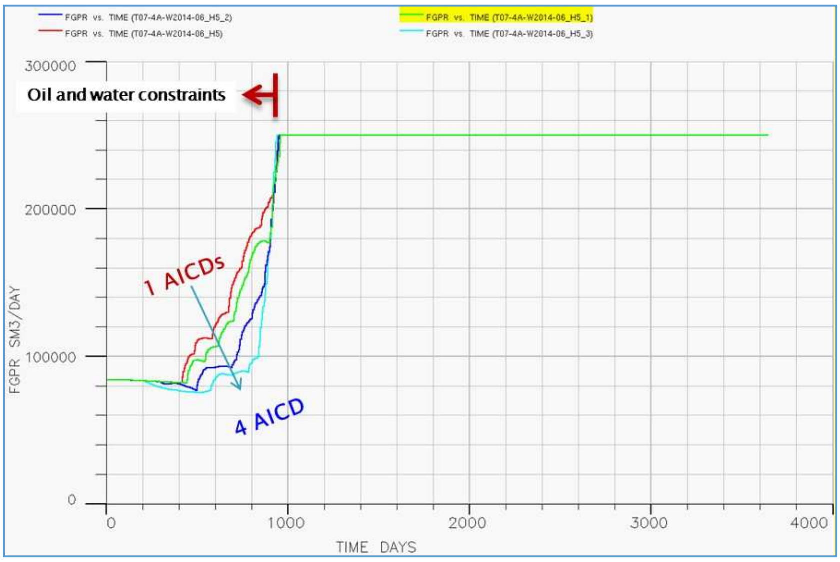

Figure 5-33: Model-X, AICD-1 Gas production rate for 1, 2, 3 and 4 AICDs/joint

This result can be understood by looking at the performance of the individual segments in terms of the Figure 5-29 AICD-1 model behaviour. The segments' oil, water and gas production behaviour was observed to depend on:

1. **The distance to an Oil-Water or Gas-Oil contact:**

   Two performance types were observed. These depended on the closeness to the OWC or the GOC.

2. **The number of joints per segment (i.e. the total number of AICDs)**:

   There is a variable number of AICDs/segment (an average of 6 with a maximum > 13). However, the overall performance of the segment depends on its distance from the fluid contacts (point 1 above).

3. **The active simulation constraint:**

   The active simulation constraint changes successively from Oil Rate to Water Rate to Gas Rate control.

5.7.3.4 Conclusions from Model-X

1) Fine grid resolution was required to capture the saturation changes near the wellbore, e.g. the gas-oil contact movement and the gas cusp development were less obvious for the upscaled model.
2) The recorded oil production increased as the level of LGR cell size reduction increased. The level of LGR had a greater effect on the recorded level of gas production than the presence of an AICD completion in this field model which is sensitive to gas flow. Which signify the importance of near wellbore modelling.
3) The AICD-1 completion improved the oil production. However, the overall change in oil recovery achieved by LGR model cell size reduction was found to be greater. The Table 5-5 values suggest that adding an AICD-completion increased the oil recovery by 4%, whereas LGR cell size reduction changed the recorded increase in oil recovery between 8 to 21%.
4) An interesting observation is that the relative oil gain from the AICD completion was less sensitive (almost independent) to the grid size for the applied completion and AICD model. This observation gives the impression that an AICD completion can be optimised for a large grid model, though the absolute value of the oil recovery will affect the economic calculations. Furthermore, there are other effects, such as annular flow phenomena, that occur in the real field but have not been fully captured in these simulations (e.g. despite modelling the actual well trajectory, full annulus isolation was assumed).
5) All the segments along the well, produced with a more than 50% water cut from day one. This implies that the AICDs reaction (increased flow resistance) during simulation was mainly to control the water rather than the gas. In fact, the AICD-1 completion will produce more gas as long as there is some oil and water co-production, i.e. there is not a very high (almost 100% volume fraction) level of gas production.
6) The results presented above, emphasize the importance of dynamic modelling and coupling of well and reservoir models when assessing the advantages and added value from the AFCD new technology. The well trajectory (undulation), the length, the location and number of valves, the impact of MPF within the wellbore

and the flow dynamics in the near wellbore area as well as the influence of the nearby wells etc. all should be considered.

5.8 Conclusions

Several ICD completion design methods are available for passive FCDs (ICDs). ICD completion design involves optimizing the strength and type of these devices along the wellbore. There is no an AFCD completion optimisation workflow widely adopted yet. The AFCD completion offers an extra degree of freedom by adding a phase-selective functionality to the passive performance of an ICD.

In this chapter we have developed novel methodology to carry out and analyse such an optimization. The methodology includes:

1) A workflow to translate the optimised ICD-completion design into an AFCD completion.
2) The AFCD completion optimisation workflow.
3) A method to plot the optimisation results and to identify the optimum level of fluid selectivity of the AFCDs required for a particular application.
4) Example workflow results and their analysis to relate the AFCD restrictive mechanisms to the reservoir and production conditions.
5) A new method for comparing passive and active FCD’s performance in various reservoir models putting more insights into the added value of the AFCDs’ spontaneous reaction to unwanted fluids.
6) Evaluating the impact of MPF uncertainty on AFCD-completion performance and value prediction.

This methodology can be used by well completion engineers when selecting and optimising the downhole flow control completion, including the autonomous flow control options.

The analysis shows that the maximum value from AFCD can be gained when both the oil flow equalization and water-restriction capabilities of AFCDs are optimised.

Controlling and (potentially) equalising the production profile along the wellbore can improve the oil recovery (sweep efficiency) and delay the breakthrough of unwanted fluid. However, evenly distributed production along the entire well length does not necessarily guarantee the optimal well performance.

The examples considered show that it is important to consider both the AFCD's oil-restrictive and water-restrictive performance. The latter increases in importance as the formation's heterogeneity increases.

Advanced (A)FCD completion design, optimization and selection will benefit from early identification of reservoir challenges and sensing of completion scenarios and options. These include: production mode, identifying unwanted effluent influx (water and gas), balancing inflow profile responses, the pressure along the entire wellbore and the advanced completions modelling (static and or dynamic). An AFCD alleviates the adverse effect of ignoring the uncertainty during optimal completion design by its autonomous reaction to WC.

NPV, which includes water production cost, allowed us to discriminate between the various cases studied compared to evaluating the completions performance on the volume of oil recovered when (i) analysing an AICD completion's performance and (ii) optimising the number of AICDs per segment.

The results obtained from model-X, emphasize the importance of dynamic modelling and coupling of well and reservoir models when assessing the advantages and added value from the AFCD new technology:

(1) The relative oil gain from the AICD completion was almost independent of the grid size for the chosen completion and AICD model.
(2) AICD optimisation showed that the gas production, unlike the water production, increased with a reduced number of AICDs/joint due to various effects (e.g. water production, well trajectory, AICD performance etc.)

The well trajectory (undulation), the length, the location and number of valves, the impact of MPF within the wellbore and the flow dynamics in the near wellbore area etc. all should be considered.

Chapter 6 Conclusions and Future work

6.1 Conclusion

The functions of the various wellbore completion components and their impact on the given well performance need to be fully understood to achieve the full potential of AWCs.

Inflow Control technology has been employed in several fields successfully. The recently introduced, Autonomous Flow Control Devices (AFCDs) have a great potential for further improving the well performance. Their (autonomous) discrimination and control of the different fluid phases, presents new modelling challenges that require extension of today's wellbore/reservoir models and workflows. Their success reported in field trials, their optimisation potential, and the new modelling challenges associated with this new technology (AFCDs) stimulate research to unlock their added value and to suggest improvements for well and technology performance.

AFCD-completions are often designed using steady-state well production simulators, though input from a dynamic, reservoir simulator is preferred. This is of particular importance in evaluating and understanding new concepts and ideas in the context of their long-term value, e.g. improved oil recovery. This way the enhanced prediction, optimization and quantification of the AWC's Added Value can be done. This thesis has strongly focused on the area of stand-alone AFCD and AFCD-completion performance modelling, design, and evaluation both in the long- and short-term production context.

6.1.1 Major problems that were addressed in this thesis:

a) To date, commercial reservoir simulators provide just one equation to describe the performance of all AFCD types using three calibration parameters: x, y, a_{AICD}. To our knowledge, no guidance or proof is available as to whether it captures the multi-phase performance of AFCDs accurately, or the trio of parameters x, y, a_{AICD} can be translated to the situation of different fluid properties, or what combinations of x, y, a_{AICD} are actually physically possible (in the AFCD completion design studies).

b) Limited published laboratory test data on the AFCD (stand-alone) multi-phase flow performance is available. Rules or models must be in place to translate this data into a given reservoir production situation.

c) The MPF configuration in the wellbore, especially in advanced completions, is complex due to the varying, well trajectory, pressure drops (due to FCDs' reaction), rates along the well and influx from the reservoir (phases and rates), etc. However, its modelling is greatly simplified, in the coupled well/reservoir modelling tools available today. This is due to the assumption that the fluids behave as a homogeneous mixture whose properties were averaged (volume weighted) from the individual phases' properties. Such currently used wellbore MPF modelling approach, that was suitable enough for a passive-FCD completion, can be highly inaccurate for modelling the modern, phase selective FCDs and therefore is recognised as needing update.

d) Engineering data provided by Production Logging Tools (PLT) in a real well or by experiments in the laboratory, have indicated stratified multiphase flow to be the most frequently encountered flow environment in horizontal and highly deviated wellbores. Considerable differences in phase velocities and holdup values resulting from small ($\pm 1^0$) changes in wellbore inclination from the horizontal have been observed. A so-called horizontal well is almost never actually horizontal. Several challenges can hinder the originally planned trajectory resulting in a shorter well, varying inclinations and perhaps different target (sand unit) in some cases. Assumptions such as "perfectly horizontal" trajectory and wellbore model gridding/scaling should be evaluated when modelling advanced completions.

e) The physics above should be included in the modelling workflow. It has a considerable impact on the predicted performance of the AFCDs behaviour. The problem is further exacerbated by accumulation of the denser fluid at low points and the lighter (e.g. gas) at the high points of the well trajectory.

f) Finally, several ICD completion design methods are available for passive FCDs (ICDs). ICD completion design involves optimizing the strength and type of these devices along the wellbore. There is no AFCD completion optimisation workflow widely adopted yet. This is despite the AFCD completion offering an extra degree of freedom by adding a phase-selective functionality to the passive performance of an ICD.

6.1.2 Solutions provided

This thesis has provided detailed guidelines for AFCD performance modelling along with workflows, formulae, sensitivity and optimisation studies that allow engineers to evaluate the viability of an AFCD completion and its potential added-value while recognizing the implication of various (routinely) made assumptions and overlooked physics. New methods for analysing, comparing and evaluating AWCs' performance are presented.

6.1.2.1 The following have been developed and presented in this thesis:

a) AFCD performance models that honour the published data. Equations and modelling recommendations for several commercial AFCDs along with a range of modelling options are presented with the pros and cons of each identified. Impact of MPF on the stand-alone AFCDs' performance was evaluated. Equations are provided (e.g. Equation 4-4) which incorporate both, the improved single phase performance formula {Equation 3-18} and a MPF expression that has been found to match data generated during testing AFCDs in a multi-phase flow loop.

b) The methods and workflows have been validated using either actual data wherever possible or synthetic data, and have been implemented in several scenarios which are representative of typical oil field production management cases. The analysis of these scenarios was made possible by the development of a novel methodology to verify the applicability of different types of AFCDs and their impact on production which also allowed optimization of the AFCD-design.

c) Recommendation for increasing the accuracy of commercial well/reservoir simulators when modelling AFCD completions were made by evaluating the impact of the well trajectory, the reservoir/well segmentation and the multiphase flow performance, emphasized the implication of various (routinely) made assumptions and overlooked physics.

d) A novel, extended, Multi-Segment Well (MSW) model application was developed. It captures the impact of annular fluid stratification on (A)FCD performance. This model, was successfully validated against published AICV performance. It can be used to identify the optimum AFCD design performance (e.g. AICV shut-in threshold) for each application.

   (1) The method allowed answering different completion optimisation questions (within the context of well and reservoir interaction) as well as testing various MPF effects, scenarios and concepts in the context of AWC performance.

   (2) The studied examples have shown that an autonomous reaction potentially improves production. However, it was concluded that each AFCD type (available today) provides a fixed performance/resistance for unwanted fluids' inflows (or a fixed shut-in threshold, e.g., for AICVs). The (wider) optimum "intelligent" AFCD ought to capture both, (a) the improvement in oil production through optimal unwanted fluid control (case specific) and (b) allowing the 'good' water

and (or) gas necessary for the sufficient recovery and/or well's outflow performance.

e) Novel methods to visualise and optimise AFCD completions. It has been used successfully to understand the added value from this latest technology, its range of application, success measures, the optimisation techniques and the possible improvements in the valve's physical design and function.

6.1.2.2 Conclusions drawn from this thesis

1) Quantifying the added value from an AWC can be a challenging task. It requires a thorough knowledge about the reservoir, and competent modelling capabilities. It was shown that different types of AWCs will need different modelling approach.
2) The (A)FCDs' performance can be incorporated in a commercial reservoir simulator's wellbore model as: (a) a formula and (b) a tabulated input – the latter approach was found to be more comprehensive and provided a greater flexibility in wellbore modelling; it has been thoroughly explored in this thesis for the purpose of modelling AFCD's newly developed performance formulae as well as for the MPF performance modulation.
3) The formula available today in the commercial software {Equation 3-12} does not suite all AFCD types. The parameterization method presented in this thesis {Figure 3-8} allows using this formula to model the commercial AICD types consistently with the valve dimensions as well as the fluid properties for the given production conditions.
4) Further to the point above, the dimensionally consistent formula {Equation 3-18} allows for a more conclusive match of the AFCD test results with an updated AFCD performance model using the reduced number of performance modelling parameters. This formulation has been extended to allow for better incorporation of MPF (see points 11 – 13 below).
5) The AICV is shown to be different in its performance to other types of AICDs. It is recognised as being a stepwise device (i.e. it changes from one mode to another depending on a specific threshold). It should be modelled differently in a reservoir simulator than the methods proposed for AICDs. A model/formulae to solve this problem has been derived.
6) Extensive modelling of FCD completion performance in a range of reservoir models indicated the following parameters to be important for AWC modelling and design:

1- Fluid properties, and how to translate the AFCD laboratory test performance parameters from the test fluids to the reservoir fluids.
2- AFI configuration is an important factor to be considered, e.g. the number and location of packers. The appropriate wellbore model segmentation with the resolution to capture the AFI should be specified.
3- The well's liquid production rate.
4- The pressure distribution across the AWC and its possible constraints e.g. due to total and critical coning flow rates, sand production, artificial lift, etc., when modelling the well under drawdown or BHP constrained production. The resulting drawdown should be considered during completion optimization.

7) The presented results show that, the ICD completion apply high pressure drop across the completion. Furthermore, the inevitable loss in ICD-completed well's PI at the early production life limit their design flexibility to allow for more oil production initially. AFCDs on the other hand, have different design philosophy. They are used mainly to control the unwanted fluid upon breakthrough. However, they can still be used to apply the necessary initial control where required.
8) An AFCD design implies testing its sensitivity on the:
   a) Optimum single-phase oil control.
   b) MPF response: very important since majority of the well's life will be in this condition for most of the time.
   c) Optimum reaction to single phase unwanted flow (important consideration should be given to the well outflow performance.

   Five reservoir models were examined. The study showed that it is important to consider both the AFCD's oil-restrictive and water-restrictive performance. The latter increases in importance as the formation's heterogeneity increases (Details in Chapters 4 and 5).
9) The MPF configuration in the AWC is complex. Generally, it is understood that the AWC's will flow a series of varying phases with different compositions, between 100% oil to 100% gas (or) water to mixture. Such effects may have a relatively short time scale (e.g. minutes), resulting from the varying rates along the well and influx from the reservoir (phases and rates). Within the context of reservoir simulation however, the sparser timescale modelling is required. The reservoir simulation is not "normally" detailed, as such, in terms of simulation time steps (normally month(s) long), nor in terms of capturing the spatial reality surrounding the wellbore as well as deep in the reservoir (geological uncertainty). An AFCD completion performance

model has been presented to translate the fast multi-mode flow into a reservoir simulator.

10) The multiphase flow is greatly simplified, in the coupled well/reservoir modelling tools available today. The problem is further exacerbated by accumulation of the denser fluid at low points and the lighter (e.g. gas) at the high points of the well trajectory. As far as AFCD completion modelling is concerned, this was recognised as needing update.

11) Section 3.4.1 illustrates the impact of the stand-alone AFCD MPF assumptions on the AICD completion modelling. In section 4.2.3 a generalised equation {Equation 4-4} is provided. It incorporates both, the improved single phase performance formula {Equation 3-18} and a MPF expression that has been found to match data generated during testing AFCDs in a multi-phase flow loop. Equation 4-4 is dimensionally consistent and assumes pseudo-volumetric averaging of single-phase AFCD response. 4 variables (parameters) were employed to match the AFCD single-phase and MPF performance. The methodology presented here facilitates incorporating the MPF performance within the current simulators capabilities while capturing the fluid stratification effects.

12) MPF in the wellbore was modelled by the means of Equation 4-5 where the following wide range of MPF performance curves has been observed during extensive AFCD flow loop laboratory tests (personal communication):
    i) A “slow”, or tolerant, AFCD response to an increase in the water or gas fraction.
    ii) A “fast”, or highly restrictive, AFCD response to the unwanted fluid phase.
    iii) A “linear” response to MPF performance.

13) The analysis of the impact of traditional wellbore segmentation and MPF modelling on AFCDs when a stratified flow environment exists shows that:
    a) The pressure drop across the AICD increases and the rate decreases as the device’s response to water becomes more restrictive due to stratification.
    b) A considerable difference in the system performance (flow rate) is observed at various WC for the MPF designs used (i.e. ‘slow’, ‘linear’ and ‘fast’ [response to WC] models).
    c) The total flow rate for segregated annular flow is lower than when modelled with homogeneous annular flow. This sometimes can be alleviated by introduction of a pseudo MPF performance where MPF parameters can be calculated (iteratively) to emulate the stratified flow performance while actually modelling the homogeneous flow. The workflow (2) joins the well’s inflow/outflow, and

the AFCD performance to obtain (b, v) values allowing the homogeneous AFCD MPF to incorporate the fluid stratification effects while accurately capturing the single-phase performance.

d) Segmentation sensitivity has shown that the AWC modelling precision requires a fine resolution model along with the true well trajectory so that a more detailed calculation can be encompassed encouraging the fluid separation and slippage effects to be captured; therefore the fluid sensitive AWCs' (AFCDs) response can be examined.

14) Observations from the conducted MPF AWC modelling includes:

   a) Fine grid resolution plays a significant rule in capturing the saturation changes near the wellbore, e.g. the gas-oil contact movement and the gas cusp development. So much so that in terms of the AFCDs added value – its dependence on the level of LGR had higher impact on the recorded level of gas production than the actual presence of the gas-controlling AICD completion in the tested field

   b) The relative oil gain from the AICD completion was less sensitive (almost independent) to the grid size for the applied completion and AICD model. This observation is interpreted as the AICD completion can be optimised for a large grid model, though the absolute value of the oil recovery will affect the economic calculations.

   c) In three phase flow conditions, the interaction between the AFCD response to water and gas should be considered. E.g. the modelled valves in model-X case study, imply that, the optimum production depends more on water production control than gas control due to the employed greater resistance to water.

   d) The presented results show that fluid segregation in the wellbore promotes a higher pressure loss across the AFCD-completions. This should be accounted for while designing the well completion (or adjusting the design at wellsite).

15) An ICD completion may require a high level of flow equalization to delay water breakthrough, while an optimized AFCD completion allows for greater oil production with higher initial area open for flow. This has a direct impact on the well's Inflow performance and early life oil production.

16) Correct modelling of inflow control devices and annulus flow (see points 3 - 6, 11 - 14) will improve reliability of simulation results and eliminate related convergence problems.

17) Workflow (3) described in Figure 5-1 provides a new insight for AFCD-completion optimisation. Methods to plot the optimisation results and to compare the passive and active FCD's performance in various reservoir models are presented. The sensitivity and optimisation study in chapter 5 shows that:
    - An optimized AFCD completion provides greater (than ICDs) flexibility to deal with the reservoir uncertainties. This is because the ICD completion is designed to permanently restrict the flow delaying the breakthrough of unwanted fluids. Such design is reservoir model based and is, therefore, more sensitive to uncertainty, pressure and rates.
    - An optimum AFCD -completion shows a clear improvement in production and recovery for the selected case studies as compared with the conventional or ICD completion. Incremental oil production depends on well's production conditions.
    - NPV, which includes water production cost, allowed us to further discriminate between the various AFCD designs studied compared to evaluating the completions performance based on the volume of oil recovered when (i) analysing an AICD completion's performance and (ii) optimising the number of AICDs per segment.
18) AFCD designs should always consider well deliverability (inflow/outflow) at later times when unwanted fluid BT and pressure depletion prevail. The higher robustness of an optimum selected AFCD design for geological uncertainty, compared with passive ICD design, is shown in chapter 5.
19) Each AFCD type (available today) provides a fixed performance/resistance for unwanted fluids' inflows (or a fixed shut-in threshold, e.g., for AICVs). The modelling results presented here show that, one AFCD type applied to all sections may not be the global optimum. Furthermore, increasing the resistance to water without optimisation may hinder the maximum oil recovery objective. The (wider) optimum "intelligent" AFCD ought to capture both, (a) the improvement in oil production through optimal unwanted fluid control (case specific) and (b) allowing the good water and (or) gas necessary for the well's outflow performance.
20) The analysis of the results presented in this thesis, emphasizes the importance of dynamic modelling and coupling of well and reservoir models when assessing the advantages and added value from the AFCD new technology. The well trajectory (undulation), the length, the location and number of valves, the impact of MPF within

the wellbore and the flow dynamics in the near wellbore area as well as the influence of the nearby wells etc. were all found to be important.

6.2 Future work

The effort to advance our numerical simulation capabilities in accurately modelling, optimising and capturing the physics involved in AFCD-completions performance/response downhole is far from complete. Many areas for research and improvements remain; constrained, however, by the limited access to performance data due to information confidentiality and companies' publishing procedure. Based on the work presented in this thesis, the followings points for future work are recommended:

1) One conclusion from this thesis shows that: The (wider) optimum "intelligent" AFCD ought to capture both, (a) the improvement in oil production through optimal unwanted fluid control (case specific) and (b) allowing the good water and (or) gas necessary for the well's outflow performance. This conclusion should be followed by a further research which can lead to the development of a new "more intelligent" AFCD.
2) A simple workflow for the optimal AFCD-completion response based on the work presented in this thesis is required. This is of particular importance at the completion installation stage when the (A)FCD completion design is revised at the wellsite against the new geological information obtained after drilling the well (e.g. open-hole well log). A short time is allocated for this important analysis.
    - This includes: Developing an understanding of AFCDs' interaction with the reservoir at various field/fluid conditions (uncertainty assessment), then investigate the possibility of using a simpler (snap-shot based) modelling approach for optimizing the AFCD-completion expected (dynamic) performance.
3) Further investigation is required on the inflow/outflow interaction for wells completed with AFCDs. This step is very important especially for AFCDs with a strict resistance to unwanted fluids' flow (e.g. AICVs).
4) AFCD completion impact on recovery in full-field applications is required enlightened with the methods and findings presented in this thesis:
    - AFCDs implementation in multi-lateral wells; especially when combined with ICVs, etc.
    - Wells' interaction.

5) The AFCDs' application envelope should be further investigated. AFCDs provide a wide range of reaction to unwanted fluids. The impact of the MPF on the objective function for various geological scenarios needs further effort for research.
6) AFCDs can potentially deliver high oil production (initially) while still being able to control unwanted fluids at breakthrough. This work have shown that early oil production provided extra "Added Value" from AFCDs when compared with ICDs. Such added value requires further evaluation.
7) Further assessment and optimization of the added value from AFCDs is required for:
   a) SAGD.
   b) Fractured reservoir.
   c) Producers within a water injection scheme.
   d) Exiting wells suffering a localised high water production.
   e) Gas fields to stop/control water production.
   f) Other applications.
8) Evaluation and comparison between the effect of ICV, ICD and AFCDs on clean-up process in advanced well completions. Further investigation to demonstrate when irregular clean-up in AFCD completed well will be a problem i.e. some AFCD might open faster affecting the performance of others.
9) Further investigation is required to reveal the impact of Re dependency on passive FCD-completion performance when detailed MPF modelling is considered (e.g. stratified flow environment or undulating/inclined well trajectories).
10) Optimal placement of annular flow isolation (packers) require further research along with other uncertainties and risks (e.g. formation of emulsion or scale and its implications on AFCD performance and added value.
11) Other new types of AFCDs introduced require further research.
12) The AFCDs' performance during backflow or crossflow should be investigated. The AFCDs' injection performance (countercurrent/crossflow flow) is not published (the software calculations are based on reversing the flow sign).
13) A Transient wellbore simulator (e.g. OLGA) able to model the multi-phase flow regimes accurately inside the wellbore is required for further investigation of MPF impact on AFCDs' performance. A comparison study should be carried out between OLGA/ROCX simulator and Eclipse reservoir simulator. The work requires constructing same reservoir models in Eclipse and ROCX simulators.

Appendices

The value of the computation is only as good as the engineer's creativity and understanding of the modelled system in terms of his/her selection of the data in-put and the level of the analysis of the results. Computation is a powerful tool. It allows the engineers to design and test the efficiency/applicability of various ideas. However, with such power comes a great responsibility. One should be aware of the limitations and areas of applications of the tool being used. This also implies taking into considerations the uncertainties in the field of application.

Appendix (1): Successful AWC implementation

Checklist for successful implementation [18]

AICD BENEFITS	BEFORE DRILLING	UNDER DRILLING (Until bit reaches total depth)
1. Enhance and equalize production, delay and minimize the flow of unwanted fluids such as water and or gas into the vertical, horizontal or deviated wellbore **2.** Adjust pressure along the entire wellbore, especially important in new and mature field re-vitalization **3.** Balance production through the interval, and for stimulation or acidizing **4.** Help increase recoverable reserves and extend well production life **5.** Utilizes innovative technology to direct flow **6.** Increase reliability through design simplicity **7.** Reduce cost and risk of handling unwanted fluid at surface	**1.** Well placement, length, dimensions, sensitivities **2.** Flow control with AICDs, zone isolation, compartmentalization, design process **3.** Effects and benefits of AICD gravel packing vs. conventional completions, both in injection and production modes **4.** Early water entry and coning (which can occur anywhere along the wellbore) **5.** Permeability ranges, heterogeneity and anisotropy tendencies **6.** Pressure balancing and equalization **7.** Fluid saturations variations **8.** Vertical anisotropy **9.** Wellbore damage and skin	**1.** Preliminary completion tally **2.** Calibration with LWD petrophysical interpretation **3.** Very important to interrogate initial water and oil saturations **4.** Compartmentalization **5.** Identify intervals with potential for fines migration and isolate this intervals **6.** Bypassing non-pay zones **7.** Prevent fine particles from entering permeable sections like consolidated formations **8.** In mature fields, prepare several scenarios related to rock and fluid properties vs. all available a-priori data **9.** Wellbore damage and skin scenarios **10.** Wellbore cleanup options
	10. Production performance, initial conditions **11.** Preliminary tally of alternatives as an aid to hardware and completion tools logistics, preparation and readying for field operations start date, early start of production.	**11.** Use PVT tables as a function of temperature (e.g., CSS injection conformance) **12.** Final completion tally **13.** Production performance

AICD POST-COMPLETION FOLLOW-UP	VALUE-ADDED WORK-OVERS
1. Future alternative completion scenarios **2.** Minimizing uncertainties **3.** Post-well production follow-up e.g., matching PLT logs **4.** Lessons learned – sharing knowledge **5.** Future alternative completion at group or field level	Already completed producer or injector wells will require a historical in-depth revisit of all available data and often with more than triple annulus geometry pre-existing hardware (not easy to dynamically simulate) to assess, screening and recommendation of re-completion potentials, often will require verification data measurements for fine tuning and calibration.

Appendix (2): Issues related to completion components' utilization in AWC

AWC component	Some major challenges and characteristics	Reviewed in
Inflow Control Device (ICD)	1- Need to choose between the different types available (e.g. Nozzle, tube, orifice) 2- Provides passive control only	[6, 97, 98]
Interval Control Valve (ICV)	1- Need to choose between the different types available (e.g. on/off and multiple positions) 2- Number of devices which can be installed along the completion is limited. 3- Selection of real-time control strategy can be non-trivial. 4- Downhole information is required for optimum control.	[42, 99, 100]
Autonomous Inflow Control Device (AICD)	1- Need to choose from various types available due to differences in operating principles. 2- Modelling and design challenges due to device performance depending on the produced fluid properties. 3- Requires advanced modelling techniques and completion optimization workflows 4- Their performance correlation in multiphase flow environment is not publicly available 5- Further field experience required to increase industry confidence.	[1, 18, 33, 59]
Autonomous Inflow Control Valve (AICV)	1- Shuts (1% by-pass) or restricts (up to 20% by-pass flow) when unwanted fluid fraction reaches critical level at valve location. 2- Valve performance depends on fluid properties, but multiphase flow performance correlations are not publicly available. 3- Requires advanced modelling techniques and completion optimization workflows.	[24, 34, 70]
Screen	1- Screen stand-off (annulus between the screen and base pipe) may affect AWC functions in heavy oil production (Oyeka et al.2014). 2- Studies on the impact of fluid flow regime across various completion components under North Sea conditions available.	[4, 101]

Packer	1- Various types and rating available. 2- The optimum number and location of packers in AWC can be a non-trivial design challenge 3- Installation risks need to be considered.	[6, 84, 102]
Gravel pack (GP)	1-Can be operationally difficult to combine with AWC. 2-Axial flow isolation efficiency of the Gravel pack may not be complete.	[21]
Blank pipes	1-Normally installed across intervals with specific reservoir properties: e.g. shale, fractures, super K, etc... 2-Annulus isolation efficiency/reliability across such zones needs to be designed carefully.	[6]
End-of-completion valve - and other completion accessories	Malfunctioning of down-hole completion accessories degrades AWC performance.	[103]
Sliding sleeve circulating device	Used as a contingency to bypass the AICDs. Valuable when the well productivity is lower than expected.	[45]

Appendix (3): The procedure to predict horizontal-well performance with (A)FCDs

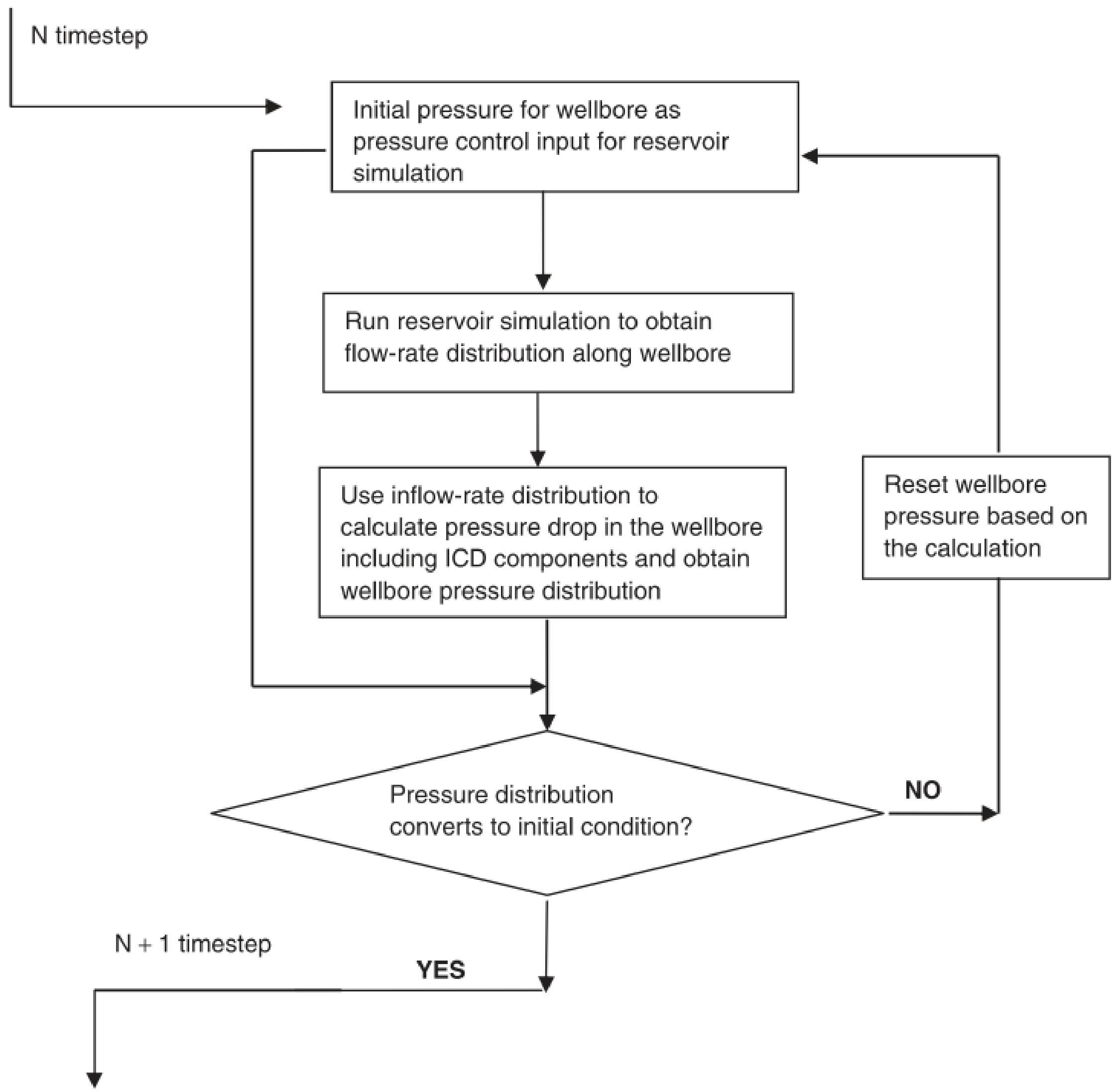

The procedure to predict horizontal-well performance with ICDs [68]

Appendix (4): Problem of modelling a well segment equipped with AICVs

In the case of oil and water/gas flow, the multi-modal response of the device makes a unique case. The segregated flow in the annulus makes the device(s) react sequentially to either oil or water/gas, as opposed to the "homogeneous flow" modelling approach that is traditionally assumed in reservoir simulators. Capturing the sequential reaction of the device to either oil or water in a reservoir simulator is challenging.

We are aiming to derive a model, formulae to solve this problem, and offer a more accurate way of modelling AFCD completion performance in a commercial reservoir simulator. Note that this concept of a flow control dependent on the inflow performance is relatively new to the industry (and so is the AFCD!). Normally the AFCD completion is installed to control a particular type of the unwanted fluid, e.g. water in the case of heavy oil production, or gas in the case of light-oil production. In the below derivations we will be assuming water-oil case to be specific, although the result is valid for gas-oil cases since the gas compressibility effect in the small annular space can be neglected in this problem.

It is believed that some AFCDs react to water only when the WC reaches certain limit, despite of the annulus water HU and whether the AFCD is submerged to water or not. Other AFCDs are believed to respond to water only when submerged to water, i.e. when the annulus water HU reaches a certain critical value (not necessarily corresponding to level of the AFCD position). We assume the situation of the "critical" condition, i.e. the condition when the critical HU or WC is reached and the device(s) starts responding to both oil and water flows. If there are multiple AFCDs in one well segment, then this happens when all but one are already in the 100% water production mode, while the last AFCD (e.g. the one at the top of the segment, or the farthest from the water source) is intermittently exposed to either oil or water flow.

The completion performance when the WC is below the above-defined critical condition is relatively straightforward to model traditionally with the single-phase AFCD performance curve, and has been extensively described elsewhere . Unfortunately, such "non-critical" period can be short, let alone the AFCDs completions are designed to actually react to water, so by default to operate within the "critical" condition. So the relevance of this work findings is appropriate.

Deriving the flow performance model for a well segment equipped with a single AFCD

Consider a well segment – i.e. the section between two adjacent packers. Assume it is equipped with one AFCD.

We aim to ultimately be able to describe the well segment performance using the classical ICD terminology, i.e. to describe the pressure drop across a single AFCD as

$$\overline{dP}_{AFCD} = \overline{a}_{AFCD} \cdot \overline{Q}_l^2$$

where $\overline{a}_{AFCD} = f(inflow\ performance, a_{AFCD,w}, a_{AFCD,o})$

Where the bars represent the time averages of the reservoir simulation time step. This format makes at it easy to incorporate this performance into most of the available reservoir simulators.

See the notation below.

Notation and Nomenclature

- Operator $\overline{f}$ means averaging *f* over a reservoir simulation time-step (usually 1-3 months) at a particular time-step. We are essentially looking for thus averaged performance because a reservoir simulator does not need to (and even is preferred not to) consider processes happening at a faster rate.
- *a* is strength. We understand it as a constant relating the pressure change across a device to the liquid rate square flowing across the device. In the case of AFCD with stratified flow in the annulus we distinguish two instantaneous AFCD strengths:

  $dP_{AFCD} = a_{AFCD,w} \cdot Q_w^2$ when there is only water flow across the device ("water mode"), and

  $dP_{AFCD} = a_{AFCD,o} \cdot Q_o^2$ when there is only oil flow across the device ("oil mode").

  Note that ideally the AFCD is designed so that $a_{AICV,o} \ll a_{AICV,w}$

  It is an assumption that the performance of a single AFCD can be matched to the single-phase oil or water flow as a quadratic function of rate, although this is often the case, andi i not the AFCD-paraemtric studies can be used to obtain an acceptable match (Eltazy et al 2014).

- J_l is a liquid productivity index of the well segment, i.e. $J_l(P_{reservoir} - P_{annulus}) = Q_l$
- Q_{inflow} is the instantaneous rate flowing **into** the well segment annulus from the reservoir
- $Q_{outflow}$ is the instantaneous rate flowing **from** the well segment annulus to the tubing across the AFCD
- $\Delta P \equiv P_{reservoir} - P_{tubing}$ (definition)

- WC_{inflow} is the water cut of the fluid flowing into the well segment annulus from the reservoir

Problem statement:

5. A single AFCD is installed across the well segment.
6. The AFCD performance can be described as $dP_{AFCD} = a_{AFCD,w} \cdot Q_w^2$ in the water mode and $dP_{AFCD} = a_{AFCD,o} \cdot Q_o^2$ in the oil mode.
7. Flow rates are such that the flow in the annulus is stratified (or, more generally, segregated). This means that the AFCD can be open to either water or to oil flow at a time.
   Note: In a more complete study one has to check the critical velocities/rates, fluid properties, and wellbore configuration where this assumption is violated.
8. P_{tubing} (also called *BHP* or P_{wf}) and $P_{reservoir}$ can be considered constant during a reservoir simulation time-step. This also means that ΔP can be considered constant during a reservoir simulation time-step. (The validity of this condition is confirmed by reservoir simulation studies.)

Assumptions:

5. Assume there is a critical water hold up $HU_{w,crit}$ in the annulus so that when $HU_w >= HU_{w,crit}$ the AFCD is mostly exposed to water, and otherwise – to oil.
   NB1: For instance this can be a water hold up so that the water surface is across the AFCD position, or it can be some experimental value (e.g. 98%), or other.
   NB2: Note that we are only assuming that this $HU_{w,crit}$ is constant during a simulation time-step, not necessarily throughout the whole production period.
   NB3: As long as this assumption is valid we can ignore the well segment trajectory or other well geometry or flow related factors at this stage in this study.
6. Consider a situation when the annulus water hold-up HU_w is such that $HU_w = HU_{w,crit}$. Then the AFCD is going to be exposed to a series of oil and water flows. *This is easy to comprehend assuming that the water hold up is suddenly higher than the critical water hold-up. The AFCD will be exposed mostly to water and the well segment outflow will be water only $Q_{l,outflow}=Q_{w,outflow}$, while the well segment inflow Q_{inflow} will consist of both oil and water (given that $0< WC_{inflow}<1$). Moreover, $Q_{l,intflow}=Q_{w,outflow}$ from the mass balance considerations when the $P_{annulus}$ is stabilised at a particular mode. So basically the segment outflows water which is replaced by water and oil. Essentially, the water hold up in the annulus*

will be decreasing until it reaches the critical value, after which the AFCD will generally "switch" to the oil mode and the process will continue in the oil mode. We are not concerned at this stage how often the AFCD will be exposed to oil or water. This may depend on the transient flow effects in the system, segregated flow regime parameters, CFD effects, etc.

Our assumption is that such fluctuations will happen at least twice during the simulation time step (e.g. duration_of_1_oil_mode + duration_of_1_water_mode <= 1-3 months).

7. Linear Inflow Performance Relationship assumption is valid during a simulation time step. I.E. $J_l(P_{res} - P_{annulus}) = Q_l$ applies.
8. Frictional pressure drop in the annulus is negligible compared to the drops across the reservoir and completion (normally holds true mainly because the AFCD completion is designed and installed to act so).

Derivation lemmas:

a. Because the AFCD can adapt to the new (oil or water) mode fast (known to be in the order of minutes), and also because this study discusses the liquid flow only (note that the liquids are slightly compressible unlike gasses), the well segment pressures are expected to react fast when the mode changes with minimal wellbore storage effects in the annulus. We believe the speed of change of the annulus pressure after a mode "switch" will be mostly governed by the slowest process - the transient reservoir response (i.e. the build-up or draw-down times). In low-to-very high permeability formations the transient response is in the order of hours or days, which is by far less than the simulation time step (1-3 months). So we can state as a first order of accuracy that the annular pressure stabilises fast (compared to 1-3 months) after the AFCD switches modes. *Note that this statement may be violated in tight formations and/or viscous oil reservoirs.*

Now, since the annular pressure does not change during a single oil or water flow mode, the mass balance dictates that $Q_{l,intflow}=Q_{l,outflow}$.

See also discussions in Assumption 2 above.

b. Assumption 2 states that there will be a series of mode switches during a simulation time step, so the average $WC_{outflow}$ can be calculated using the times $\overline{t_w}$ and $\overline{t_o}$ the AFCD needs to "suck-off" extra water or extra oil respectively ("extra" here has the same sense as above – the excessive phase volume above or below the critical water hold up). This gives

$$\overline{WC_{outflow}} \equiv \frac{\overline{Q_{w,outflow}}}{\overline{Q_{w,outflow}} + \overline{Q_{o,outflow}}} = \frac{Q_{w,outflow} \cdot \overline{t_w}}{Q_{w,outflow} \cdot \overline{t_w} + Q_{o,outflow} \cdot \overline{t_o}}$$

(1)

c. It is possible to derive mathematically, but is also intuitively understood that the average outflow water cut equals the inflow water cut. In a nut shell, the system periodically "sucks off" extra phases, and when averaged over a simulation time-step the average phase outflow equals the inflow. So we have:

$$\overline{WC_{outflow}} = WC_{inflow}$$

(2)

d. Naturally, on average the system will have to "suck off" the volumes dV of phases relating as oil and water rates, i.e.: $\frac{dV_o}{dV_w} = \frac{1-WC}{WC}$. Otherwise, this would violate the material balance in the system (e.g. otherwise it would be that more oil is been produced from the segment than flowing into the segment while assuming that on average the oil does not accumulate in the segment for a given simulation time step duration).

Derivation in brief:

The nodal system balance gives:

$$P_{tubing} = P_{reservoir} - (P_{reservoir} - P_{annulus}) - (P_{annulus} - P_{tubing}) = P_{reservoir} - \frac{Q_{l,inflow}}{J_l} - a_{AFCD} \cdot Q^2_{l,outflow}$$

(3)

which is rearranged as

$$a_{AFCD} \cdot Q^2_{l,outflow} + \frac{Q_{l,inflow}}{J_l} - \Delta P = 0$$

(4)

Note that $Q_{l,intflow}$=$Q_{l,outflow}$ (Lemma a).

As discussed above, in the water mode $a_{AICV} = a_w$ and $Q_{l,outflow} = Q_{w,outflow}$, while in the oil mode $a_{AFCD} = a_o$ and $Q_{l,outflow} = Q_{o,outflow}$.

Solution to Equation 4 gives

$$Q_{w,outflow} = \frac{\sqrt{1+4J_l^2 a_w \Delta P} - 1}{2J_l a_w}$$ during the water mode; and

(5)

$$Q_{o,outflow} = \frac{\sqrt{1+4J_l^2 a_o \Delta P} - 1}{2J_l a_o}$$ during the oil mode.

(6)

Consider an extra volume dV of a phase exceeding the critical hold up. If it is oil, then the average time for the system to suck this extra oil volume off is

$$\overline{t_o} = \frac{dV_o}{Q_{o,outflow}} = \frac{dV \cdot 2J_l a_o}{\sqrt{1+4J_l^2 a_o \Delta P} - 1}$$

(7)

If it is water then the time is

$$\overline{t_w} = \frac{dV_w}{Q_{w,outflow}} = \frac{dV_w \cdot 2J_l a_w}{\sqrt{1+4J_l^2 a_w \Delta P} - 1}$$

(8)

On average the system will be sucking off the excess oil for

$\frac{\overline{t_o}}{\overline{t_w} + \overline{t_o}}$ *100% of the time (during the given reservoir simulation time step).

Average outflow liquid rate during a simulation time step is given by the instantaneous outflow, oil or water rates and the times of producing oil or water:

$$\overline{Q_{l,outflow}} = Q_{o,outflow} \frac{\overline{t_o}}{\overline{t_w} + \overline{t_o}} + Q_{w,outflow} \frac{\overline{t_w}}{\overline{t_w} + \overline{t_o}}$$

or, using the definition of WC (also remember $\overline{WC_{outflow}} = WC_{inflow}$):

$$\overline{Q_{l,outflow}} = \frac{Q_{o,outflow}}{1 - \overline{WC_{outflow}}} \frac{\overline{t_o}}{\overline{t_w} + \overline{t_o}} = \frac{Q_{o,outflow}}{1 - WC_{inflow}} \frac{\overline{t_o}}{\overline{t_w} + \overline{t_o}}$$

(9)

Equation 9 can be rearranged using Equations 5,6,7,8 as (note that for simplicity we write WC instead of WC_{inflow}):

$$\overline{Q_{l,outflow}} = \frac{\sqrt{1+4J_l^2 a_o \Delta P} - 1}{2J_l a_o \left(1 - WC + WC \frac{a_w}{a_o} \frac{\sqrt{1+4J_l^2 a_o \Delta P} - 1}{\sqrt{1+4J_l^2 a_w \Delta P} - 1} \right)} \tag{10}$$

We are looking for $\overline{a}_{AFCD} = f(\textit{inflow performance}, a_{AFCD,w}, a_{AFCD,o})$ where $\overline{dP}_{AFCD} = \overline{a}_{AFCD} \cdot \overline{Q}_l^2$.

Averaging Equation 4 gives

$$\bar{a}_{AFCD} \cdot \bar{Q}^2_{l,outflow} + \frac{\bar{Q}_{l,outflow}}{J_l} - \Delta P = 0$$

(11)

From Equation 11:

$$\bar{a}_{AFCD} = \frac{\Delta P - \dfrac{\bar{Q}_{l,outflow}}{J_l}}{\bar{Q}^2_{l,outflow}}$$

(12)

Finally, expanding the terms in Equation 12 using Equation 10 we find the exact solution of the time-step averaged AFCD strength:

$$\bar{a}_{AFCD} = \left(\Delta P - \frac{\sqrt{1+4J_l^2 a_o \Delta P} - 1}{2J_l^2 a_o \left(1 - WC + WC \dfrac{a_w}{a_o} \dfrac{\sqrt{1+4J_l^2 a_o \Delta P} - 1}{\sqrt{1+4J_l^2 a_w \Delta P} - 1} \right)} \right) \Bigg/ \left(\frac{\sqrt{1+4J_l^2 a_o \Delta P} - 1}{2J_l a_o \left(1 - WC + WC \dfrac{a_w}{a_o} \dfrac{\sqrt{1+4J_l^2 a_o \Delta P} - 1}{\sqrt{1+4J_l^2 a_w \Delta P} - 1} \right)} \right)^2$$

(13)

The average AFCD strength is now a function of the inflow performance as well as of the AFCD performance. Note that the critical water hold-up value is not present and its value is therefore irrelevant here.

We will now simplify Equation 13 to make it more usable.

Simplification of Equation 13

Additional assumptions:

3. The AFCD is designed to promote and reasonably equalise oil inflow so that

   $dP_{AFCD,oil\,mode} \le \left(P_{reservoir} - P_{annulus,oil\,mode} \right)$

4. The AFCD is designed to restrict water inflow so that

   $dP_{AFCD,water\,mode} >> \left(P_{reservoir} - P_{annulus,water\,mode} \right)$

Additional derivation in brief:

Additional Assumptions 1 and 2 allow us presenting the Solutions 5 and 6 as a first and second order Taylor series respectively (the infinitesimal terms are $4J_l^2 a_o \Delta P \le 1$ for oil mode and $1 << 4J_l^2 a_w \Delta P$ for water mode). This gives

$$Q_{w,outflow} \approx \sqrt{\frac{\Delta P}{a_w}}$$

(14)

$$Q_{o,outflow} \approx J_l \Delta P \left(1 - J_l^{\,2} a_o \Delta P\right)$$

(15)

Using Equations 1, 7, 8, 9, 12 gives:

$$\overline{a_{AFCD}} \approx \frac{1}{\Delta P J_l}\left(\left(1-WC\right)(1+J_l^{\,2}a_o\Delta P)+J_lWC\sqrt{\Delta P a_w}-1\right)\left(1-WC+J_lWC\sqrt{\Delta P a_w}\right)$$

(16)

Now, keeping only the first order accuracy, the average AFCD strength can be found as:

$$\overline{a_{AFCD}} \approx a_o\left(1-WC\right)+a_wWC^2+\frac{WC\left(1-WC\right)}{J_l}\sqrt{\frac{a_w}{\Delta P}}$$

(17)

Note that when WC=0 then $\overline{a_{AFCD}} = a_o$ *while when WC=1 then* $\overline{a_{AFCD}} = a_w$.

For simplicity, we recommend incorporating into the reservoir simulators a further simplified version of Eq. 17 when the WC is high enough for the system to start flowing in the oil-water mode sequentially:

$$\overline{a_{AFCD}} \approx a_w WC^2$$

(18)

Note that:

4. This particular derivation is valid for a well segment containing a single AFCD. So it should be applied in the situations where the annular flow isolation is modelled across each well segment (e.g. for the no annular flow option in Eclipse).
5. In case of multiple AFCDs per well segment we expect to have multiple, critical water hold-up values resulting in a multistage curve $\bar{a}_{AFCD} = f\,(inflow\ performance, a_{AFCD,w}, a_{AFCD,o}, N_{AFCDs\ per\ segment})$. Derivation of such a system is provided below.
6. Note that if the single-phase performance of an AFCD cannot be acceptably described as a quadratic function of rate, and instead is proportional to the rate in the power of x, then it is possible to make adjustments to the derived formulae based on the (x-2)/2 order.

Performance of a well segment with multiple AFCD

Consider a well segment – i.e. the section between two adjacent packers. Assume it is equipped with n AFCDs of the same type.

Assume the performance of each single AFCD can be matched to the single-phase oil or water flow quadratically as described above.

The WC or HU is around its critical value – so all but one AFCDs are already in the 100% water production mode, while the last AFCD (e.g. the one at the top of the segment, or the farthest from the water source) is intermittently exposed to either oil or water flow.

The changes we need to make to extend the "single-AFCD segment" case to the multiple-AFCD case are as follows:

1. The volumes of oil and water produced from the well segment for a given (simulation time-step) duration now related differently due to the fact that when one AFCD is producing oil, the other n-1 AFCDs are producing water:
   dV_w in Eq. 8 will change to:
   $$dV_{w\_nAFCD\_case} = dV_{w_{1AFCD_{case}}}\left(1 - \frac{1-WC}{WC}\gamma(n-1)\right) \quad (19)$$
   where γ is defined as $\gamma \equiv \sqrt{\frac{a_o}{a_w}}$
   This also means that the min WC for which all these derivations are valid is:
   $$WC_{min} = 1/(1 + 1/\gamma(n-1)) \quad (20)$$
   because for the lower values of WC the assumption that the system is at the critical condition – i.e. only one out of n AFCDs can be exposed to oil, does not hold. Note that for the n=1 the minimum WC = 0% as expected.
2. The same fact that when the last AFCD is in the oil flow mode, the other (n-1) AFCDs are producing water, also leads to the following changes to Eqs. 5 and 6:
   $$Q_{w,outflow} = \frac{n\sqrt{n^2 + 4J_l^2 a_w \Delta P} - 1}{2J_l a_w}$$ during the water mode; and
   (21)
   $$Q_{o,outflow} = \frac{\sqrt{\left(1+\gamma(n-1)\right)^2 + 4J_l^2 a_o \Delta P} - 1 - \gamma(n-1)}{2J_l a_o}$$ during the oil mode.
   (22)

With changes, following the same derivation workflow as in the section above we find:

$$\overline{Q_{l,outflow}} = \frac{\sqrt{\left(1+\gamma(n-1)\right)^2 + 4J_l^{\,2} a_o \Delta P} - 1 - \gamma(n-1)}{2J_l a_o (1-WC)\left(1 + \left(\frac{WC}{1-WC} - \gamma(n-1)\right)\frac{a_w}{a_o}\frac{\sqrt{\left(1+\gamma(n-1)\right)^2 + 4J_l^{\,2} a_o \Delta P} - 1 - \gamma(n-1)}{n\sqrt{n^2 + 4J_l^{\,2} a_w \Delta P} - 1}\right)}$$

(23)

Finally, the equation that can be used to describe every single AFCD in the well segment to adequately capture the segment performance, is:

$$\overline{a}_{1AFCDout\,of\,n} = n^2 \cdot \left(\Delta P - \frac{\sqrt{\left(1+\gamma(n-1)\right)^2 + 4J_l^{\,2} a_o \Delta P} - 1 - \gamma(n-1)}{2J_l^{\,2} a_o (1-WC)\left(1 + \left(\frac{WC}{1-WC} - \gamma(n-1)\right)\frac{a_w}{a_o}\frac{\sqrt{\left(1+\gamma(n-1)\right)^2 + 4J_l^{\,2} a_o \Delta P} - 1 - \gamma(n-1)}{n\sqrt{n^2 + 4J_l^{\,2} a_w \Delta P} - 1}\right)}\right) \Bigg/ \left(\frac{\sqrt{\left(1+\gamma(n-1)\right)^2 + 4J_l^{\,2} a_o \Delta P} - 1 - \gamma(n-1)}{2J_l a_o (1-WC)\left(1 + \left(\frac{WC}{1-WC} - \gamma(n-1)\right)\frac{a_w}{a_o}\frac{\sqrt{\left(1+\gamma(n-1)\right)^2 + 4J_l^{\,2} a_o \Delta P} - 1 - \gamma(n-1)}{n\sqrt{n^2 + 4J_l^{\,2} a_w \Delta P} - 1}\right)}\right)^2$$

(24)

It's simplified version (same assumptions as above) is:

$$\overline{Q_{l,outflow}} \approx \Delta P J_l \Bigg/ \left(\left(1-WC\right)\left(\gamma(n-1)+1\right) + \left(WC - (1-WC)\gamma(n-1)\right)\frac{J_l\sqrt{\Delta P a_w}}{n}\right) \tag{25}$$

$$\overline{a_{AFCD}} \approx \frac{n^2}{J_l^{\,2}\Delta P}\left[\left(1-WC\right)\left(\gamma(n-1)+1\right) + \left(WC-(1-WC)\gamma(n-1)\right)\frac{J_l\sqrt{\Delta P a_w}}{n} - 1\right] \cdot$$
$$\cdot\left(\left(1-WC\right)\left(\gamma(n-1)+1\right) + \left(WC-(1-WC)\gamma(n-1)\right)\frac{J_l\sqrt{\Delta P a_w}}{n}\right)$$

(26)

Further, simplifying this equation for high WC values gives a result similar to Eq. 18, with a minor correction (can be ignored in many cases) due to the multiple AFCDs in a segment:

$$\overline{a_{AFCD}} \approx WC^2 a_w\left(1 - \frac{n}{WCJ_l\sqrt{\Delta P a_w}}\right) \tag{27}$$

Appendix (5) Model-X (properties)

```
-- Generated [
-- Format      : ECLIPSE keywords (ASCII)
-- Exported by : Petrel 2013.4 (64-bit) Schlumberger
-- User name   : eltazy khalid
-- Date        : Friday, April 17 2015 10:07:49
-- Project     : 12June13.pet
-- Generated ]

ROCKOPTS                          -- Generated : Petrel
  1* 1* ROCKNUM /

ROCK                              -- Generated : Petrel
     158.2000     0.000285 /

PVTW                              -- Generated : Petrel
         215      1.0132  3.9795E-005      0.39851           0 /

RSCONSTT                          -- Generated : Petrel
      8.7645          40 /

PVDO                              -- Generated : Petrel
          40      1.0527      72.191
      56.316      1.0492       73.85
      72.632      1.0473      75.546
      88.947       1.046      77.282
      105.26      1.0452      79.058
      121.58      1.0446      80.875
      137.89      1.0441      82.733
      154.21      1.0438      84.634
      170.53      1.0435      86.579
      186.84      1.0432      88.568
      203.16       1.043      90.603
      219.47      1.0428      92.685
      235.79      1.0427      94.815
      252.11      1.0426      96.993
      268.42      1.0424      99.222
      301.05      1.0422      103.83
      333.68      1.0421      108.66
  /

DENSITY                           -- Generated : Petrel
      958.38      1020.3     0.81172 /

INCLUDE                           -- Generated : Petrel
'TEST_2AICD_1_2_1_PROP_PROPS.GRDECL' /

FILLEPS                           -- Generated : Petrel
```

Please note: End point scaling option was activated in this model.

SWOF -- Generated : Petrel

0	0	1	1827.8
0.0165	6.04E-07	0.9394	1444.5
0.025	2.27E-06	0.90809	1269.4
0.033	6.63E-06	0.87928	1135.5
0.0495	2.70E-05	0.824	916.02
0.05	2.80E-05	0.82239	910.02
0.066	7.33E-05	0.77316	745.97
0.075	0.000114	0.74703	670.02
0.0825	0.000159	0.72601	613.4
0.099	0.000301	0.68191	510.31
0.1	0.000312	0.67932	504.64
0.1155	0.000516	0.64032	427.55
0.125	0.00068	0.61735	387.59
0.132	0.000824	0.60083	360.88
0.1485	0.001246	0.56315	307.25
0.15	0.001291	0.55981	302.8
0.165	0.001805	0.52705	263.02
0.175	0.002222	0.50588	240.13
0.1815	0.002527	0.49238	226.49
0.198	0.003438	0.45902	196.33
0.2	0.003563	0.45506	192.98
0.2145	0.004566	0.4269	170.93
0.225	0.00541	0.40709	156.92
0.231	0.00594	0.39598	149.52
0.2475	0.007593	0.36624	131.49
0.25	0.00787	0.36184	128.97
0.264	0.009556	0.33768	116.04
0.275	0.011053	0.31929	107.01
0.2805	0.011863	0.31029	102.81
0.297	0.014549	0.28409	91.473
0.3	0.015081	0.27946	89.568
0.3135	0.017649	0.25911	81.631
0.325	0.020074	0.24242	75.563
0.33	0.0212	0.23535	73.09
0.3465	0.025237	0.21285	65.672
0.35	0.02616	0.20824	64.212
0.363	0.029798	0.1916	59.155
0.375	0.033463	0.17695	54.929
0.3795	0.034918	0.17164	53.436
0.396	0.040632	0.15295	48.411
0.4	0.042111	0.14861	47.277
0.4125	0.046976	0.13554	43.953
0.425	0.05222	0.1232	40.922

0.429	0.053982	0.1194	40.004
0.4455	0.061682	0.10452	36.5
0.45	0.063907	0.10068	35.608
0.462	0.070107	0.090871	33.365
0.475	0.077273	0.08097	31.135
0.4785	0.079284	0.078428	30.565
0.495	0.08924	0.067154	28.058
0.5	0.092415	0.063961	27.348
0.5115	0.099999	0.057005	25.801
0.525	0.10941	0.049507	24.125
0.528	0.11158	0.047935	23.77
0.5445	0.12402	0.039891	21.938
0.55	0.12835	0.037427	21.366
0.561	0.13732	0.032815	20.278
0.575	0.1493	0.027527	18.994
0.5775	0.15151	0.026647	18.775
0.594	0.16661	0.021325	17.41
0.6	0.17233	0.019587	16.944
0.6105	0.18265	0.016785	16.166
0.625	0.19755	0.013389	15.166
0.627	0.19966	0.01296	15.034
0.6435	0.21768	0.009786	13.999
0.65	0.22507	0.008698	13.616
0.66	0.23677	0.007195	13.052
0.675	0.25509	0.005292	12.262
0.6765	0.25698	0.005123	12.186
0.693	0.27841	0.003507	11.391
0.7	0.28789	0.002943	11.073
0.7095	0.30117	0.002283	10.659
0.725	0.32389	0.001438	10.025
0.726	0.32541	0.001392	9.9857
0.7425	0.35132	0.000777	9.3659
0.75	0.36371	0.000572	9.1
0.759	0.37913	0.000381	8.7933
0.775	0.40816	0.000157	8.2799
0.7755	0.4091	0.000152	8.2644
0.792	0.44147	4.18E-05	7.7751
0.8	0.45818	1.62E-05	7.5508
0.8085	0.47613	4.63E-06	7.3213
0.825	0.51002	0	6.9009
0.85	0.5662	0	6.32
0.875	0.62665	0	5.7994
0.9	0.69159	0	5.3318
0.925	0.7612	0	4.9107
0.95	0.83567	0	4.5308
0.975	0.9152	0	4.1872

1	1	0	3.8758
/			
0	0	1	4040.6
0.0165	6.04E-07	0.9394	3234.5
0.025	2.27E-06	0.90809	2864.5
0.033	6.63E-06	0.87928	2578.9
0.0495	2.70E-05	0.824	2105.4
0.05	2.80E-05	0.82239	2092.4
0.066	7.33E-05	0.77316	1734.6
0.075	0.000114	0.74703	1567.4
0.0825	0.000159	0.72601	1442.2
0.099	0.000301	0.68191	1212.2
0.1	0.000312	0.67932	1199.5
0.1155	0.000516	0.64032	1025.8
0.125	0.00068	0.61735	935.12
0.132	0.000824	0.60083	874.25
0.1485	0.001246	0.56315	751.05
0.15	0.001291	0.55981	740.8
0.165	0.001805	0.52705	648.61
0.175	0.002222	0.50588	595.21
0.1815	0.002527	0.49238	563.27
0.198	0.003438	0.45902	492.17
0.2	0.003563	0.45506	484.25
0.2145	0.004566	0.4269	431.86
0.225	0.00541	0.40709	398.4
0.231	0.00594	0.39598	380.65
0.2475	0.007593	0.36624	337.15
0.25	0.00787	0.36184	331.06
0.264	0.009556	0.33768	299.65
0.275	0.011053	0.31929	277.61
0.2805	0.011863	0.31029	267.31
0.297	0.014549	0.28409	239.41
0.3	0.015081	0.27946	234.7
0.3135	0.017649	0.25911	215.03
0.325	0.020074	0.24242	199.91
0.33	0.0212	0.23535	193.73
0.3465	0.025237	0.21285	175.11
0.35	0.02616	0.20824	171.44
0.363	0.029798	0.1916	158.67
0.375	0.033463	0.17695	147.95
0.3795	0.034918	0.17164	144.15
0.396	0.040632	0.15295	131.32
0.4	0.042111	0.14861	128.42
0.4125	0.046976	0.13554	119.89
0.425	0.05222	0.1232	112.07
0.429	0.053982	0.1194	109.7

0.4455	0.061682	0.10452	100.6
0.45	0.063907	0.10068	98.283
0.462	0.070107	0.090871	92.432
0.475	0.077273	0.08097	86.591
0.4785	0.079284	0.078428	85.094
0.495	0.08924	0.067154	78.494
0.5	0.092415	0.063961	76.618
0.5115	0.099999	0.057005	72.521
0.525	0.10941	0.049507	68.066
0.528	0.11158	0.047935	67.12
0.5445	0.12402	0.039891	62.229
0.55	0.12835	0.037427	60.696
0.561	0.13732	0.032815	57.775
0.575	0.1493	0.027527	54.316
0.5775	0.15151	0.026647	53.724
0.594	0.16661	0.021325	50.032
0.6	0.17233	0.019587	48.767
0.6105	0.18265	0.016785	46.652
0.625	0.19755	0.013389	43.923
0.627	0.19966	0.01296	43.562
0.6435	0.21768	0.009786	40.729
0.65	0.22507	0.008698	39.676
0.66	0.23677	0.007195	38.124
0.675	0.25509	0.005292	35.94
0.6765	0.25698	0.005123	35.73
0.693	0.27841	0.003507	33.526
0.7	0.28789	0.002943	32.642
0.7095	0.30117	0.002283	31.49
0.725	0.32389	0.001438	29.721
0.726	0.32541	0.001392	29.611
0.7425	0.35132	0.000777	27.873
0.75	0.36371	0.000572	27.125
0.759	0.37913	0.000381	26.261
0.775	0.40816	0.000157	24.812
0.7755	0.4091	0.000152	24.768
0.792	0.44147	4.18E-05	23.382
0.8	0.45818	1.62E-05	22.745
0.8085	0.47613	4.63E-06	22.092
0.825	0.51002	0	20.893
0.85	0.5662	0	19.23
0.875	0.62665	0	17.731
0.9	0.69159	0	16.379
0.925	0.7612	0	15.156
0.95	0.83567	0	14.047
0.975	0.9152	0	13.039
1	1	0	12.122

/

0	0	1	2011
0.0165	6.04E-07	0.9394	1609.7
0.025	2.27E-06	0.90809	1425.6
0.033	6.63E-06	0.87928	1283.5
0.0495	2.70E-05	0.824	1047.9
0.05	2.80E-05	0.82239	1041.4
0.066	7.33E-05	0.77316	863.29
0.075	0.000114	0.74703	780.08
0.0825	0.000159	0.72601	717.78
0.099	0.000301	0.68191	603.31
0.1	0.000312	0.67932	597
0.1155	0.000516	0.64032	510.56
0.125	0.00068	0.61735	465.4
0.132	0.000824	0.60083	435.1
0.1485	0.001246	0.56315	373.79
0.15	0.001291	0.55981	368.69
0.165	0.001805	0.52705	322.81
0.175	0.002222	0.50588	296.23
0.1815	0.002527	0.49238	280.33
0.198	0.003438	0.45902	244.95
0.2	0.003563	0.45506	241.01
0.2145	0.004566	0.4269	214.94
0.225	0.00541	0.40709	198.28
0.231	0.00594	0.39598	189.45
0.2475	0.007593	0.36624	167.8
0.25	0.00787	0.36184	164.77
0.264	0.009556	0.33768	149.13
0.275	0.011053	0.31929	138.16
0.2805	0.011863	0.31029	133.03
0.297	0.014549	0.28409	119.15
0.3	0.015081	0.27946	116.81
0.3135	0.017649	0.25911	107.02
0.325	0.020074	0.24242	99.492
0.33	0.0212	0.23535	96.417
0.3465	0.025237	0.21285	87.153
0.35	0.02616	0.20824	85.324
0.363	0.029798	0.1916	78.969
0.375	0.033463	0.17695	73.635
0.3795	0.034918	0.17164	71.745
0.396	0.040632	0.15295	65.36
0.4	0.042111	0.14861	63.915
0.4125	0.046976	0.13554	59.666
0.425	0.05222	0.1232	55.775
0.429	0.053982	0.1194	54.594
0.4455	0.061682	0.10452	50.069

0.45	0.063907	0.10068	48.914
0.462	0.070107	0.090871	46.002
0.475	0.077273	0.08097	43.095
0.4785	0.079284	0.078428	42.35
0.495	0.08924	0.067154	39.066
0.5	0.092415	0.063961	38.132
0.5115	0.099999	0.057005	36.093
0.525	0.10941	0.049507	33.876
0.528	0.11158	0.047935	33.405
0.5445	0.12402	0.039891	30.971
0.55	0.12835	0.037427	30.208
0.561	0.13732	0.032815	28.754
0.575	0.1493	0.027527	27.032
0.5775	0.15151	0.026647	26.738
0.594	0.16661	0.021325	24.9
0.6	0.17233	0.019587	24.271
0.6105	0.18265	0.016785	23.218
0.625	0.19755	0.013389	21.86
0.627	0.19966	0.01296	21.68
0.6435	0.21768	0.009786	20.27
0.65	0.22507	0.008698	19.746
0.66	0.23677	0.007195	18.974
0.675	0.25509	0.005292	17.887
0.6765	0.25698	0.005123	17.782
0.693	0.27841	0.003507	16.686
0.7	0.28789	0.002943	16.246
0.7095	0.30117	0.002283	15.673
0.725	0.32389	0.001438	14.792
0.726	0.32541	0.001392	14.737
0.7425	0.35132	0.000777	13.872
0.75	0.36371	0.000572	13.5
0.759	0.37913	0.000381	13.07
0.775	0.40816	0.000157	12.349
0.7755	0.4091	0.000152	12.327
0.792	0.44147	4.18E-05	11.637
0.8	0.45818	1.62E-05	11.32
0.8085	0.47613	4.63E-06	10.995
0.825	0.51002	0	10.398
0.85	0.5662	0	9.5704
0.875	0.62665	0	8.8247
0.9	0.69159	0	8.1517
0.925	0.7612	0	7.5429
0.95	0.83567	0	6.9909
0.975	0.9152	0	6.4895
1	1	0	6.0332

/

Well-UN survey

MD (m)	Inclination angle	well length (m)	TVD (m)
2327.44	85	0	2327.44
2419.1	85	91.3	2335.54
2555.53	92	227.6	2334.77
2640.63	95	312.47	2328.47
2768	91	439.77	2325.26
2921.03	89	592.79	2326.67
3025.36	86	696.95	2332.59
3193.86	89	865.4	2336.31
3358.51	92	1030	2332.46
3447.46	94	1118.72	2326.28
3628.83	89	1300.03	2326.41
3746.3	87	1417.05	2336.19

Appendix (6) Multiphase flow in pipes

The fundamental MPF phenomenon occurring in horizontal and vertical pipes for oil-gas, water-oil, etc. include the concepts of SLIP and HOLD UP. The accumulation of the denser phase in the pipe (or the annulus) is "an equilibrium phenomenon i.e. the in- and out-let flow rates of a particular phase flowing in the pipe are the same". These concepts are best illustrated by the aid of the following mathematical expressions and the Figure (Davies D., 2007) [87]:

Subscripts g, L, o and w refer to the gas, liquid, oil and water phases respectively, while Q is the phase volume flow rate, V the velocity and A_p the cross sectional area of the pipe.

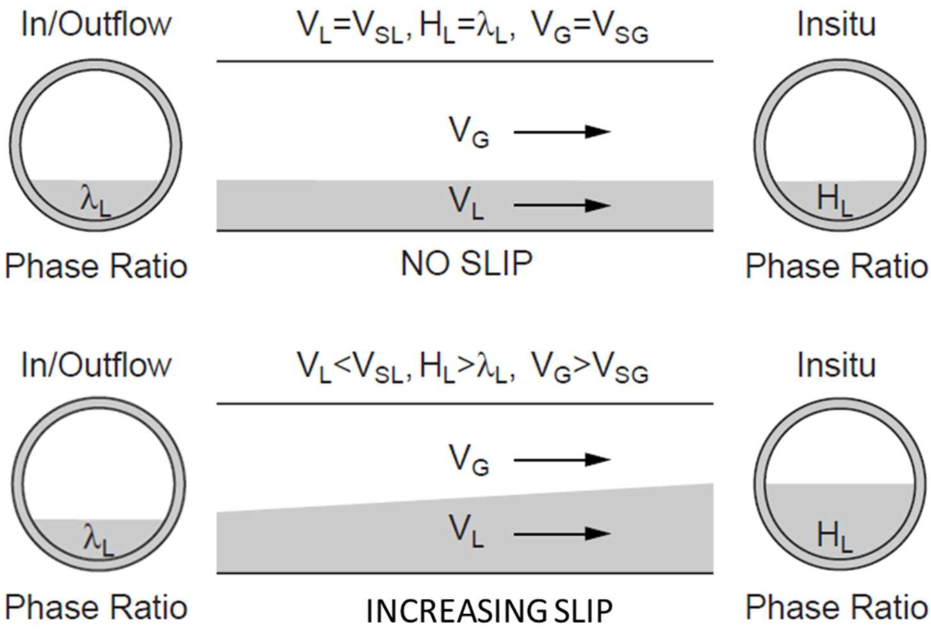

Figure (6a): Volume fraction changes when slip occurs during flow [87]

Superficial phase velocities (V_{SL} and V_{SG}) are given by:

$$V_{SL} = {Q_L}/{A_p} \quad \text{and} \quad V_{SG} = {Q_g}/{A_p} \qquad \text{Equation (28)}$$

In situ (or actual) velocities (V_S and V_G) are given by:

$$V_L = {Q_L}/{A_L} \quad \text{and} \quad V_G = {Q_g}/{A_G} \qquad \text{Equation (29)}$$

where A_L and A_G are the actual areas of the pipe occupied by that liquid and phases respectively.

A_L and A_G under NO SLIP conditions can be calculated from the in- and out-flow phase rates

$$A_L = {Q_L}/{(Q_L + Q_g)} \quad \text{and} \quad A_g = {Q_g}/{(Q_L + Q_g)} \qquad \text{Equation (30)}$$

The slip condition can be quantified by the liquid Holdup (HL) defined as the Fraction of the pipe filled with liquid:

$$H_L = {A_L}/{A_p} \quad \text{and} \quad H_g = {A_g}/{A_p} = 1 - H_L \qquad \text{Equation (31)}$$

and the No slip holdup:

$$\lambda_L = {Q_L}/{(Q_L + Q_g)}$$ Equation (32)

where λ_L is the input liquid volume fraction. The relationship between all these variables is illustrated in Figure.

Hence if slip occurs, then the slip velocity, Vs, is given by:

$$V_s = V_g - V_L = {V_{Sg}}/{H_g} - {V_{SL}}/{H_L}$$ Equation (33)

Appendix (7) MATLAB 3D plotting

For plotting 3D surfaces:

```
a = unique(oneto8(:,2));
b = unique(oneto8(:,3));
c = unique(oneto8(:,4));

z = zeros(length(a),length(b), length(c));

indi =[];

for ii=1:length(a)
    for jj=1:length(b)
        for kk=1:length(c)
            index =
find((oneto8(:,2)==a(ii))&(oneto8(:,3)==b(jj))&(oneto8(:,4)==c(kk)));
            indi = [indi index];
            z(ii,jj,kk) = oneto8(index,1);
        end
    end
end

c1=ones(12,12);
c2=c1+1;
c3=c1+2;
c4=c1+3;

figure(2)
surf(b,a,z(:,:,1),c1);
hold on
surf(b,a,z(:,:,2),c2);
hold on
surf(b,a,z(:,:,3),c3);
hold on
surf(b,a,z(:,:,4),c4);
hold on
```

References

1. Halvorsen, Martin, Geir Elseth, and Olav Magne Naevdal, Increased oil production at Troll by autonomous inflow control with RCP valves, in SPE Annual Technical Conference and Exhibition. 2012: SPE 159634.
2. Saeverhagen, Erland, Arve Thorsen, Sveinung Gard, and Richard Jones. Troll West Oilfield Development? How a Giant Gas Field Became the Largest Oil Field in the NCS Through Innovative Field and Technology Development. in IADC/SPE Drilling Conference. 2008. IADC/SPE 112616.
3. Salamy, Salam Phillip, Hassan K. Al-Mubarak, Drew E. Hembling, and Mohammad Saad Al-Ghamdi, Deployed Smart Technologies Enablers for Improving Well Performance in Tight Reservoirs-Case: Shaybah Field, Saudi Arabia, in SPE Intelligent Energy Conference and Exhibition held in Amsterdam, The Netherlands. 2006, Society of Petroleum Engineers: SPE 99281.
4. Aadnoy, Bernt and Geir Hareland, Analysis of Inflow Control Devices, in SPE Offshore Europe Oil & Gas Conference & Exhibition held in Aberdeen, UK. 2009: SPE 122824.
5. Ouyang, Liang-Biao, Practical consideration of an inflow-control device application for reducing water production, in SPE Annual Technical Conference and Exhibition. 2009: SPE 124154.
6. Al-Khelaiwi, Faisal Turki Manee, A comprehensive approach to the design of advanced well completions, in Institute of Petroleum Engineering, A thesis submitted for the degree of Doctor of Philosophy. 2013, Heriot-Watt University.
7. Thomas, Sally A., Technology Focus: Offshore Production and Flow Assurance. Journal of Petroleum Technology, 2015. 67(11): p. 1.
8. Gualdrón, M. B. Gómez, A. Florez Anaya, Y. E. Araujo, W. Parra, M. Uzcategui, V. Bolaños, E. Mayorga, and F. A. Porturas, Autonomous Inflow Control Devices (AICD) Application in Horizontal Wells Completions in Rubiales Area, Heavy Oil Reservoir, in SPE Middle East Intelligent Oil & Gas Conference & Exhibition held in Abu Dhabi, UAE. 2015, Society of Petroleum Engineers: SPE-176752-MS.
9. Corona, Georgina, Stephen Greci, Brandon Least, Weiqi Yin, and Jacqueline Plumlee, Fluidic Diode Autonomous ICD Single-Phase Testing, in SPE Deepwater Drilling & Completions Conference held in Galveston, Texas, USA. 2016, Society of Petroleum Engineers: SPE-180303-MS.

10. Halvorsen, Martin, Martin Madsen, Mathias Vikøren Mo, Ismail Isma Mohd, and Annabel Green, Enhanced Oil Recovery On Troll Field By Implementing Autonomous Inflow Control Device, in SPE Bergen One Day Seminar held in Bergen. 2016, Society of Petroleum Engineers: SPE-180037-MS.
11. Awannegbe, Edohamen Patrick, Characterization of flow regime of highly viscous oils using conventional ICD and BECH AICD. Master's thesis in Petroleum engineering, University of Stavanger, Norway, 2014.
12. Konopczynski, Michael, Intelligent wells can improve reservoir performance. Drilling contractor, 2004. 60(2): p. 37-38.
13. Brekke, Kristian and Sc Lien, New and simple completion methods for horizontal wells improve the production performance in high-permeability, thin oil zones. SPE Drilling & Completion, 1994. 9(03): p. 205-209.
14. Birchenko, Vasily Mihailovich, Analytical modelling of wells with inflow control devices, in Institute of Petroleum Engineering, A thesis submitted for the degree of Doctor of Philosophy. 2010, Heriot-Watt University.
15. Mackay, E. J., S. Al-Mandhari, J. Peacock, and B. Hammond, Improved Accuracy of Modelling for Optimization of Squeeze Design, in SPE International Symposium on Oilfield Chemistry held in Houston, Texas, U.S.A. 2005, Society of Petroleum Engineers: SPE 93375.
16. Lien, S. C., Knut Seines, S. O. Havig, and Torgeir Kydland, The First Long-Term Horizontal-Well Test in the Troll Thin Oil Zone. Journal of petroleum technology, 1991: p. 914 - 973.
17. Haug, B. T., The Second Long-Term Horizontal Well Test in Troll: Successful Production From a 13-in. Oil Column With the Well Partly Completed in the Water Zone, in Annual Technical Conference and Exhibition of the Society of Petroleum Engineers held in Washington, DC. 1992, Society of Petroleum Engineers: SPE 24943.
18. Porturas, F., Enhanced Production with ICD and AICD Completions in Oil Wells: Case Studies From Latin America, in SPE Latin America and Caribbean Heavy and Extra Heavy Oil Conference held in Lima, Peru. 2016, Society of Petroleum Engineers: SPE-181204-MS.
19. Prakasa, Bona, Khafiz Muradov, and David Davies, Rapid Design of an Inflow Control Device Completion in Heterogeneous Clastic Reservoirs Using Type Curves, in SPE Offshore Europe Conference & Exhibition held in Aberdeen, Scotland. 2015, Society of Petroleum Engineers: SPE-175448-MS.

20. Joshi, Sada D, Horizontal well technology. 1991: PennWell Books.
21. Negrescu, Matei and Ivan Landim Frota Leitao Junior, ICD/AICD for Heavy Oil - Technology Qualification at the Peregrino Field, in Offshore Technology Conference Brasil held in Rio de Janeiro, Brazil. 2013, Offshore Technology Conference: OTC 24503.
22. Eltaher, Eltazy Khalid, Khafiz Muradov, and David R Davies, Combined surface and subsurface control Adds Value during the production of wells subject to gas coning. SPE Integrated Intelligent-Well Completions Workshop, Rio de Janeiro, 2014.
23. Mjaavatten, Are, Robert Aasheim, Steinar Saelid, and Oddvar Groenning, A Model for Gas Coning and Rate-Dependent Gas/Oil Ratio in an Oil-Rim Resevoir, in SPE Reservoir Evaluation & Engineering, pages, 842 - 847. 2008. p. 842-847.
24. Eltaher, Eltazy Mohammed Khalid, Morteza Haghighat Sefat, Khafiz Muradov, and David Davies, Performance of Autonomous Inflow Control Completion in Heavy Oil Reservoirs, in International Petroleum Technology Conference. 2014, International Petroleum Technology Conference: IPTC-17977-MS.
25. Stalder, John, Test of SAGD Flow-Distribution-Control Liner System in the Surmont Field, Alberta, Canada. Journal of Canadian Petroleum Technology, 2013: p. 95-100.
26. Abd Elfattah, Mahmoud, Karam Al-Yateem, Hassan Qahtani, and Behzad Rajabian, Variable Nozzle-Based Inflow Control Device Completion: Inflow Distribution Comparison, Analysis, and Evaluation, in International Petroleum Technology Conference held in Beijing, China. 2013, International Petroleum Technology Conference: IPTC 17168.
27. Ahmed, Tarek, Reservoir engineering handbook. Third Edition ed. page 870 - 874. 2006, ELSEVIER.
28. Fall 2013 European Gas Well Deliquification Workshop. 2013 [cited 19 April 2017; Presentations Given at the Workshop]. Available from: http://www.alrdc.com/workshops/2013_2013europeangaswell/presentations.htm.
29. Regulacion, Rhandy and Noman Shahreyar. Inflow Control Devices Minimize Annular Velocity in Gas Wells with Stand-Alone Screen Completions. in SPE European Formation Damage Conference. 2011. SPE 142700.
30. Kavle, Vinod Manik, Salem Mohamed Elmsallati, Eric James Mackay, and David R. Davies, Impact of Intelligent Wells on Oilfield Scale Management, in SPE

Europec/EAGE Annual Conference and Exhibition held in Vienna, Austria. 2006, Society of Petroleum Engineers: SPE 100112.

31. Lee, Byung Oh, Fahad Sulaiman Al-Fassam, Artyom Galimzyanov, Syed Abu Faizal, and Roberto Vicario. ICD Evaluation Study Using Numerous PLT Runs to Optimise Design Practice and Maximise ICD Value. in International Petroleum Technology Conference. 2014. IPTC-17882-MS: International Petroleum Technology Conference.

32. Chertenkov, Mikhail, Sergej Deliya, Dmitry Semikin, George Brown, Ainur Bayanova, Edward Kanevsky, Marat Nukhaev, Alexay Shapovalov, and Yan Pormeyster. Gas Breakthrough Detection and Production Monitoring From ICD Screen Completion on Lukoil. in SPE Annual Technical Conference and Exhibition. 2012. SPE 159581.

33. Semikin, Dmitry, Alexander Senkov, Albert Surmaev, Alexey Prusakov, and Edmund Leung, Autonomous ICD Well Performance Completed With Intelligent Inflow Tracer Technology in the Yuri Korchagin Field in Russia, in SPE Russian Petroleum Technology Conference held in Moscow, Russia. 2015, Society of Petroleum Engineers: SPE-176563-MS.

34. Kais, Ransis, Vidar Mathiesen, Haavard Aakre, Glenn Woiceshyn, Amr Elarabi, and Ricardo Hernandez, First Autonomous Inflow Control Valve AICV Well Completion Deployed in a Field Under an EOR Water & CO2 Injection Scheme, in SPE Annual Technical Conference and Exhibition held in Dubai, UAE. 2016, Society of Petroleum Engineers: SPE-181552-MS.

35. Grebenkin, Ivan Mikhailovich, A New Optimisation Procedure for Uncertainty Reduction by Intelligent Wells during Field Development Planning, in Institute of Petroleum Engineering, thesis submitted for the Degree of Doctor of Philosophy. 2013, Heriot-Watt University.

36. Al-Khelaiwi, Faisal T. and David R. Davies, Inflow Control Devices: Application and Value Quantification of a Developing Technology, in International Oil Conference and Exhibition in Mexico held in Veracruz, Mexico. 2007, Society of Petroleum Engineers: SPE 108700.

37. Mayer, Christian Sebastian Jakob, Matthew Spiecker, Chris E. Shuchart, Russell Conway Burkey, Adam Ufford, and Jessica Brysch, Multiphase Flow Performance of Inflow Control Devices - Characterizing Downhole Flow Behavior in Lab Experiments, in Abu Dhabi International Petroleum Exhibition

and Conference held in Abu Dhabi, UAE. 2014, Society of Petroleum Engineers: SPE-171890-MS.

38. Jain, Rachna, Ted A. Long, Jasper Dickson, Scott V. Brown, and Edmond Shtepani, Experimental Investigation of Pressure-Drop/Flow-Rate Relationship for Small-Aperture Holes for High-Viscosity Fluids, in SPE Production & Operations, pages 114 - 121. 2014, Society of Petroleum Engineers: SPE Annual Technical Conference and Exhibition, San Antonio, Texas, USA, SPE 159735.

39. Al-Khelaiwi, Faisal T. and David R. Davies, Advanced Sand-Face Completion Design and Application in Gas and Gas-Condensate Fields, in SPE Asia Pacific Oil & Gas Conference and Exhibition held in Brisbane, Queensland, Australia. 2010, Society of Petroleum Engineers: SPE 133603.

40. Gurses, Sule Fatma and Adam Charles Vasper, Optimized Modeling Workflows for Designing Passive Flow Control Devices in Horizontal Wells, in SPE Reservoir Characterisation and Simulation Conference and Exhibition held in Abu Dhabi. 2013, Society of Petroleum Engineers: SPE 166052.

41. Grebenkin, Ivan, Khafiz Muradov, and David Davies, A stochastic approach for evaluating where On/Off zonal production control is efficient. Journal of Petroleum Science and Engineering, 2015. 132: p. 28-38.

42. Ebadi, Farhad and David R. Davies, Should "Proactive" or "Reactive" Control be Chosen for Intelligent Well Management?, in SPE Intelligent Energy Conference and Exhibition held in Amsterdam, The Netherland. 2006, Society of Petroleum Engineers: SPE 99929.

43. Eltaher, Eltazy Khalid, Khafiz Muradov, and David R Davies, “Value from Advanced Wells: New Frontiers”, Inflow Control Technology. Forum - Calgary 2014, in SPE Annual Technical Conference and Exhibition held in Amsterdam, The Netherlands. SPE-170780-MS.

44. Halliburton. EquiFlow Autonomous Inflow Control Device. 2017 [cited 19 April 2017; Available from: http://www.halliburton.com/en-US/ps/completions/sand-control/screens/inflow-control/equiflow-autonomous-inflow-control-device.page?node-id=hfqel9w4.

45. Least, Brandon, Autonomous ICD Installation Success in Ecuador Heavy Oil: A Case Study, in SPE Annual Technical Conference and Exhibition held in New Orleans, Louisiana, USA. 2013: SPE 166495.

46. Hydro-Oil, Hydro Oil & Energy booklet. Hydro Oil Energy, 2007. pp. 20, 48-49, 2007.

47. Freyer, Rune, Fejerskov Morten, and Huse Arve. An Oil Selective Inflow Control System. in SPE 13th European Petroleum Conference held in Aberdeen, Scotland, U.K. 2002. SPE 78272.
48. Sætre, G., Oil Selector - A solution for complete reservoir management. presentation to the SPE Stavanger Section, 2007.
49. Crow, Stephen, Martin Coronado, and Rustom Mody, Means for Passive Inflow Control Upon Gas Breakthrough, in SPE Annual Technical Conference and Exhibition held in San Antonio, Texas, U.S.A. 2006: SPE 102208.
50. Sang, Guangsen, Zhenhai Jiang, Qingjie Zhang, Jianguang Wei, and Tianjun Zhang, A Novel Autonomous Inflow Control Device Design Based on Water Swelling Rubber, in IADC/SPE Asia Pacific Drilling Technology Conference and Exhibition held in Bangkok, Thailand. 2014, Society of Petroleum Engineers: IADC/SPE 170506.
51. Zeng, Quanshu, Zhiming Wang, Xiaoqiu Wang, Yiwei Li, Weilin Zou, Jingnan Xiao, Tian Chen, Gang Yang, and Quan Zhang, A Novel Autonomous Inflow Control Device Design: Improvements to Hybrid ICD, in International Petroleum Technology Conference held in Kuala Lumpur, Malaysia. 2014, International Petroleum Technology Conference: IPTC-17776-MS.
52. Aadnoy, Bernt. Autonomous Flow Control Valve or “intelligent” ICD. 2008 [cited 19 April 2017; Available from: http://hansenenergy.biz/HANSEN_Energy_Solutions/InflowControl2008B.pdf.
53. Bowen, Eddie G. and Bernt Sigve Aadnoy, A Quasi Intelligent Flow Control Device for Water Injectors, in IADC/SPE Asia Pacific Drilling Technology Conference. 2014, Society of Petroleum Engineers: IADC/SPE-170463-MS.
54. Delia, S. V., M. V. Chertenkov, A. V. Zhakovschikov, V. V. Matsashik, O. N. Zhuravlev, and R. V. Shchelushkin, Field Tests of a New Generation of Flow Control Unit Able to Prevent the Gas Breakthrough in Oil Wells, in SPE Russian Petroleum Technology Conference held in Moscow, Russia. 2015, Society of Petroleum Engineers: SPE-178417-MS.
55. Vasily Y. Volkov, Alexander P. Skibin, Oleg N. Zhuravlev, Marat T. Nukhaev, Roman V. Shchelushkin, R. V. , Adaptive Inflow Control System. Cornell University Library, August 2014.
56. Wang, Xiaoqiu, Zhiming Wang, and Quanshu Zeng, A Novel Autonomous Inflow Control Device: Design, Stracture Optimization, and Fluid Sensitivity Analysis,

in International Petroleum Technology Conference. 2014, International Petroleum Technology Conference: IPTC-17758-MS.

57. Aadnoy, Bernt S. Autonomous inflow control, water removal and water stop technologies. in Presentation at the Inflow Control Technology Forum. 2016. Dubai.

58. Krohn-Fagervoll, Siri, An Untapped Resource for the Oil and Gas Industry. Scandinavian oil-gas magazine, 2013. 7/8(2013): p. 18-19.

59. Fripp, Michael, Liang Zhao, and Brandon Least, The Theory of a Fluidic Diode Autonomous Inflow Control Device, in SPE Middle East Intelligent Energy Conference and Exhibiiton held in Dubai, UAE. 2013, Society of Petroleum Engineers: SPE 167415.

60. Aakre, Haavard, Britt Halvorsen, B. Rnar Werswick, and Vidar Mathiesen. Smart Well With Autonomous Inflow Control Valve Technology. in 18th Middle East Oil & Gas Show and Conference (MEOS). 2013. SPE 164348-MS.

61. Mathiesen, Vidar, Bjernar Werswick, Haavard Aakre, and Geir Elseth, Autonomous Valve, A Game Changer Of Inflow Control In Horizontal Wells, in Society of Petroleum Engineers. 2011, Society of Petroleum Engineers: SPE-145737-MS.

62. Tendeka. Tendeka announce 10,000 FloSure AICD installations globally. 2015 [cited 19 April 2017; Available from: http://www.tendeka.com/news-and-events/tendeka-celebrates-10000-flosure-aicd-installations-globally/.

63. Benn a Voll, Ismarullizam Mohd Ismail, Iko Oguche. Inflow control. 2015 [cited 19 April 2017; Available from: http://www.oedigital.com/engineering/item/8647-inflow-control.

64. Zhao, Liang, Brandon Least, Stephen Greci, and Angel Wileman, Fluidic Diode Autonomous ICD Range 2A Single-Phase Testing, in SPE Oilfield Water Management Conference and Exhibition held in Kuwait City, Kuwait. 2014, Society of Petroleum Engineers: SPE-170993-MS.

65. Least, Brandon, Stephen Greci, Russell Burkey, Adam Ufford, and Angel Wilemon. Autonomous ICD Single Phase Testing. in SPE Annual Technical Conference and Exhibition. 2012. SPE 160165.

66. Halliburton. EquiFlow Autonomous Inflow Control Devices. 2016 [cited 19 April 2017; Inflow Control Technology Brochure]. Available from: http://www.halliburton.com/public/cps/contents/Data_Sheets/web/H/H08364-EquiFlowAICD.pdf.

67. Einar Haugen, Nils O. Ostbye, Tore Gronvold, Knut Straith, and Thomas G. Theting, Statoil Asa, Lessons Learned from Further Development of the Peregrino Heavy Oil Field Offshore Brazil, in EUROPEC 2015 held in Madrid, Spain. 2015: SPE-174341-MS.
68. Li, Zhuoyi , Preston Fernandes, and Ding Zhu. Understanding the Roles of Inflow-Control Devices in Optimizing Horizontal-Well Performance. in September 2011 SPE Drilling & Completion, pages 376 - 385. 2009. SPE Annual Technical Conference and Exhibition, New Orleans, Louisiana, SPE 124677.
69. Mathiesen, Vidar, Bjornar Werswick, and Haavard Aakre, The Next Generation Inflow Control, the Next Step to Increase Oil Recovery on the Norwegian Continental Shelf, in SPE Bergen One Day Seminar held in Grieghallen, Bergen, Norway. 2014, Society of Petroleum Engineers: SPE 169233.
70. Eltaher, Eltazy Khalid, Khafiz Muradov, David R Davies, and Ivan Mikhailovich Grebenkin. Autonomous Inflow Control Valves-their Modelling and" Added Value". in SPE Annual Technical Conference and Exhibition held in Amsterdam, The Netherlands. 2014. SPE-170780-MS: Society of Petroleum Engineers.
71. Ouyang, Liang-Biao, Nicholas Petalas, Sepehr Arbabi, Donald E. Schroeder, and Khalid Aziz, An Experimental Study of Single-Phase and Two-Phase Fluid Flow in Horizontal Wells, in SPE Weatem Regional Meeting held in Bakersfield, California,. 1998, Society of Petroleum Engineers: SPE 46221.
72. Ouyang, Liang-Biao, Single phase and multiphase fluid flow in horizontal wells. 1998, Stanford University, Department of Petroleum Engineering: Thesis submitted for the degree of Doctor of Philosophy.
73. Holmes, J. A., T. Barkve, and O. Lund, Application of a Multisegment Well Model to Simulate Flow in Advanced Wells, in SPE European Petroleum Conference held in The Hague, The Netherlands. 1998, Society of Petroleum Engineers: SPE 50646.
74. Schlumberger, ECLIPSE Reference Manual. 2014.
75. Shi, Hua, Jonathan A. Holmes, Louis J. Durlofsky, Khalid Aziz, Luis Diaz, Banu Alkaya, and Gary Oddie, Drift-Flux Modeling of Two-Phase Flow in Wellbores, in SPE Annual Technical Conference and Exhibition held in Denver, Colorado, U.S.A. 2003, Society of Petroleum Engineers: SPE 84228.
76. Hagedorn, Alton R. and Kermit E. Brown, Experimental Study of Pressure Gradients Occurring During Continuous Two-Phase Flow in Small-Diameter Vertical Conduits. 1965.

77. Thornton, Kim, Design of Autonomous Inflow Control Device Completions in Heavy Oil for Complex Reservoir Structures, in SPE Latin America and Caribbean Heavy and Extra Heavy Oil Conference held in Lima. 2016, Society of Petroleum Engineers: SPE-181144-MS.
78. Eltaher, Eltazy, Khafiz Muradov, David Davies, and Peter Grassick. Autonomous Flow Control Device Modelling and Completion Optimisation. in ASME 2017 36th International Conference on Ocean, Offshore and Arctic Engineering. 2017. Trondheim, Norway.
79. Eltaher, Eltazy, Khafiz Muradov, David Davies, and Peter Grassickn, Autonomous Flow Control Device Modelling and Completion Optimisation, in SPE Production and Operations. 2017: Awaiting company's approval to be submitted.
80. Grassick, Peter, A Review of Processes for the Simulation of Autonomous Infow Control Devices, in Institute of Petroleum Engineering, Thesis submitted for MSc Individual Project Report. 2016, Heriot-Watt University.
81. Hauge, J. and T. Horn, The Challenge Of Operating And Maintaining 115 Subsea Wells On The Troll Field, in Offshore technology conference. 2005, Offshore Technology Conference: OTC 17111.
82. Lundberg, Bruce Alan, Well and Reservoir Behavior with Varying Associated Gas/Oil Ratio, in SPE Middle East Oil and Gas Show and Conference held in Manama, Bahrain. 2011, Society of Petroleum Engineers: SPE 142617.
83. Konieczek, J, The concept of critical rate in gas coning and its use in production forecasting, in SPE Annual Technical Conference and Exhibition. 1990: SPE 20722.
84. Moradi, Mojtaba, Khafiz Muradov, and David Davies, Novel Workflow to Optimise Annular Flow Isolation in Advanced Wells, in International Petroleum Technology Conference. 2014: IPTC-17716-MS.
85. Aakre, Haavard, Britt Halvorsen, Bjornar Werswick, and Vidar Mathiesen. Autonomous Inflow Control Valve for Heavy and Extra-Heavy Oil. in SPE Heavy and Extra Heavy Oil Conference: Latin America. 2014. SPE-171141-MS: Society of Petroleum Engineers.
86. Bamforth, Steve, Christian Besson, Ken Stephenson, Colin Whittaker, George Brown, Gérard Catala, Gilles Rouault, Bernard Théron, Gilbert Conort, and C Lenn, Revitalizing Production Logging. Oilfield Review, 1996. 8: p. 44-60.

87. Davies, David, Prduction technology Module for the MSc Petroleum Engineering program. Vol. I/II. 2007: Heriot-Watt univeristy.
88. Espinoza, Irina Baca, Roberto Vicario, and Imam Affandi. Production Logging Interpretation Challenges in Evaluating Highly Deviated Wells with Advanced ICD Completions. in SPE Middle East Oil & Gas Show and Conference. 2015. SPE-172742-MS: Society of Petroleum Engineers.
89. Oddie, G., H. Shi, L. J. Durlofsky, K. Aziz, B. Pfeffer, and J. A. Holmes, Experimental study of two and three phase flows in large diameter inclined pipes. International Journal of Multiphase Flow, 2003. 29(4): p. 527-558.
90. Morris, C. W., C. P. Lenn, and I. J. Albertin, Water production logging in horizontal wells. Journal of Petroleum Science and Engineering, 1999. 22(4): p. 217-227.
91. Petex, IPM suite Reveal software, P.E.I. 8.1, Editor. 2017.
92. Schlumberger, Petrel help center, P. Software, Editor. 2017.
93. Lauritzen, Jon Eric and Ingvild Berg Martiniussen, Single and Multi-phase Flow Loop Testing Results for Industry Standard Inflow Control Devices, in SPE Offshore Europe Oil and Gas Conference and Exhibition held in Aberdeen, UK. 2011, SPE Offshore Europe Oil and Gas Conference and Exhibition held in Aberdeen, UK: SPE 146347.
94. Becze, A., C. M. Nascimento, D. F. B. Jackson, C. J. Virues, and A. Wang, The Impact of Well Trajectory on Horn River Shale Gas Production in a Multi-Well Pad: A New Approach Using Steady State and Transient Simulation, in SPE Unconventional Resources Conference-Canada held in Calgary, Alberta, Canada. 2013, Society of Petroleum Engineers: SPE 167210.
95. Nugraha, Ikhsan, Terki K. Albassam, Alessandro Gallelli, and Vidar Mathiesen, Optimizing Reservoir Performance through Utilization of Autonomous Inflow Control Valve – Lessons Learnt from the World's First Installation, in SPE Kingdom of Saudi Arabia Annual Technical Symposium and Exhibition held in Dammam, Saudi Arabia. 2016, Society of Petroleum Engineers: SPE-182755-MS.
96. V. M. Birchenko, A. V. Usnich, D. R. Davies, Impact of frictional pressure losses along the completion on well performance. Journal of Petroleum Science and Engineering, 2010. 73(3-4): p. 204-213.
97. Al-Khelaiwi, Faisal, Vasily Birchenko, Michael Konopczynski, and David Davies, Advanced Wells: A Comprehensive Approach to the Selection Between

Passive and Active Inflow-Control Completions. SPE Production & Operations, 2010. 25(3): p. 305-326.

98. Birchenko, Vasily M., Faisal T. Al-Khelaiwi, Michael R. Konopczynski, and David R. Davies, Advanced Wells: How To Make a Choice Between Passive and Active Inflow-Control Completions, in SPE Annual Technical Conference and Exhibition held in Denver, Colorado, USA. 2008, Society of Petroleum Engineers: SPE 115742.

99. Grebenkin, Ivan and David Davies. A Novel Optimisation Algorithm for Inflow Control Valve Management. in SPE Europec/EAGE Annual Conference. 2012. SPE 154472.

100. Carvajal, G. A., I. Boisvert, and S. Knabe, A Smart Flow for SmartWells: Reactive and Proactive Modes, in SPE Intelligent Energy Conference & Exhibition. 2014: SPE 167821-MS.

101. Oyeka, Onyema, Frederic Felten, and Brandon Least, Screen-Inflow-Design Considerations with Inflow Control Devices in Heavy Oil, in SPE Heavy Oil Conference-Canada held in Alberta, Canada. 2014, Society of Petroleum Engineers: SPE-170097-MS.

102. Gavioli, Paolo, Gonzalo Garcia, and Juan Serrano. Design, Analysis, and Diagnostics for Passive Inflow Control Devices with Openhole Packer Completions. in Offshore Technology Conference. 2010. OTC 20348.

103. Al-Khanferi, Mohammed, Ahmed Bubshait, Mahmoud Abd El-Fattah, Hussain Al-Shabibi, and Mustafa Bawazir, How Malfunctioning Completion Accessories Affect Well Performance in Offshore Saudi Arabia, in SPE-SAS Annual Technical Symposium & Exhibition held in Al Khobar, Saudi Arabia. 2014, Society of Petroleum Engineers: SPE-172238-MS.